Ontario

Ministry of
Northern Development
and Mines

Mines and
Minerals
Division

Ontario Geological Survey
Open File Report 5694

The Geraldton Gold Camp: The Role of Banded Iron Formation

1988

©Queen's Printer for Ontario 1988
Printed in Ontario, Canada

MINES AND MINERALS DIVISION

ONTARIO GEOLOGICAL SURVEY

Open File Report 5694

The Geraldton Gold Camp:
The Role of Banded Iron Formation

by

A.J. Macdonald

1988

Parts of this publication may be quoted if credit is given. It is recommended that reference to this publication be made in the following form:

Macdonald, A.J.

1988: The Geraldton Gold Camp: The Role of Banded Iron Formation; Ontario Geological Survey, Open File Report 5694, 173p., 93 figures, 5 tables, and 1 map in back pocket.

Ontario
Ministry of
Northern Development
and Mines

89-06126/

Ontario Geological Survey

OPEN FILE REPORT

Open File Reports are made available to the public subject to the following conditions:

This report is unedited. Discrepancies may occur for which the Ontario Geological Survey does not assume liability. Recommendations and statements of opinions expressed are those of the author or authors and are not to be construed as statements of government policy.

This Open File Report is available for viewing at the following locations:

(1) Mines Library
Ministry of Northern Development and Mines
8th floor, 77 Grenville Street
Toronto, Ontario M7A 1W4

(2) The office of the Regional or Resident Geologist in whose district the area covered by this report is located.

Copies of this report may be obtained at the user's expense from a commercial printing house. For the address and instructions to order, contact the appropriate Regional or Resident Geologist's office(s) or the Mines Library. Microfiche copies (42x reduction) of this report are available for $2.00 each plus provincial sales tax at the Mines Library or the Public Information Centre, Ministry of Natural Resources, W-1640, 99 Wellesley Street West, Toronto.

Handwritten notes and sketches may be made from this report. Check with the Mines Library or Regional/Resident Geologist's office whether there is a copy of this report that may be borrowed. A copy of this report is available for Inter-Library Loan.

This report is available for viewing at the following Regional or Resident Geologists' offices:

Beardmore-Geraldton: 435 James St. S., Thunder Bay,
P7E 6E3

The right to reproduce this report is reserved by the Ontario Ministry of Northern Development and Mines. Permission for other reproductions must be obtained in writing from the Director, Ontario Geological Survey.

V.G. Milne

V.G. Milne, Director
Ontario Geological Survey

0.1 Foreword

In 1981, the Mineral Deposits Section of the Ontario Geological Survey embarked upon a program to investigate and describe the geological controls upon gold mineralization in the Province. The initial objectives of the program were to address several discrete factors pertaining to gold mineralization by individual, detailed geological mapping studies in key localities in a variety of gold camps.

One of the initial investigations focussed upon the well-known association between gold and banded iron formation. The Geraldton gold camp was selected for this program, because it hosts a number of significant, past-producing gold mines, such as the Hard Rock and MacLeod-Cockshutt mines, from which a considerable portion of gold was mined from an oxide facies, banded iron formation.

The results of this investigation, including a detailed study of an open stope in the Hard Rock Mine, are presented in this report. This work concludes that gold mineralization is largely controlled by structures developed in contrasting rock types, as earlier inferred by geologists who mapped the area in the 1950's for the Ontario Department of Mines. Little evidence has been found to support the contention that banded iron formation may be a protore source of gold in Archean lode deposits.

The observations recorded in the report will be useful to anyone searching for gold in the Beardmore - Geraldton area, and the conclusions drawn from those observations are applicable to gold exploration elsewhere in the Archean.

V.G. Milne
Director
Ontario Geological Survey

Table of Contents

Page

1.0 Introduction....1

2.0 History of Mineral Development and Geological Investigations....6

3.0 Geological Overview of the Geraldton Camp....11
3.1 Volcano-sedimentary Stratigraphy....11
3.1.1 Volcanic Rocks....13
3.1.2 Sedimentary Rocks....14
3.2 Intrusive Rocks....17
3.3 Quaternary Geology....24

4.0 Structural Geology....26
4.1 Folding....26
4.2 Faulting....29

5.0 Metamorphism....33

6.0 Styles of Mineralization 35

7.0 Timing of Mineralization in the Geraldton Camp....47

8.0 Hard Rock Open Stope - Geology....55
8.1 Field Relationships in the Hard Rock Open Stope....58
8.1.1 Iron Formation....61
8.1.2 Porphyritic Rock....69
8.1.3. Wacke and Siltstone....76
8.2 Structure in the Hard Rock Open Stope....78
8.2.1. Soft Sedimentary Structures....78
8.2.2. Structural Geology of the North Zone, Hard Rock and MacLeod-Cockshutt Mines....86
8.2.3. Structural Geology of the Hard Rock Open Stope....94
8.2.3.1. Banded Iron Formation 94
8.2.3.2. Wacke and Siltstone....104
8.2.3.3. Soft Sedimentary Structures....106
8.2.3.4. Porphyry....109

9.0. Mineralization in the Hard rock Open Stope....................114
9.1. Mineralization - Veins and Selvages....................114
9.2. Carbonate Veins in BIF....................114
9.3. Quartz veins in BIF....................115
9.4. Veins in Porphyry....................136
9.5. Veins in Wacke....................142
9.6. Summary of Vein Types and a Structural Analysis.........150

10. Summary and Interpretation....................159

11. Implications for Mineralization in the Geraldton Camp..........164

12. Acknowledgements....................167

13. References....................168

DIAGRAMS

Figure Page

1 Location Map of the Geraldton Gold Camp....2
2 Flowchart of Research Strategy....3
3 Geological Map of Ashmore, Errington and Croll Townships....5
4 A Stratigraphic Column for the Geraldton Area....12
5 Polymict conglomerate, Geraldton....15
6 Photomicrograph of albite porphyry....20
7 Albite porphyry intruding banded iron formation, Bankfield Property....21
8 Quaternary Deposits, Longlac area....25
9 Cleavage folded about Z fold, Consolidated Mosher Property....27
10 Pressure solution cleavage axial to fold....28
11 Slab of material from Bankfield-Tombill Fault Zone....30
12 Folded Veins and Veinlets, F Zone, Consolidated Mosher Property..36
13 Isometric Diagram of F Zone....37
14 Section through North Zone, MacLeod Cockshutt Mine....38
15 Plan of the Little Long Lac Mine....40
16 Section through the Bankfield Mine....41
17 Surface Geology, McLellan Property....45
18 Paragenetic Sequence of Geological Events for the Geraldton Gold Camp....48
19 Photomicrograph of porphyry with two cleavages.. 50
20 Two fabrics in wacke outcrop....51
21 Folded quartz vein cut by non-folded vein, Porphyry Hill, Hard Rock Mine....52
22 Tourmaline vein cutting non-folded vein in Figure 21....53
23 Banded Iron Formation photomicrographs....57
24 Hard Rock open stope....59
25 Geological sketch map overlain upon Figure 24(b)....60
26 Ice-polished outcrop of Banded Iron Formation, Hard Rock open stope....63
27 Folded iron formation, thin mesobands (0.1 - 0.2 cm)....64
28 Interbedded red chert and magnetite mesobands....65
29 Hinge region of fold with significant limb attenuation....66
30 Carbonate veinlets cutting mesobands....67
31 Porphyry within finely banded iron formation....70
32 Photomicrograph of altered porphyry....71
33 Low angle, cross-cutting contact between porphyry and iron formation, Brton Bay Island....72
34 Photomicrograph of porphyry margin....73
35 Plan of the North Zone, Hard Rock Mine....74
36 Magnetite mesobands in highly deformed wacke, Macleod Cockshutt Property....77
37 Cleavage in wacke folded about small-scale folds, picked out by folded quartz veins, McLellan Property....79
38 Folded, clastic dike, Hard Rock open stope....80
39 Clastic dike, sub-perpendicular to bedding, Barton Bay Island....82
40 Clastic dike at acute angle to bedding, Barton Bay Island....83
41 Schematic diagram of the relationships between clastic dikes, angles to bedding, and fold hinges....84

Figure Page

42 Level plans, North Zone, Hard Rock Mine........................85
43 Section through the North Zone, Hard Rock Mine..................88
44 Isometric sketch of North Zone, Hard Rock and MacLeod Cockshutt Mines..89
45 Isoclinally folded fold axis, Consolidated Mosher Property.......90
46 Sheath Fold experiments...93
47 Similar Folds, Hard Rock open stope.............................95
48 Dip isogons on fold in Figure 26................................96
49 Dip isogons on fold in Figure 29................................97
50 Deformed wacke; carbonate layers are strained into lozenges.....100
51 Carbonate lozenges in apical region of fold....................101
52 Carbonate ellipsoids "floating" in deformed wacke..............102
53 Sketch relating formation of carbonate ellipsoids from layers to degree of deformation.........................103
54 Intensely deformed magnetite layers in wacke...................105
55 Spaced, pressure solution cleavage in wacke, Hard Rock open stope...107
56 Development of apparent S folds from Z folds through progressive shear.......................................108
57 Folded porphyry and iron formation, Hard Rock open stope........110
58 Sketch of Figure 57..111
59 Lineated grains of feldspar and amphibole in porphyry, Hard Rock open stope.....................................112
60 Photomicrograph of deformed porphyry, Hard Rock open stope......113
61 Carbonate veinlets cutting iron formation, Hard Rock open stope, tracing of slab.............................116
62 Folded iron formation and quartz-carbonate-gold vein, Hard Rock open stope...117
63 Photomicrograph of gold in pyrite..............................120
64 Photomicrograph of gold in fracture in pyrite..................121
65 Photomicrograph of gold in gangue..............................122
66 Photomicrograph of gold in fracture cutting gangue.............123
67 Sulphidation either side of vein cutting iron formation, Hard Rock open stope.....................................125
68 Quartz vein and zone of sulphidised iron formation cutting folded clastic dike, Hard Rock open stope................126
69 Photomicrographs of sulphidised iron formation, Hard Rock open stope...127
70 Sulphidation of magnetite, Hard Rock open stope................128
71 Location of channel cut through sulphidised iron formation Hard Rock open stope.....................................131
72 Major and trace element variability across sulphidised zone, Hard Rock open stope.....................................132
73 Fibrous, quartz-carbonate ladder veins at high angle to large quartz-carbonate vein, Hard Rock open stope...............133
74 Close-up of a portion of Figure 73.............................134
75 Close-up of a portion of Figure 73.............................135
76 Folded ankerite veinlet in porphyry, cut by quartz-carbonate vein, Hard Rock open stope...............................137
77 Sheeted, quartz carbonate veins in porphyry, Hard Rock open stope..138

Figure **Page**

78 Sheeted, auriferous, quartz-carbonate veins restricted to porphyry unit within Hard Rock open stope................140
79 Sketch of alteration selvage associated with quartz-carbonate vein, Hard Rock open stope.....................141
80 Foliation-parallel carbonate vein, Hard Rock open stope.........143
81 Foliation-oblique quartz-carbonate vein cuts carbonate vein of Figure 80, Hard Rock open stope......................144
82 Boudinage and intra-folial folds in adjacent quartz-carbonate veins, Hard Rock open stope.............................145
83 Two foliation-oblique quartz-carbonate veins displaying variable strain, Hard Rock open stope....................147
84 Ptygmatic elastica folds, Hard Rock open stope. Azimuth of fold axes rotated into shear............................148
85 Ptygmatic elastica folds, Hard Rock open stope.................149
86 Contoured, equal area, lower hemisphere projection of pi-poles to cleavage in wacke, Hard Rock open stope..........151
87 Contoured, equal area, lower hemisphere projection of pi-poles to cleavage in porphyry, Hard Rock open stope.......152
88 Contoured, equal area, lower hemisphere projection of pi-poles to veins in iron formation, Hard Rock open stope....154
89 Contoured, equal area, lower hemisphere projection of pi-poles to veins in porphyry, Hard Rock open stope..........155
90 Contoured, equal area, lower hemisphere projection of pi-poles to transverse veins in porphyry, Hard Rock open stope..156
91 Typical fabrics in a shear zone...............................158
92 Effect of temperature, pressure and pore fluid pressure upon deformation style.......................................160
93 Exponential decrease of contained gold in deposits of the Geraldton Camp from east to west.........................165

Geological Map : Hard Rock Open Stope, Geraldton : Back Pocket

TABLES

Table		Page
I	The Geraldton Gold Camp : Production Statistics	8
II	The Geraldton Gold Camp : Previous Work	9
III	Chemistry of unaltered BIF, Hard Rock open stope	68
IV	Chemistry of porphyry, Hard Rock open stope	75
V	Chemistry of altered BIF, Hard Rock open stope	129

Abstract

An exposure of the North Zone, Hard Rock Mine, Geraldton, reveals the geology in and around an open stope from which gold was extracted prior to 1950. The principal host rock is banded magnetite iron formation, which lies within a shale and wacke sequence. Porphyritic units are found within both chemical and clastic sediments.

Gold mineralisation, while hosted by all three major rock types in the Hard Rock North Zone, shows a marked spatial association with a 50 m wavelength, Z-shaped fold, most prominent in banded iron formation. Gold is within two sets of quartz ± iron-bearing carbonate veins, which are younger than a barren set of carbonate veinlets. Gold is also hosted by zones of sulphidation, up to a metre in width, that are peripheral to quartz-carbonate veins; while present in all rock types, sulphidation zones attain optimal development within iron formation, where iron and arsenic sulphides form at the expense of magnetite.

Structures in the North Zone, including folds and faults in the host rocks, deformed clastic dikes and veins and veinlets, are all consistent with a period of progressive, dextral shear punctuated by transient brittle failure within an overall ductile strain regime. Brittle failure was triggered by massive fluid influx from an external source. The fluid introduced components such as gold, carbon dioxide, arsenic, sulphur and silica.

THE GERALDTON GOLD CAMP:
THE ROLE OF BANDED IRON FORMATION

A.J. Macdonald
Precambrian Geology Section
Ontario Geological Survey
77 Grenville Street
Toronto, Ontario, M7A 1W4

Manuscript approved for publication by V.G. Milne, Director, Ontario Geological Survey, July 19, 1988.

This report is published with the permission of V.G. Milne, Director, Ontario Geological Survey, Toronto.

THE GERALDTON GOLD CAMP : THE ROLE OF BANDED IRON FORMATION

1.0 Introduction

This report investigates gold mineralization in the Geraldton camp, 250 km northeast of Thunder Bay, Ontario (Figure 1). Following brief descriptions of the history of mining development in the area and previous geological mapping, a synopsis of the geology of the area is provided together with a brief description of the types and timing of mineralization. The relationship between gold mineralization and banded iron formation is examined in more detail. The study investigated the geometry of auriferous zones with respect to host lithologies, the effects of alteration and deformation in ores and host rocks, and the characteristics of geochemical signatures in both barren and mineralized material. This initial and critical phase of the research was designed to test the hypothesis that gold may be an integral, synsedimentary component of banded iron formation in the Geraldton Camp. If the hypothesis received support from field mapping and geochemical studies, subsequent research would be designed to investigate the mobility of gold in post-sedimentary processes, such as diagenesis, deformation and metamorphism.

If on the other hand, the competing hypothesis indicating that gold was introduced at some stage subsequent to sedimentation, is better supported by field data, efforts would be made to determine the timing of gold introduction with respect to (a) deformation (b) alteration (c) metamorphism. Finally, potential gold sources would be investigated, to assess whether the metal may have been locally or distally derived.

These two alternative hypotheses, outlining a strategy for research designed in 1982 at commencement of the project, are shown diagramatically in a flowchart, Figure 2.

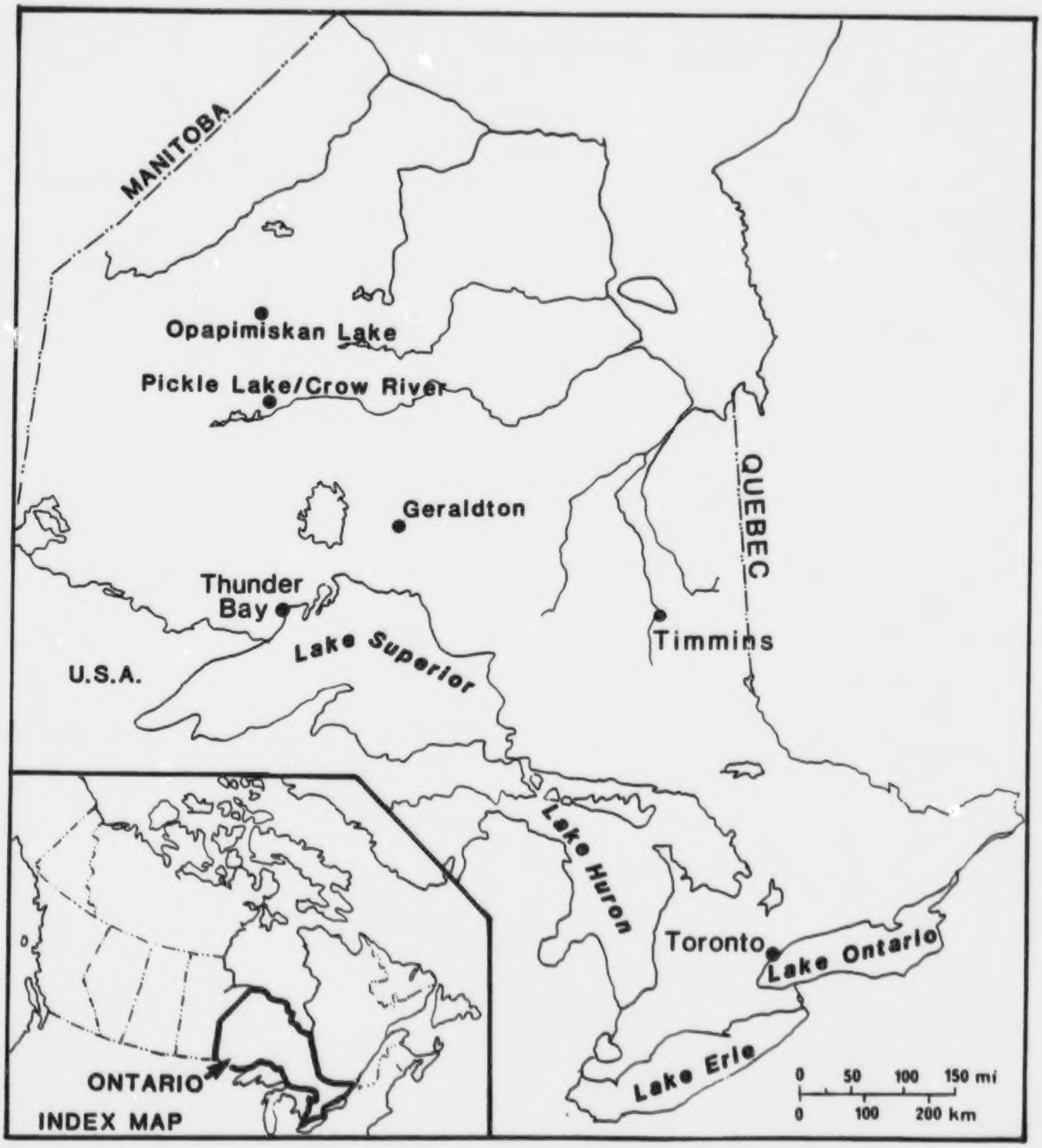
MANITOBA
Opapimiskan Lake
Pickle Lake/Crow River
Geraldton
Thunder Bay
Lake Superior
U.S.A.
QUEBEC
Timmins
Lake Huron
Toronto
Lake Ontario
Lake Erie
0 50 100 150 mi
0 100 200 km
ONTARIO
INDEX MAP

Figure 1 : Location of the Geraldton Gold Camp, Northern Ontario

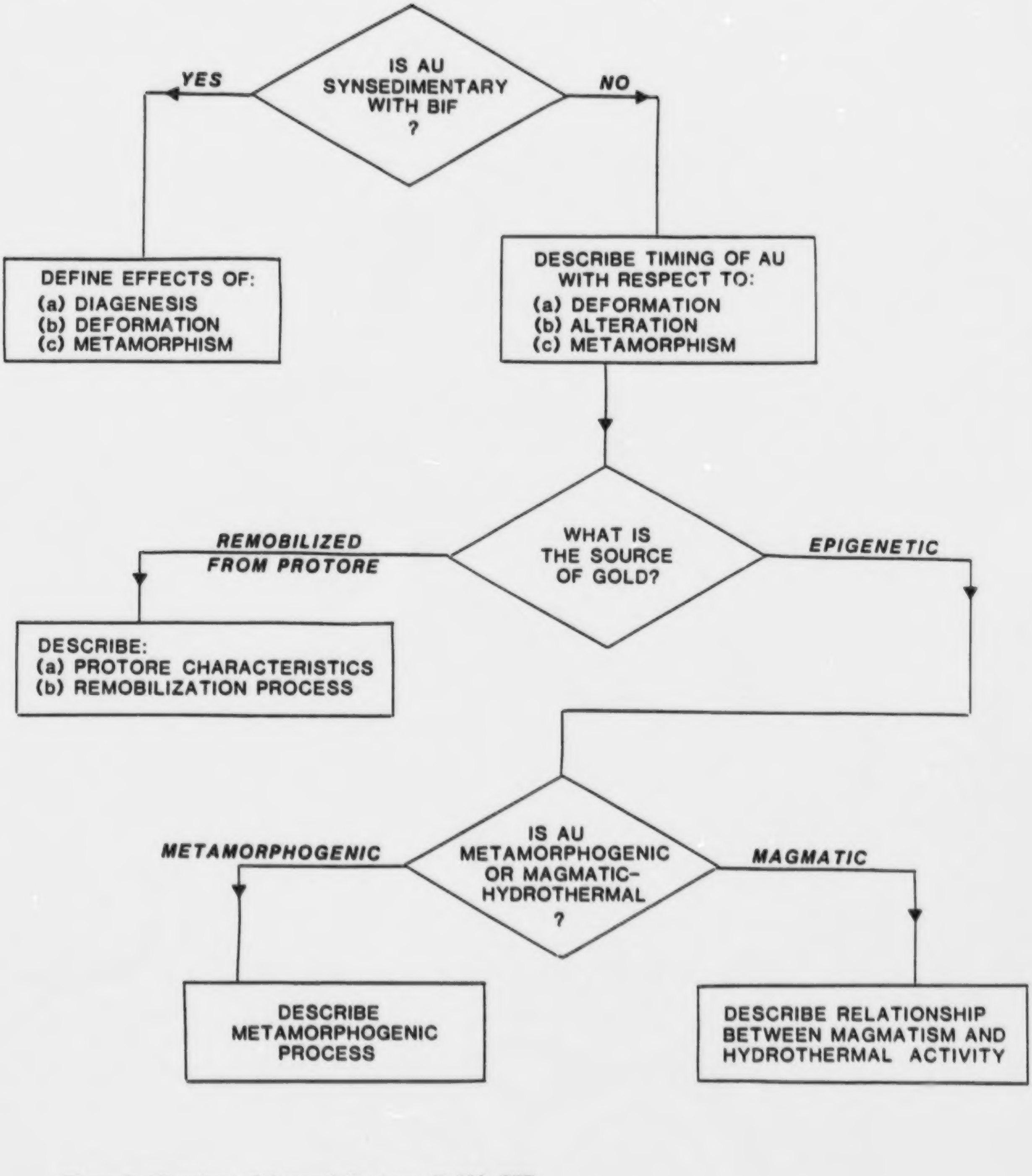
IS AU SYNSEDIMENTARY WITH BIF ?
YES
NO
DEFINE EFFECTS OF:
(a) DIAGENESIS
(b) DEFORMATION
(c) METAMORPHISM
DESCRIBE TIMING OF AU WITH RESPECT TO:
(a) DEFORMATION
(b) ALTERATION
(c) METAMORPHISM
WHAT IS THE SOURCE OF GOLD?
REMOBILIZED FROM PROTORE
EPIGENETIC
DESCRIBE:
(a) PROTORE CHARACTERISTICS
(b) REMOBILIZATION PROCESS
IS AU METAMORPHOGENIC OR MAGMATIC-HYDROTHERMAL ?
METAMORPHOGENIC
MAGMATIC
DESCRIBE METAMORPHOGENIC PROCESS
DESCRIBE RELATIONSHIP BETWEEN MAGMATISM AND HYDROTHERMAL ACTIVITY

Figure 2 : Flowchart of Research Strategy : Gold in BIF

During this study, research into mineralization in the Geraldton Camp developed into two parts:

(A) the relationship between gold and banded iron formation (BIF);

(B) the relationship between the mineralizing event and felsic magmatic activity.

The bulk of the field work for the Au-BIF study was completed in 1982 (Macdonald, 1982, 1983a), with follow-up work in 1983 (Macdonald, 1983b) and 1984 (Macdonald, 1984a, 1984b). A reconnaissance traverse in Croll Township during the fall of 1982 suggested evidence of a large hydrothermal system near the township line with Ashmore Township (see Figure 3). The bulk of the field work to investigate the relationship between gold mineralization and felsic magmatism was completed in 1983, with follow-up in 1984.

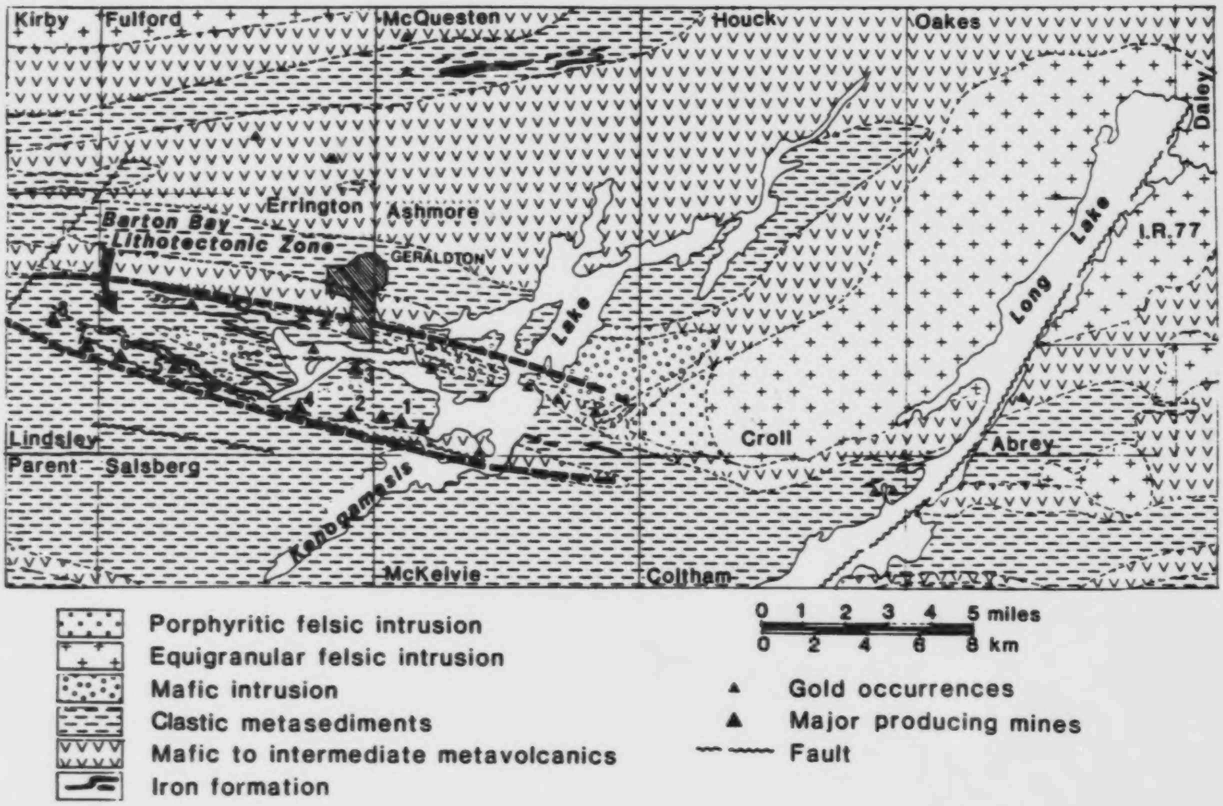
Kirby
Fulford
McQuesten
Houck
Oakes
Daley
Errington
Ashmore
Barton Bay
Lithotectonic Zone
GERALDTON
Lake
Long Lake
I.R.77
Croll
Abrey
Lindsley
Parent
Salsberg
Kenogamisis
McKelvie
Coltham
1
2
3
0 1 2 3 4 5 miles
0 2 4 6 8 km
Porphyritic felsic intrusion
Equigranular felsic intrusion
Mafic intrusion
Clastic metasediments
Mafic to intermediate metavolcanics
Iron formation
Gold occurrences
Major producing mines
Fault

Figure 3 : Geological Map of the Geraldton-Long Lake area (modified from Pye, 1951, and Horwood and Pye, 1951).

2.0 History of Mineral Development and Geological Investigations in the Geraldton Area

During World War I, Tony Oklend discovered an auriferous boulder while trapping along the shore of Kenogamasis Lake, 5 km south of the present Geraldton Townsite (Figure 3). Claims were staked but were subsequently allowed to lapse. In 1931, W.W. (Hard Rock) Smith found gold on a small peninsula in Kenogamasis Lake, ultimately the site of the Hard Rock No. I shaft. During the same year, T.A. Johnson discovered gold in quartz on a small island in the middle of Magnet Lake, in the western portion of Errington Township (Figure 3) and staked a group of 18 claims that eventually became the property of Bankfield Consolidated Mines. In June 1932, Johnson and Oklend, prospecting together, found some quartz veins under water on the south shore of Barton Bay (Figure 3). The area was staked over the next two days and formed a property that evolved into the first producing mine in the Geraldton Camp, the Little Long Lac, which commenced production in November 1934 at a capacity of 350 tons per day. This mine was the the foundation of the Lac Minerals Group of Companies.

Prospecting activity soon increased markedly, with ground staked to the west of Smith's property by F. MacLeod and A. Cockshutt. Both Smith's Hard Rock property and the MacLeod-Cockshutt property were examined underground, leading to some limited development in 1936. Production from both mines commenced in 1938. A number of other smaller mines also began producing at this time: Bankfield (1937), Jellicoe (1939), Magnet (1938), Talmora-Long Lac (1942), Theresa (1935) and Tombill (1938). Underground development on the MacLeod-Cockshutt Mine, on a westerly plunging ore body, led to development on the adjacent property to the west of the Mosher Long Lac Mine, which began production in 1962.

Mining ceased in the Geraldton Camp in 1968, principally in response to a depressed worldwide gold market rather than exhausted reserves. Production statistics are given in Table I. The interested reader requiring a more extensive historical account is referred to many of the references in Table II, particularly those of Bruce (1935), Horwood and Pye (1951) and Pye (1951).

As can be seen from Table I, the largest single producing mine in the Geraldton Camp has been the McLeod-Cockshutt Mine (45.9 tonnes or 1,475,728 troy ounces), which ranked 24th amongst Canadian Archean lode gold producers in 1983 (Colvine et al. 1984). The total production from the camp is nearly 93 tonnes or 3 million ounces, an order of magnitude lower than from the Hollinger-McIntyre-Coniaurum ore bodies at Timmins and approximately 30% of production from the Red Lake Camp.

Table II is a list of authors of geological reports, maps and articles relating to the Geraldton Gold Camp. Most of the earlier efforts were of a reconnaissance nature. Bruce (1935 and subsequent reports) described many of the features of ore bodies in the camp with good descriptions of their geometry. In 1941, Dr. H.C. Horwood commenced a survey of Ashmore Township. After a temporary suspension of work due to World War II, the survey resumed in 1946 and continued until Dr. Horwood's death in 1948. Dr. E.G. Pye was engaged by the Ontario Department of Mines to compile the data that had been collected by Horwood and to complete the examination of the area. In 1951, reports and maps of the geology of Ashmore Township and adjacent Errington Township to the west were published (Horwood and Pye 1951; Pye 1951). The geological maps and descriptive text provided by these two reports formed the basis for all subsequent studies in the Geraldton Camp. In 1967, Ferguson compiled much of the underground and recent surface geological information, published at a scale of 1 inch to 500 feet (Ferguson 1967).

TABLE I : THE GERALDTON GOLD CAMP : PRODUCTION STATISTICS

MINE	YEAR	Au (oz)	Ag (oz)	Tons Milled	Au grade (oz/t)	Ag grade (oz/t)
Bankfield	1937-47	66,417	7,590	231,009	0.29	0.03
Hard Rock	1938-51	269,081	9,009	1,458,375	0.18	0.01
Jellicoe	1939-41	4,238	145	10,620	0.4	0.01
Little Long Lac	1934-54 1956	605,499	52,750	1,780,516	0.34	0.03
MacLeod-Cockshutt	1938-68	1,475,728	101,388	10,337,229	0.14	0.04
Magnet Consolidated	1938-43 1946-52	152,089	16,879	359,912	0.42	0.05
Mosher Long Lac	1962-66	330,265	34,604	2,710,657	0.12	0.01
Talmora Long Lac	1942, 1948	1,417	36	6,634	0.21	0.01
Theresa	1935-38 1941-45 1950-55	4,785	202	26,120	0.18	0.01
Tombill	1938-1942 1955	69,120	8,595	190,622	0.36	0.05
	TOTAL :	2,978,639	231,198			

Mean Gold:Silver Ratio = 12.9:1

abridged from Mason & McConnell (1983)

TABLE II : THE GERALDTON GOLD CAMP : PREVIOUS WORK

Date	Name	Publication	Study
1870	R. Bell	GSC, Report of Progress, 1870-1874,p.335-337	Geological Reconaissance
1901	E.V. Needlands	ODM, Report 1901	Geological Reconnaissance
1909	A.P. Coleman	Ontario Bureau of Mines, Vol. XVIII, 1909, pt. 1, p.141	Geological Reconnaissance
1917	A.G. Burrows	Ontario Bureau of Mines, Vol. XXVI, 1917, p.227-247	Geological Mapping
1917	T.L. Tanton	GSC Summary Report, 1917, Pt. E, p.1-6 (Refs. for above see Fairbairn 1937)	Mapping (Map 313A, 1934)
1935	E.L. Bruce	ODM, Vol. XLIV, 1935, pt.3	Mapping and Geological Description
1936	E.L. Bruce	ODM, Vol. XLV, 1936, pt.3, p.118-140	Mapping and Geological Description
1937	H.W. Fairbairn	ODM, VOl. XLVI, 1936, pt.2, p.118-140	Mapping and Geological Description
1937	E.L. Bruce & W. Samuels	Economic Geology, Vol. XXXII, p.318-334	Mine Descriptions
1939	E.L. Bruce	Economic Geology, Vol. XVI, p. 282-283	Camp Geology
1940	R.D. Macdonald	ODM, Vol. LXIX, pt.7, p.12-31	Mapping and Geological Description
1940	A. Brant	ODM, Preliminary Report	Geophysics
1941	R.D. Macdonald	ODM, Vol. L, pt.3, p.1-21	Mapping and Geological Description
1943	H.S. Armstrong	Economic Geology, Vol. XXXVIV, No. 3, p.204-252	Camp Description
1945	A.E. Tyson	Canadian Mining Journal, Vol. 66, No.12, p.939-850	Camp Description
1945	J.A. Reid	Economic Geology, Vol. 40, p.786-813, No. 8	Camp Geology
1946	E.L. Bruce	Economic Geology, Vol. 41, No. 3, p.282, 283	Camp Description
1948	H.C. Horwood	CIMM Jubilee Volume, p.377-384	Camp Description
1946	A.F. Matheson	CIMM Jubilee Volume, p.377-384	Camp Description
1948	A.F. Matheson	CIMM Jubilee Volume, p.377-384	Camp Description
1948	H.F. Morrow	Precambrian, Vol. 25, p.11-16	Mine Description
1951	H.C. Horwood & E.G. Pye	ODM Annual Report, Vol. LX, pt.V, p.1-140	Township Mapping
1951	E.G. Pye	ODM, Annual Report, Vol. LX, pt. VI, p.1-105	Township Mapping
1967	S.A. Ferguson	ODM Preliminary Map, P. 435, 436, 437	Mapping and Geological Description
1981	L.G. Closs and E.V. Sado	OGS Study 22	Quaternary Geology
1982	A.J. Macdonald	OGS Miscellaneous Paper 100	Mine Geology
1982	G.P. Beakhouse	OGS Miscellaneous Paper 100	Township Mapping
1983	A.J. Macdonald	OGS Miscellaneous Paper 110	Mine Geology
1983	M.J. Lavigne	OGS Miscellaneous Paper 116	Mapping and Geological Description
1983	G.P. Beakhouse	OFR 5513	Township Mapping
1983	A.J. Macdonald	OGS, Miscellaneous Paper 116	Township Mapping
1983	M.M. Kehlenbeck	OGS, Miscellaneous Paper 116	Township Mapping
1983	P. Fralick and T. Barrett	OGS, Miscellaneous Paper 116	Sedimentology
1983	D. Marcotte and D. Webster	OGS, Open File Report 5469	Geophysics
1983	J.K. Mason and C. McConnell	OGS, Miscellaneous Paper 110	Camp Geology
1984	S. Buck and H.R. Williams	OGS, Miscellaneous Paper 119	Camp Geology
1985	C.D. Anglin and J. Franklin	GSC Paper 85-1A, p.193-201	Camp Geology
1985	J.K. Mason and C. McConnel	OFR 5538	Field Guide : Beardmore-Geraldton Belt
1985	J.L. Oliver	M.Sc. Thesis, Queen's University	Camp Geology

In 1982 the Ontario Geological Survey commenced a detailed investigation of mineralization in the Geraldton Camp, of which this study is a part. In addition to this study, Lavigne (1983), Buck and Williams (1984), Williams (1986) concentrated upon defining the style and extent of deformation in the area. Fralick and Barrett (1983) and Barrett and Fralick (1985) described the sedimentology of the banded iron formation (BIF) host to a major ore body in the Hard Rock and MacLeod-Cockshutt Mine. Anglin and Franklin (Geological Survey of Canada, 1985) also studied the role of BIF and porphyries in the mineralizing process.

Mason et al. (1985) published a geological field guide to Beardmore-Geraldton area, and in 1986 Mason and White published a compilation of gold deposits and occurrences in the area.

3.0 Geological Overview of the Geraldton Camp

The following overview is a precis of the extensive investigations by Pye (1951) and Horwood and Pye (1951). The geological data base is taken from their work, with only minor modification. Mapping in Croll Township, to the east of those townships mapped by Horwood and Pye, has demonstrated that the Croll Lake Stock extends farther to the west then shown on the existing compilation map (Tashota-Geraldton Sheet, OGS Map 2102). These modifications are shown in Figure 3.

3.1 Volcano-sedimentary stratigraphy

The Geraldton Gold Camp lies to the north of the subprovince boundary between the Wabigoon volcano-sedimentary terrain and the Quetico sedimentary[*] and migmatitic terrain, as defined by Stockwell (1964).

The exact location of the boundary is subject to debate. Ayres (1969) suggested a gradational contact between the volcanic-dominated terrain of the Wabigoon Subprovince and the sediments of the Quetico Subprovince. McGlynn (1970) further suggested that the boundary occurs at the southern contact of a relatively thin metavolcanic belt extending eastward from Lake Nipigon to the Geraldton area and Long Lake (Figure 3).

---

[*] N.B. All rocks described in this report are metamorphosed to some extent. For purposes of brevity, the prefix "meta" is omitted hereafter, but is understood.

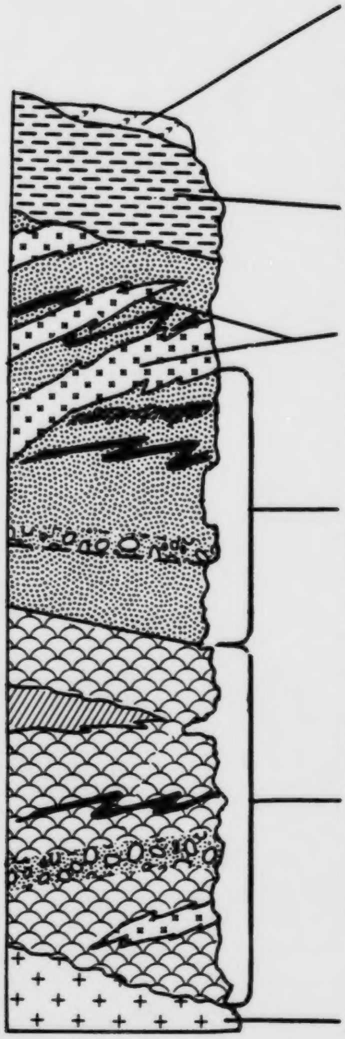

Quaternary Geology. Ground moraines, largely sandy tills, well developed eskers and kames are abundant in some areas. Fluvial sands and outwash features are associated with the Wildgoose Esker Complex.

Keweenawan Diabase. Sills and dikes of Nipissing diabases and porphyritic diabases.

Post Timiskaming Intrusions. Quartz diorites, albite porphyry, quartz albite porphyry, plagioclase diorite porphyry, diorite, hornblende diorite, possibly of Algoman age.

Timiskaming Sediments. Conglomerates, arkoses, greywackes, slates, iron formations. Probable low angle unconformable contact with Keewatin volcanic rocks.

Keewatin Volcanics. Dominated by mafic flows and pillow volcanics. Lesser fine to coarse grained mafic pyroclastic rocks. May contain inter volcanic chemical, and fine grained clastic, sediments. Restricted distribution of felsic flows and pyroclastic rocks.

Sialic Basement.

Figure 4 : Idealised stratigraphic column for the Geraldton Area (Oliver, 1983)

Williams (1986) has reappraised the geology of the Beardmore-Geraldton Belt and has suggested that it may be a fore-arc, accretionary prism assemblage.

3.1.1 Volcanic rocks

A stratigraphic column for the Geraldton area (Oliver 1985) is shown in Figure 4. The oldest rocks described are (Keewatin?) mafic volcanic lavas, agglomerates and tuffaceous rocks in three belts that trend west-northwesterly across Errington and Ashmore Townships and are deflected around the Croll Lake Stock in Croll Township. The lavas tend to be fine- to medium grained, subhedral, granular textured and have suffered variable degrees of alteration, obscuring original mineralogy and possibly modifying the chemistry of the rock. Horwood and Pye (1951) report matted assemblages of sodic plagioclase, fibrous amphibole, chlorite, epidote, clinozoisite, carbonate, minor quartz and biotite. Thin section analysis of textures during this and other studies (e.g. Lavigne, in preparation; Buck, 1986) suggests that much of the mineral assemblage reflects secondary processes (alteration, metamorphism) suggesting lower- to mid-greenschist facies grade metamorphism (250^{o}-350^{o}C).

Flow features are rare in the volcanic rocks, and have commonly been obscured by later tectonism. Even where recognizable pillow structures are preserved, they tend to be deformed, rendering any assessment of facing direction equivocal.

While mafic tuffaceous rocks are present locally within the Geraldton area, Lavigne (1983) has demonstrated that much of the tuff breccia (unit 2, Maps 1951-2, and 1957-7 accompanying Pye (1951), and Horwood and Pye (1951)) is a tectonised and altered, intrusive hornblende diorite, described below.

3.12 Sedimentary Rocks

Horwood and Pye (1951, p.11) divided the (Timiskaming?) sedimentary rocks into four lithological groups
(i) conglomerate; (ii) conglomerate, wacke and slate; (iii) arkose or quartz wacke; and (iv) iron formation. The sediments define two wide belts that strike generally west-northwesterly. Stratigraphic contacts between sedimentary and volcanic belts are commonly obscured by deformation.

Horwood and Pye (1951) also divided the southerly sedimentary package into groups A and B, separated by a disconformity. Group A is the more northerly of the two, hosts the past-producing mines and consists of conglomerate, wacke, siltstone (slate) and banded iron formation. Group B, to the south, is a monotonous sequence of medium to coarse grained wackes with interbedded, fine grained, chloritic wacke. Anglin and Franklin (1985) have determined that these two groups are separated by a major structure, parallel to other structures in the area, such as the Bankfield-Tombill Fault (see discussion of deformation, below). Their evidence is based upon measurements of structural facing directions; structural facing is west-southwesterly to the north of the contact between Group A and Group B sediments and is east-northeasterly to the south of the contact. The conglomerates of Group A are polymict, with pebbles and cobbles of quartz, chert, quartz and feldspar porphyry granodiorite, basalt and rhyolite in a matrix of wacke to silty material. Clast size is typically 5 cm in long dimension, and rarely is as much as 30 cm. Clasts are variably deformed (Figure 5), with coarse grained clasts least stretched.

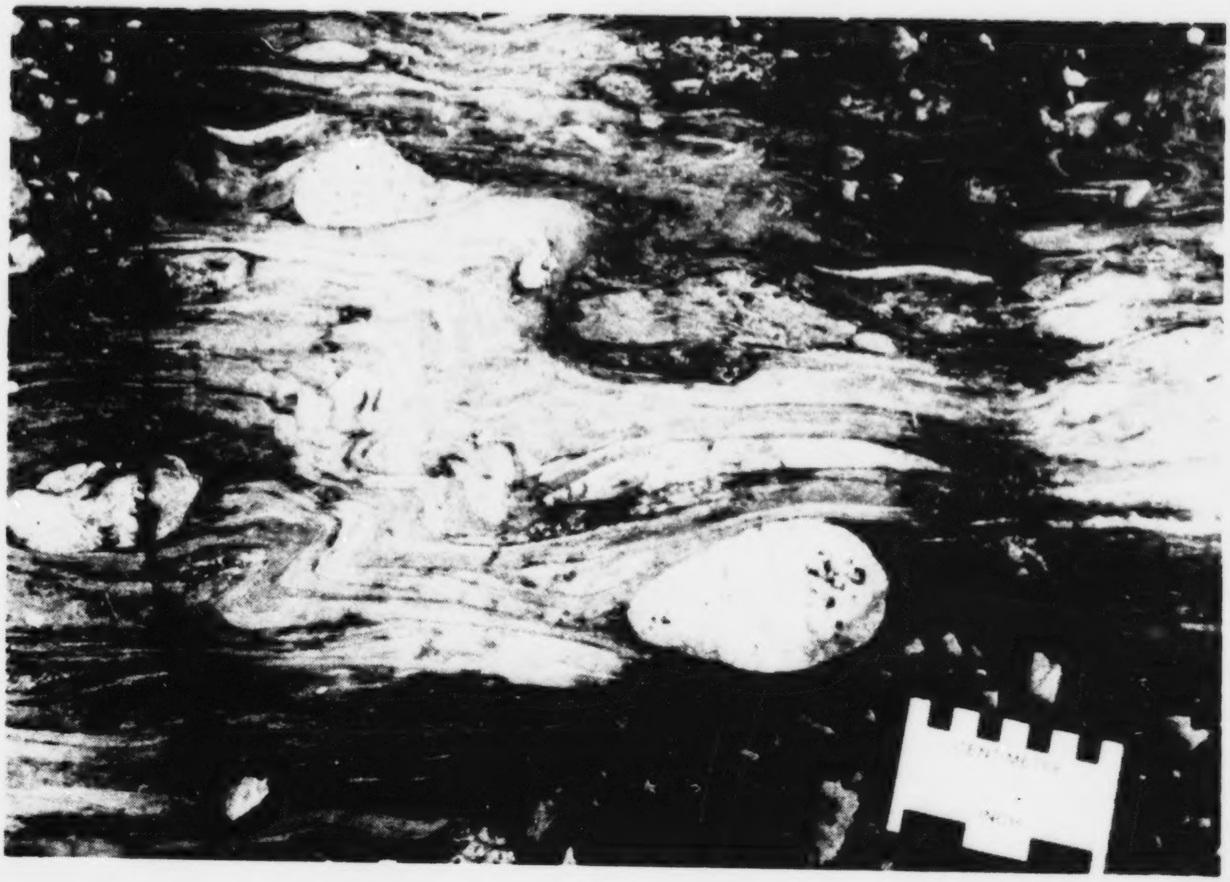

Figure 5 : Deformed Conglomerate, Geraldton.

Wackes and pelitic shales ("slate" of Horwood and Pye 1951) range in colour from light grey to green when coarse, to dark green when fine grained. Bedding is commonly well preserved and together with grain size variation permits way-up determinations in the stratigraphic column. The wacke contains angular to subangular fragments of quartz and either albite or oligoclase (15-20% of the rock) in a fine grained matrix of altered plagioclase, quartz, chlorite, sericite and carbonate, with minor amounts of epidote, magnetite, zircon and rutile.

A unit termed *arkose* was recognized as an ore host at the Little Long Lac Mine (Bruce and Samuel 1937). According to Horwood and Pye (1951) the rock contains 20% quartz grains, 10% albite, 5% orthoclase in a groundmass of 25% altered feldspar, 20% quartz, 6% chlorite, 5% sericite, 5% carbonate, 2% magnetite, 1% epidote and 0.5% each of rutile and apatite. The albite was considered secondary. Pye (1951) considers that the rock is better classified as a quartz wacke, but retains the term *arkose* as it is entrenched in the literature of the area and does not engender any misunderstanding or controversy regarding the origin of the rock.

Banded iron formation (BIF) can be traced within the Beardmore-Geraldton Belt from at least the Klotz Lake area east of Longlac to Beardmore in the west and, by aeromagnetic expression, beneath the Nipigon Plate rocks to the west of Lake Nipigon.

The BIF units tend to be less than 20 metres thick although thicknesses in excess of 60 metres are present, in areas of structural complexity; e.g. the island in Barton Bay (Figure 3).

The BIF consists of mesobands of principally magnetite with minor hematite alternating with mesobands of either chert or siltstone. Barrett and Fralick (1985) recognized sedimentary structures in the BIF, including graded bedding, parallel lamination and load casts, which they interpreted to indicate deposition of clastic beds and magnetic material by turbidity currents, i.e. suggesting that the original chemical sedimentary component (magnetite, or its iron hydroxy-oxide precursor prior to diagenesis) was redeposited together with a fine grained clastic component. Clastic mesobands, principally siltstone, may coarsen and thicken upward, passing eventually into a 100% clastic succession. Barrett and Fralick (1983, 1985) suggest that many of these features are compatible with progradation of clastic sediment lobeson a submarine fan.

Subsequently, Devaney and Fralick (1985) provided supporting evidence top this interpretation from the western portion of the Beardmore-Geraldton Belt, where they interpret a sequence, from north to south, of braided rivers and fluvial fans into submarine, prograding clastic wedges.

3.2 Intrusive Rocks

The oldest intrusive rocks recognized in the Geraldton area are a suite of dioritic to gabbroic sills or dikes ranging in thickness from a few centimetres to in excess of a kilometre. They strike generally east, tend to be thickest in the east and pinch out towards the west. One such unit shows a strong spatial association with one of the major faults in the area, the Bankfield-Tombill Fault (see description below). Where severely deformed, this body of mafic rock has been erroneously mapped as tuff breccia (Pye 1951; Horwood and Pye 1951) as demonstrated by Lavigne (1983).

The mafic intrusive rocks are dark green to grey, medium grained and characterized by blocky crystals of hornblende or, rarely, arborescent aggregates of hornblende crystals. In addition to hornblende, which has locally been uralitized and chloritized, the rocks contain altered andesine plagioclase or unaltered albite, epidote, quartz, sericite carbonate and leucoxene (Horwood and Pye 1951). Much of the mineralogy reflects regional metamorphism, although there is some doubt as to the origin of hornblende in the rock. Lavigne (Resident Geologist, Ministry of Northern Development and Mines, Red Lake, personal communication, 1985) has studied the regional effects of metamorphism and has determined that the rocks of the Geraldton gold camp did not experience pressures and temperatures in excess of middle greenschist facies. Hornblende, especially a dendritic and arborescent form, may therefore be a magmatic phase. Buck (1986) and Lavigne (in preparation) have addressed this problem.

Horwood and Pye (1951) report the presence of serpentinized material at lower levels within the Hard Rock Mine, suggesting the possibility of an ultramafic component to this suite of intrusive rocks. No ultramafic rocks have been recognized on surface.

Plagioclase-phyric diorite intrusive rocks were identified by Horwood and Pye (1951) in the southwest corner of Ashmore Township. The rock contains 25% phenocrysts of andesine plagioclase in a matrix of 45% feldspar, 20% biotite and chlorite, 10% quartz and small amounts of sericite, epidote and magnetite (Horwood and Pye 1951). The rock also contains variable quantities of hornblende, partly altered to biotite and chlorite. With increasing modal hornblende the rock appears to be transitional with hornblende diorite, described above. In more acid varieties the feldspars assume a more sodic oligoclase plagioclase composition, quartz phenocrysts become more abundant and the rock appears to be transitional toward albite porphyries described below. Horwood and Pye (1951, p.17) suggest that there may be a genetic affinity between these three rock types.

Albite and albite-quartz porphyries are exposed throughout the area, mostly as dikes or sills, except in Croll Township, where a large mass of the rock type is exposed with the Croll Lake stock (Figure 3).

The rock consists of up to 75% albite phenocrysts (Ab_{98}) and quartz. The proportion of albite to quartz is variable from almost 100% albite to rocks containing an equal amount of each. Horwood and Pye (1951) suggest that the average is 4 albite to 1 quartz. Where albite phenocrysts constitute the bulk of the rock it takes on a somewhat granular appearance and has been termed *crowded albite porphyry* (CAP) by Macdonald (1984a). The fine grained matrix consists of up to 20% quartz, 17 % feldspar, 5 % sericite, 3 % chlorite, 3 % carbonate and a small amount of apatite. Albite phenocrysts are typically one to two millimetres in diameter in the vicinity of the mines in Geraldton. To the east, however, at West Side Bay, on the shore of Long Lake (Figure 3) for example, albite phenocrysts in dikes are typically 1-2 mm (Figure 6), and up to in excess of 5 mm in diameter. Sericite and chlorite are typically developed along foliae that are deflected around albite phenocrysts. Where deformation and alteration are most intense the rock loses its massive character and takes on a waxy, light grey to pale green/yellow appearance, somewhat similar to the wackes with which it is commonly associated. The well developed fissility induced in the rock due to deformation led at one time to the suggestion that the "Hard Rock Porphyry" might in fact be of sedimentary origin (Reid 1945). The contrary suggestion, that the rock is intrusive in nature was expressed by Bruce (1946) and confirmed by underground mapping in the Hard Rock Mine (Horwood and Pye 1951). Recently exposed outcrop at the Bankfield Mine property also confirms the intrusive nature of the albite porphyry (C.D. Anglin, M.Sc. candidate, Memorial University, Newfoundland, personal communication, 1983). Here the albite porphyry clearly intrudes banded iron formation (Figure 7) and hornblende gabbro.

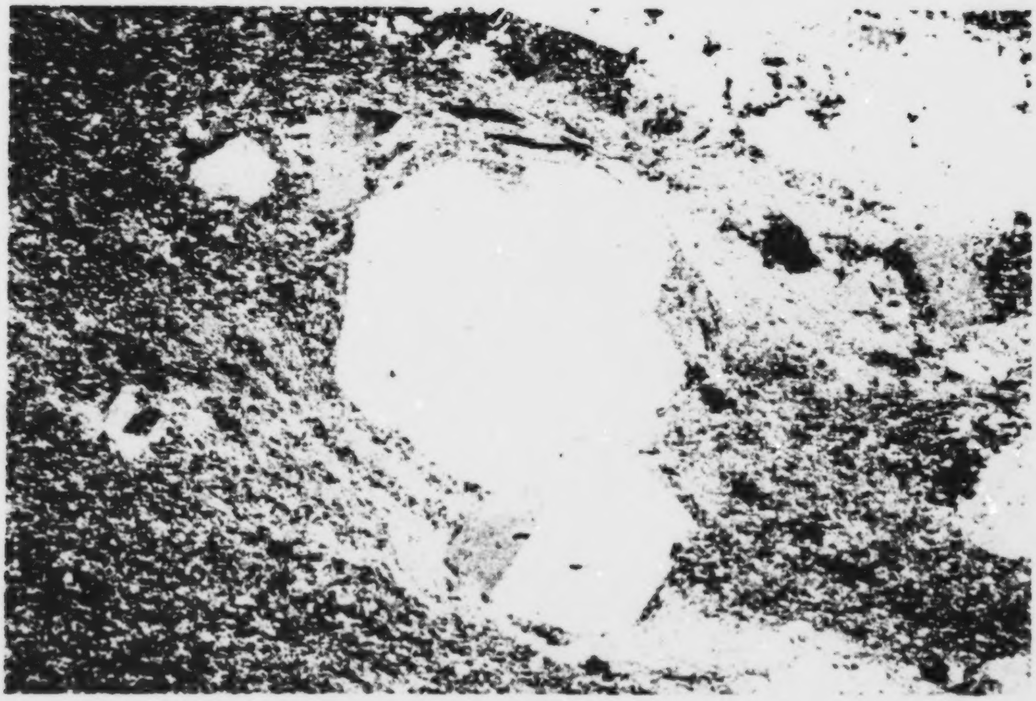

Figure 6 : Feldspar porphyry; Field of View is 5mm.

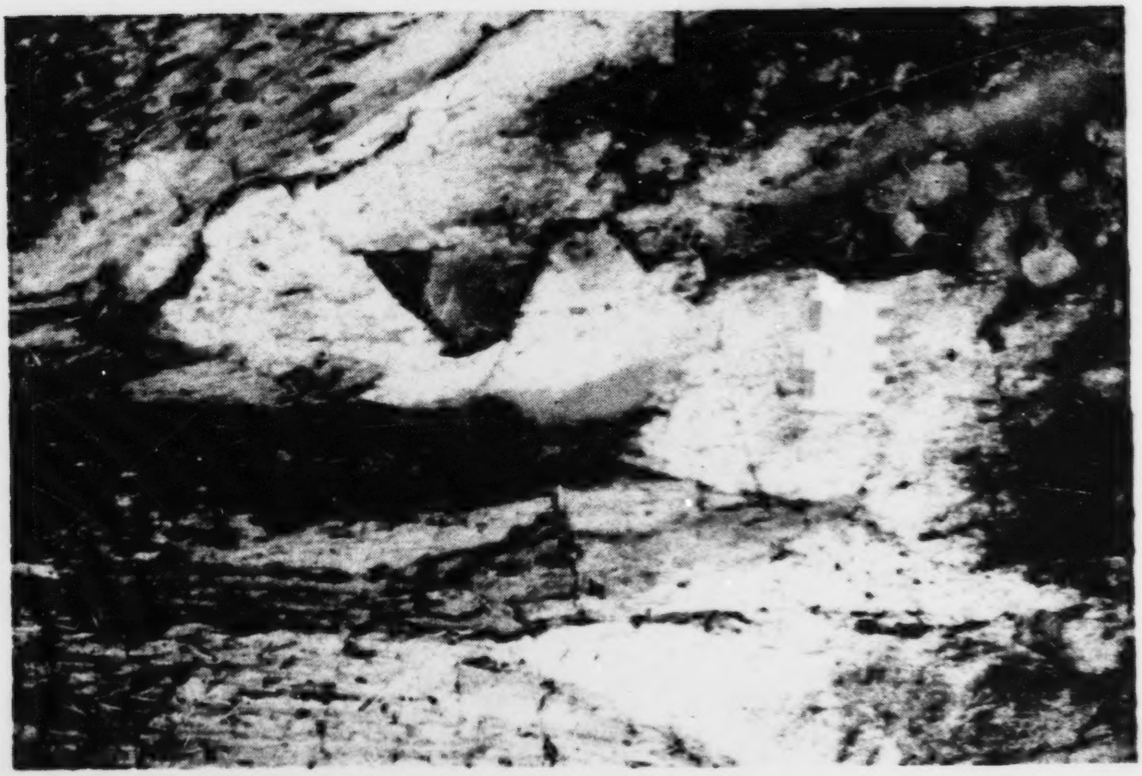

Figure 7 : Albite Porphyry intruding Banded Iron Formation, Bankfield Property, Geraldton

The albite porphyry unit (dikes or sills) is of considerable economic interest in the Geraldton Camp due to its spatial association with much of the gold mineralization. Surface mapping suggests that the unit is not present to the north or south of the 3 km wide zone (Figure 3) containing the ore-bearing lithologies (Pye 1951; Horwood and Pye 1951).

Horwood and Pye (1951) describe a few exposures of quartz diorite dikes, lenses and masses, similar in appearance to albite porphyries. They contain 40% carbonate, 30% feldspar, 15% chlorite, 10% quartz, 3% sericite and 2% magnetite. Although feldspars are commonly highly altered, a few crystals appeared to be andesine (An67). One such exposure of quartz diorite is found in the Hard Rock open stope and is described in greater detail in section 8.1.2.

Macdonald (1983b) mapped part of the granitic stock exposed in Croll Township and the Long Lac area. The bulk of the Croll Lake Stock consists of granodiorite to monzodiorite, based upon the classification of Streckeisen (1973). The western end of the stock is a porphyritic complex, which grades, from the margin of the pluton inwards, as follows: quartz porphyry, feldspar porphyry, diorite, monzodiorite and finally the dominantly granodiorite phase that constitutes the bulk of the stock.

All lithologies described above are locally host to gold mineralization in the Geraldton Camp. The following intrusive phases cut auriferous quartz veins.

Narrow dikes of lamprophyre are present in the Little Long Lac Mine (Horwood and Pye 1951), consisting of a massive, fine grained rock containing tiny plates and grains of biotite, felted aggregates of serpentine, hexagonal in outline and possibly replacing olivine, and highly altered plagioclase. Magnetite and apatite are present in accessory amounts. Carbonate is an abundant secondary constituent. Assuming olivine to be a magmatic constituent, these rocks are kersantites, using the classification of Grout (1932).

Three varieties of diabase are present in the map area: (i) feldspar-phyric quartz diabase; (ii) quartz diabase; (iii) olivine diabase. Feldspar-porphyry quartz diabase, with yellowish green phenocrysts of altered feldspar up to 4.5cm in diameter, may be correlative with the Matachewan swarm. Quartz diabase is black and fine to medium grained with interlocking laths of labradorite and clinopyroxene, and small amounts of quartz, altered amphibole (uralite), magnetite, sericite and apatite. These rocks are probably related to the Nipigon plate volcanic activity (Horwood and Pye 1951). Olivine diabase is similar in appearance to quartz diabase with the exception that olivine is present in place of quartz.

3.3 Quaternary Geology

Large portions of the area (Figure 3) are covered by sand and gravel, with thicknesses up to and locally exceeding 10 m. Best exposed are cross-stratified sands with local gravel lags (Figure 8). Horwood and Pye (1951) suggest that the deposits are of glaciofluvial origin.

The area contains at least two eskers, along the east shore of Eldee Lake and at the west margin of Errington Township (Figure 3). They trend northerly to northeasterly, parallel to the regional southwesterly direction of ice movement. The eskers reach heights of 2-25 m and lengths of up to 1 km.

Recent deposits consist of organic material in swamps, muskeg and streams. The area is located in the vicinity of the drainage divide between the Atlantic and Arctic Oceans.

Figure 8 : Quaternary Deposits, Longlac Area.

4.0 Structural Geology

The Geraldton gold camp is hosted by a suite of rocks that exhibit all scales of deformation from slightly strained to high degrees of deformation where induced fabrics may wholly destroy original rock textures, rendering identification exceedingly difficult. The structural geology of the area is complex and is the subject of considerable work in progress: Lavigne (in preparation), Buck (1986), Williams (in preparation) and Kehlenbeck (1986) have all studied various aspects of the structural geology of the area. The following brief synthesis does not attempt to summarize any unpublished studies, although all the authors in question have published preliminary observations. Much of the following is synthesized from Pye (1951), Horwood and Pye (1951) and personal observations unless stated otherwise.

4.1 Folding

Pye (1951) and Horwood and Pye (1951) outlined a number of antiforms and synforms whose axes trend generally east to east-southeast, parallel to most other structures in the area. Many minor folds with wavelengths ranging from centimetres to tens of metres are developed on the flanks of larger folds. In many cases minor folds are geometrically compatible with their location on larger fold limbs, i.e. S-shaped folds on one flank and Z-shaped on the other. Significantly, however, there are a number of locations, particularly in areas of mineralization, where in addition to *expected* S folds, many Z folds are present. These *reverse* structures have been addressed by Matheson and Douglas (1948), Horwood and Pye (1951) and Pye (1951). Pye (1951) suggests that the Z folds may have initiated in response to motion on the Bankfield-Tombill Fault (described below). This hypothesis is supported by Buck and Williams (1984), who suggest that dextral ductile shear can account for a number of the features of the Geraldton Camp, including the minor Z folds.

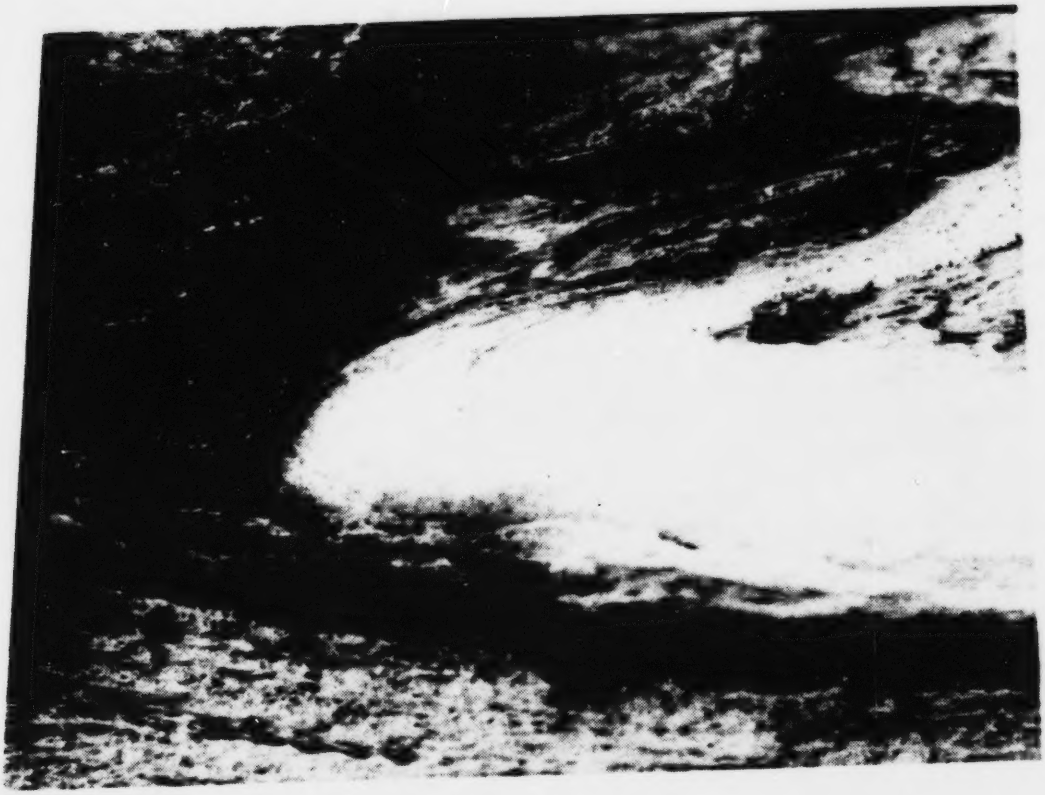

Figure 9 : Folded magnetite layers (dark) within wacke (light); note that cleavage (most visible in wacke) is also folded. Scale in centimetres.

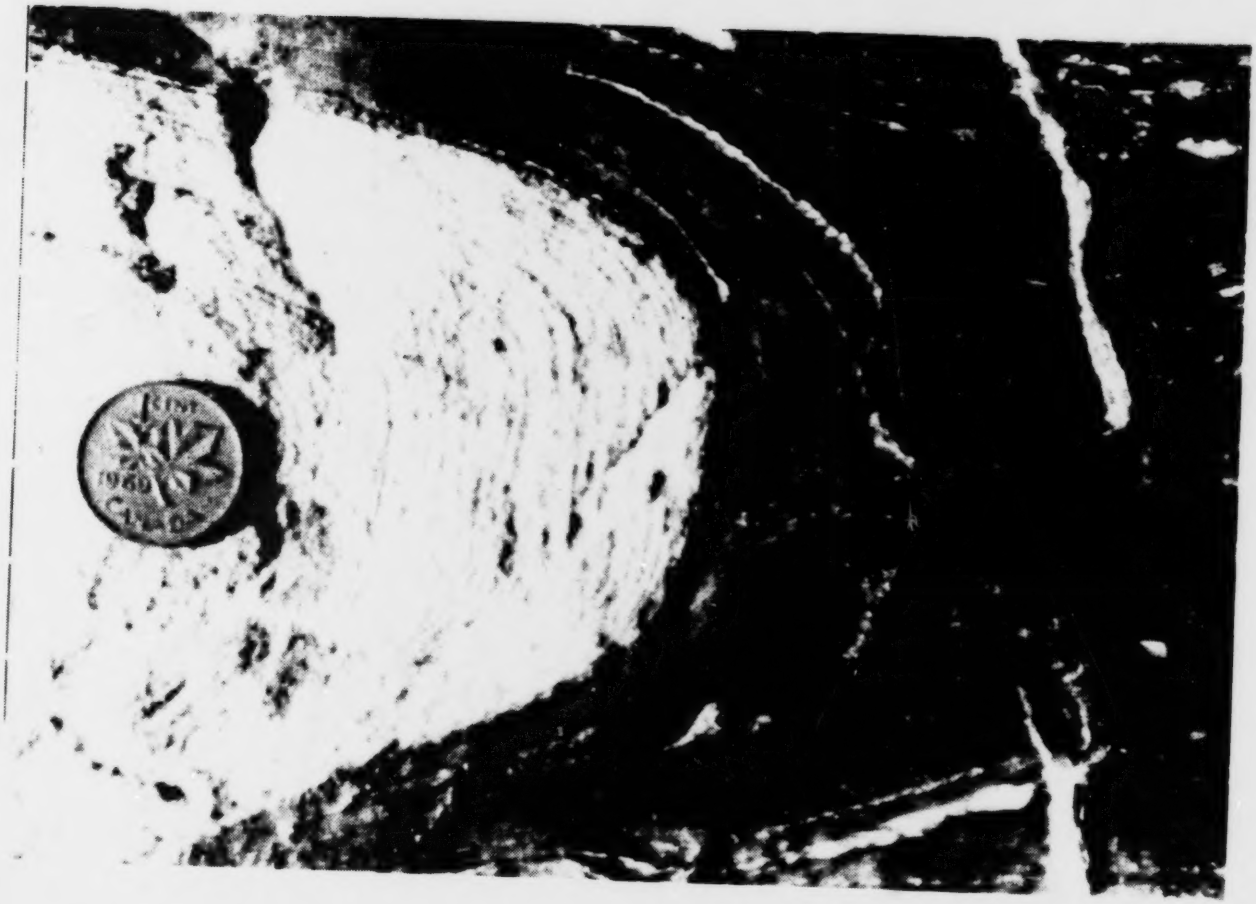

Figure 10 : Folded cleavage in wacke (light); note well-developed pressure solution cleavage in siltstone (dark), axial to fold.

Where bedding and cleavage relationships are visible in the vicinity of a minor Z-fold, the cleavage also may be folded (Figure 9), with a subsequent cleavage, locally a pressure solution fabric, developed axial to the minor fold (Figure 10). These minor Z-folds may, therefore, be termed intrafolial folds and their significance is enhanced in a later discussion of the North Zone of the Hard Rock and MacLeod-Cockshutt Mines, hosted by one such intrafolial fold, albeit larger than those shown in Figures 9 and 10. Pye (1951) and Horwood and Pye (1951) noted that both the major and minor folds plunge between 20^o and 35^o in the direction N75^o-80^{o}W.

4.2 Faulting

Two wide fault zones are present in the area, and mark the north and south boundaries of the rock suite containing gold mineralization. The most northerly of the two faults is the Little Long Lac Fault that strikes approximately east-west and dips 80^{o}S in the vicinity of the Little Long Lac Mine (Figure 3). It consists of a zone up to 20 m wide of schistose and brecciated rock, silicified, carbonatized and impregnated with $<1\%$ arsenopyrite, pyrite, pyrrhotite and chalcopyrite. The southerly fault, the Bankfield-Tombill Fault (BTF), is locally up to 65 m in width and may be followed over a strike length of at least 20 km (Figure 3). The BTF strikes N70^o - 80^{o}W and dips south at 60-70^o. With the exception of the Little Long Lac Mine, adjacent to the Little Long Lac fault, all the major producing mines in the Geraldton camp are spatially associated with the BTF,from the Hard Rock Mine in the east to the Tombill Mine in the west (Figure 3). Spatial relationships between the Jellicoe mine, just to the west of the Tombill Mine, and the BTF are obscured by overburden.

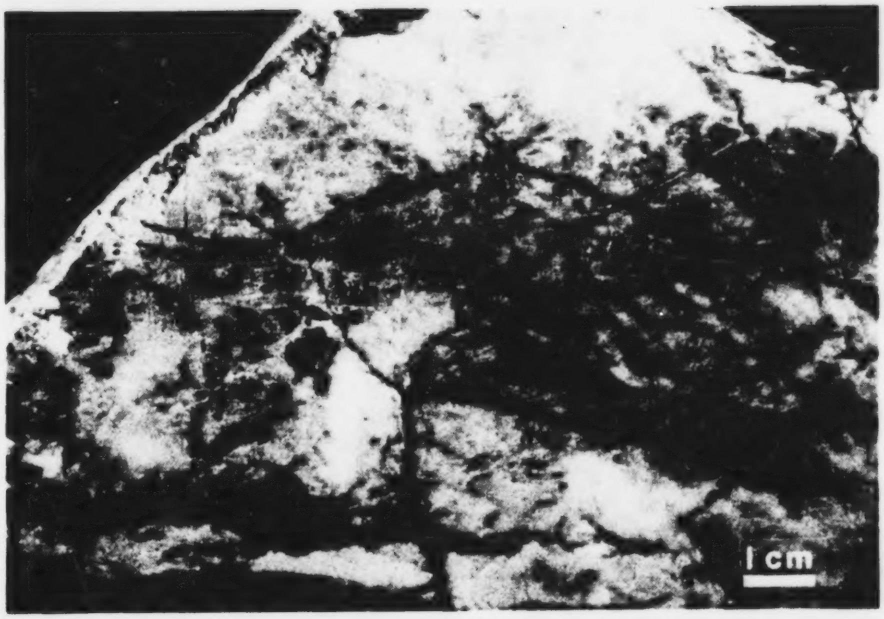

Figure 11 : Brecciated, quartz-rich material from the Bankfield-Tombill Fault, Bankfield Property.

The BTF consists of highly brecciated, siliceous and carbonate-bearing material, with small amounts of chalcopyrite and pyrite ($<1\%$). The rock consists of several generations of quartz and carbonate, and appears to have been repeatedly silicified and carbonatized, brecciated, (Figure 11).

An aggregate motion on both these major faults has yet to be determined. Pye (1951) presents evidence that the fault has ruptured on several occasions; pre-, syn- and post-ore adjustments are recorded. Pye also noted that the aforementioned intrafolial folds are only found in the vicinity of the Bankfield-Tombill fault; the geometry of the folds is suggestive of some degree of thrust motion on the fault; i.e. south side (or hanging wall) up, north side (or footwall) down. The $20\text{-}35^{\circ}$ westerly plunge on the intrafolial Z folds also suggests, as mentioned above, right lateral motion. Relative vectors of motion for the blocks on each side of the fault zone may therefore be: south side up and westwards, north side down and eastwards.

Macdonald (1984a) has pointed out that when host rocks for mineralization in the Geraldton Camp are compared with relatively barren rocks both to the north and south, two principal differences are immediately apparent:

(1) the host rocks tend to be more highly deformed;
(2) the host rocks are more lithologically diverse, with barren terrains tending to be dominated by relatively monotonous, clastic sedimentary or volcanic rocks.

To reflect both the complexity of structure in the zone bearing gold mineralization and the diversity of rock types present, Macdonald (1984a, p.417) suggested that the sequence be termed the Barton Bay Lithotectonic Zone, or BBLZ, after the large bay in Kenogamisis Lake (Figure 3). Ongoing studies have further expanded the width of the zone to as much as 5 km (Buck and Williams 1984).

Further discussion of small scale structures will be addressed in the sections (8.0, 9.0) describing the North Zone of the Hard Rock and Macleod-Cockshutt Mines.

5.0 Metamorphism

While the presence of secondary silicate phases of metamorphic origin is described by Pye (1951) and Horwood and Pye (1951), their areal distributions are not addressed. Macdonald (1944) investigated a transect along the Kenogamisis River, to the southwest of Kenogamisis Lake. Sedimentary rocks exhibit an increase in metamorphic grade from north to south, from chlorite facies in the north, to biotite facies, to garnet-bearing rocks to the south. The northernmost group of volcanic rocks investigated by Macdonald (1944) are also chlorite-bearing and lie in the chlorite zone within the sediments. The southern group of volcanics contsin hornblende and is within the biotite-bearing sedimentary zone. The southernmost sediments also contain staurolite in addition to garnet. No kyanite or sillimanite were observed.

The metamorphic zones recognized by Macdonald (1944) are subparallel to felsic intrusions and pegmatites of the Quetico belt. Macdonald (1944) attributed the distribution of metamorphic facies to contact thermal metamorphism related to the intrusive activity.

Pirie and Mackasey (1978) described a similar southward increase in metamorphic grade in the Jellicoe area, 30 km west-southwest of Geraldton. In the Jellicoe area, andalusite and cordierite were detected 4 and 5 km south of the staurolite isograd, respectively. As at Kenogamisis River, metamorphic isograds are sub-parallel to, and inferred to be related to, the belt of felsic intrusions and pegmatitic rocks of the Quetico terrain.

Beakhouse (1984) described upper greenschists to lower amphibolite facies rocks in the Grenville Lake area (Fulford, Kirby and part of McQuesten Townships) to the north of

Geraldton. While rocks to the immediate west of the known mineral deposits are drift covered, mapping to the east in Croll, Houck, Oakes and Abrey Townships indicates that, ignoring immediate contact intrusive effects, metamorphic grade rises to amphibolite facies in the Long Lake area, to the north and south of the Croll Lake Stock (Lavigne 1983; Macdonald 1983b). Lavigne (in preparation) considers that the Geraldton gold camp lies within a metamorphic "low" of lower to middle greenschist facies rocks, with metamorphic grade increasing to the north, east and south (drift covers rocks to the immediate west).

However, Williams (1986) shows that field relations and petrography of rocks from south of the Geraldton camp demonstrate that the southward increase in metamorphic grade is post-tectonic. This examination of foliation surfaces and thin sections indicates that there is a syntectonic set of mineral assemblages exhibiting variable metamorphic grades partly dependent upon lihtology. Williams, like Mackasey et al. (1976) describing similar rocks to the west, finds no evidence for any major break between the "Quetico" metasediments to the south and "Wabigoon" metasedimentary-metavolcanic terrain to the north.

6.0 Styles of Mineralization

There are several mineralization styles exhibited within the Geraldton Camp, discriminated by differing host rocks and ore structures. A simple classification scheme is not appropriate, as individual ore bodies can contain more than one mineralization style, with one type passing gradationally into another. Eight mineralization styles are described, the first three comprising the most significant, in terms of contained gold. The remaining five styles provided significant tonnage for individual mines, although on a camp scale were of less significance.

6.1 **Zones of fracturing and shearing along wacke-albite porphyry contacts**: Such zones are comprised of many tens of thin, subparallel quartz veinlets within a deformed zone up to 30 m in width (Figure 12). Not all quartz veinlets may carry gold, but a sufficient number are auriferous to permit the whole width to be mined. The largest of this type of ore body, the F Zone, is located on the hinge zone of an intrafolial fold, following the regional plunge to the west, and was mined over a plunge length of 3.5 km, on both the MacLeod-Cockshutt and Mosher Long Lac properties (Ferguson 1967). Stopes were 5 to 20 metres in width, 120 to 200 metres in height and contained in excess of 10 million tonnes at a grade of 4.25 g Au/t, i.e. approximately 42 tonnes contained gold. The relationship between the ore zone and folded CAP intrusion on the MacLeod-Cockshutt Property is shown in Figure 13. Horwood and Pye (1951) report that on the 10th level, ore was continuous for approximately a kilometre across ore widths up to 30 m.

This type of mineralization, although lower grade than others mined, constitutes the most attractive target in the Geraldton camp, due to its continuity and size.

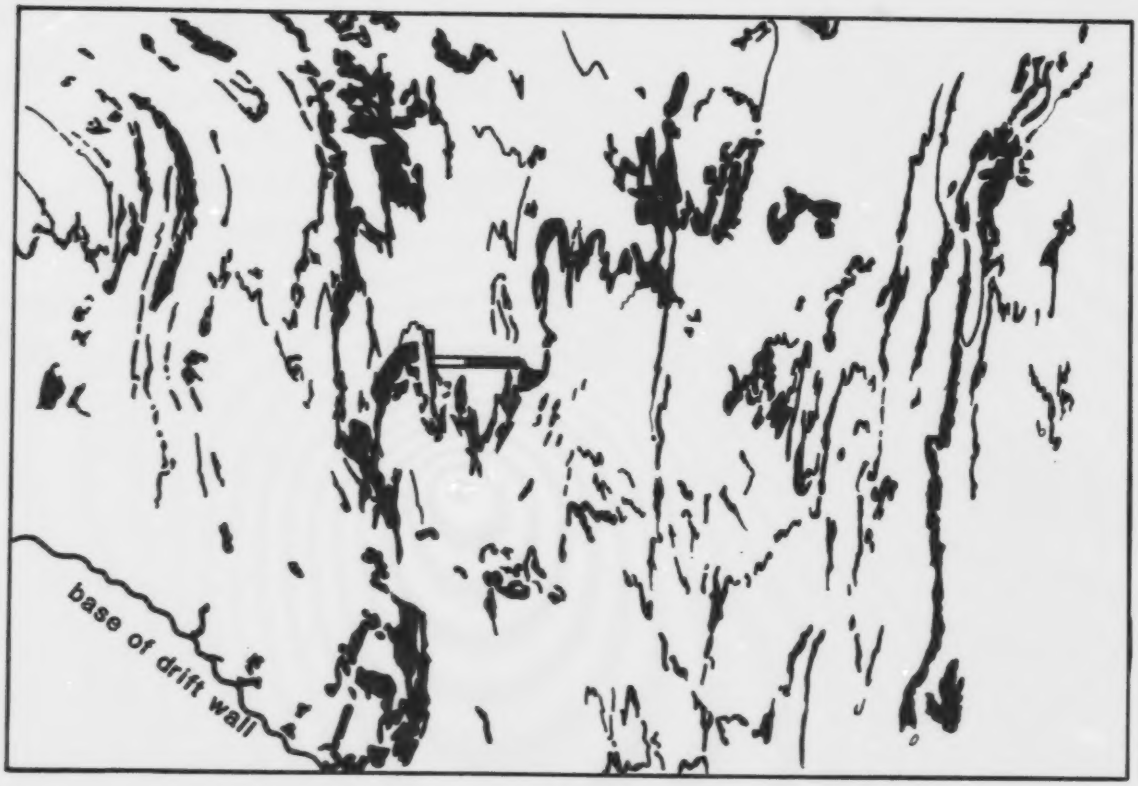
base of drift wall

Figure 12 : Deformed veins and veinlets, F Zone (Drawn from Photograph in Pye, 1951).

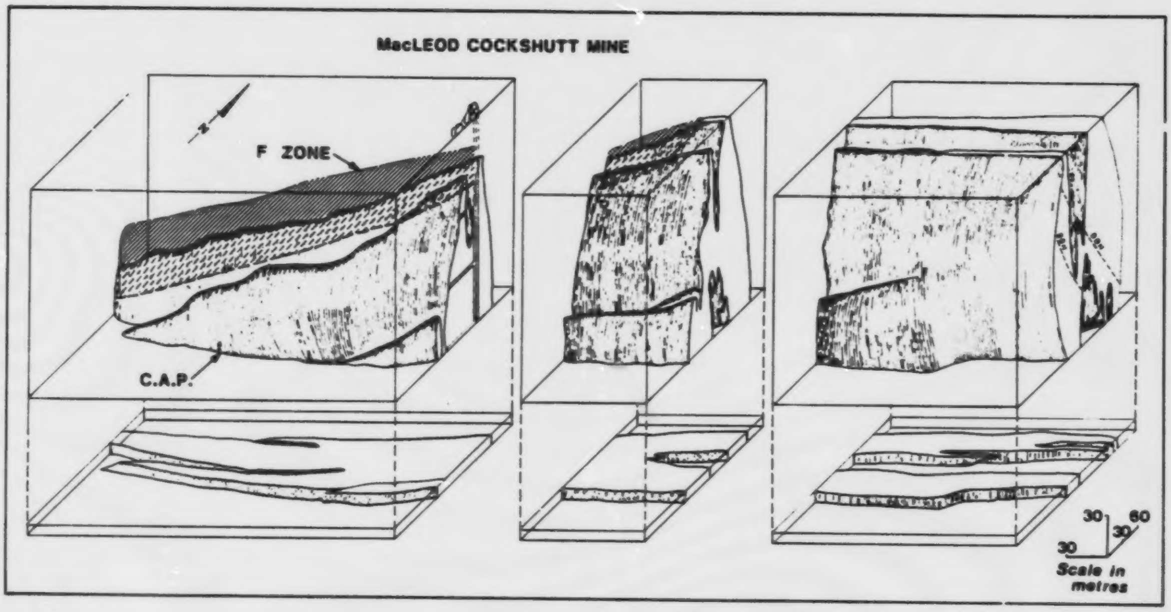
MacLEOD COCKSHUTT MINE
F ZONE
C.A.P.
30
60
30
30
Scale in metres

Figure 13 : Relationship between F Zone and folded Crowded Albite Porphyry (C.A.P.), modified from Bruce (1935).

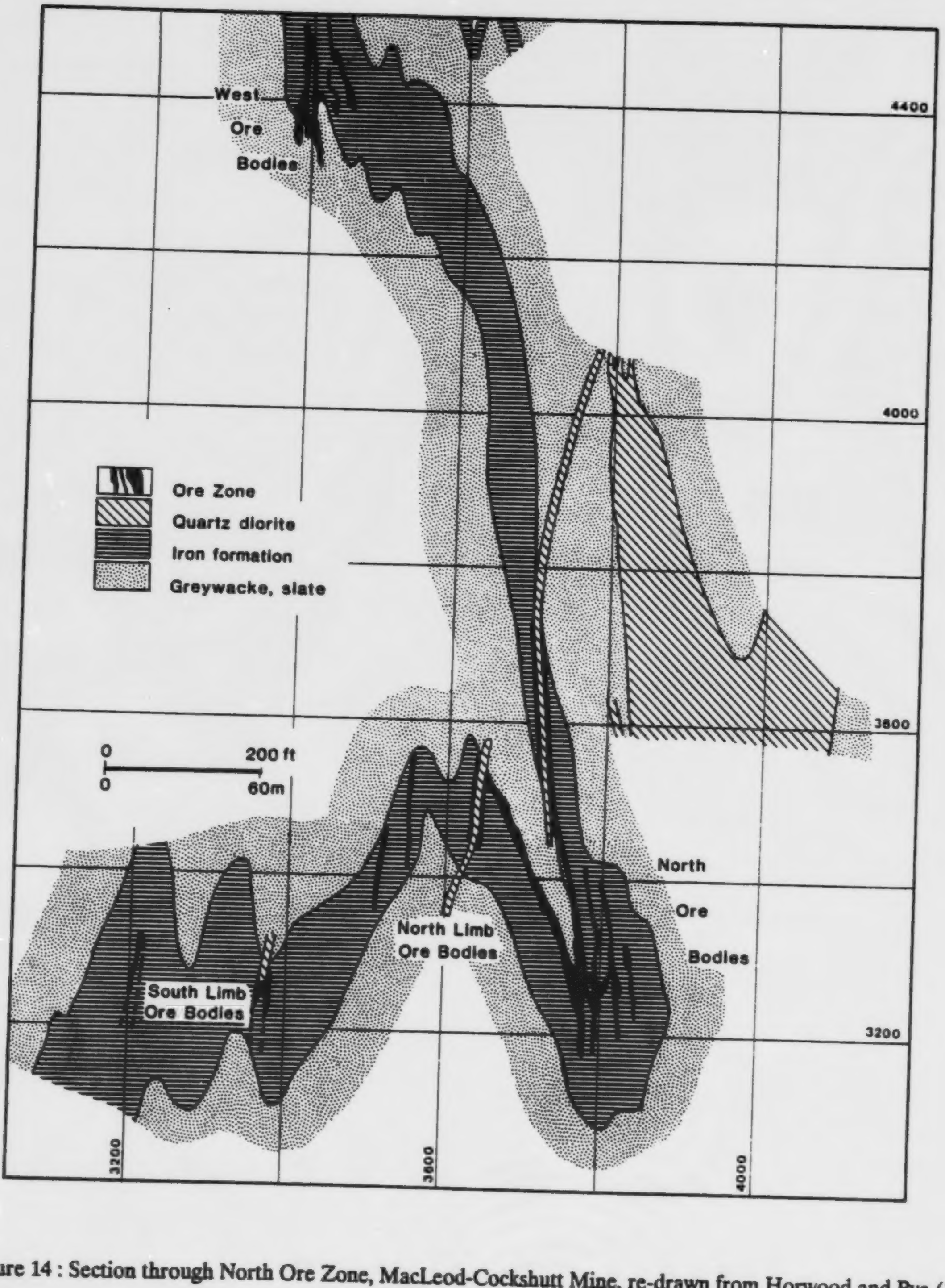
West
Ore
Bodies
4400
4000
Ore Zone
Quartz diorite
Iron formation
Greywacke, slate
3600
0
200 ft
0
60m
North
Ore
Bodies
North Limb
Ore Bodies
South Limb
Ore Bodies
3200
3200
3600
4000

Figure 14 : Section through North Ore Zone, MacLeod-Cockshutt Mine, re-drawn from Horwood and Pye (1951).

6.2 **Iron formation-hosted quartz vein and sulphide zones:** A number of deposits of this type comprise the North Zone of the Hardrock and MacLeod-Cockshutt Mines, consisting of irregular lenses of sulphide and quartz veins within deformed banded iron formation. Mineralized zones (Figure 14) either cut across the BIF in fold hinges or parallel stratification on fold limbs, where dips are steep, following the regional westerly plunge (20-40^{o}) (Horwood and Pye 1951, p.35). Production from this type of ore was approximately 3.36 million tonnes at 7.7 g Au/t, for a contained gold content of 26 tonnes.

The geology of the Hard Rock open stope within the North Zone is described in further detail in a later section (8.0).

6.3 **Quartz veins in deformed, massive quartz wacke or arkose:** Persistent and parallel quartz veins 5 to 15 cm in width, with numerous associated smaller veinlets, comprise the principal ore bodies of the Little Long Lac Mine (Figure 15). The veins are hosted solely by the more massive "arkose" (see description in Section 3.1.2). When the mineralized structures approach a contact with less massive greywacke, the veins die out. Horwood and Pye (1951, p.53) infer that the arkose fractured in a brittle manner, while the more ductilely deformed greywacke was unable to sustain a through-going brittle fracture. Similar features on a smaller scale are described in the Hard Rock open stope in a later section.

This style of mineralization is not rare in other gold camps. Notwithstanding the difference in rock types, one example in the Porcupine Camp is seen in the 55 Pit of the Hollinger Mine, where a series of stacked flows is exposed. Mineralization, in the form of late-tectonic veins, is restricted to the 99 flow, not passing into flows either above or below the 99.

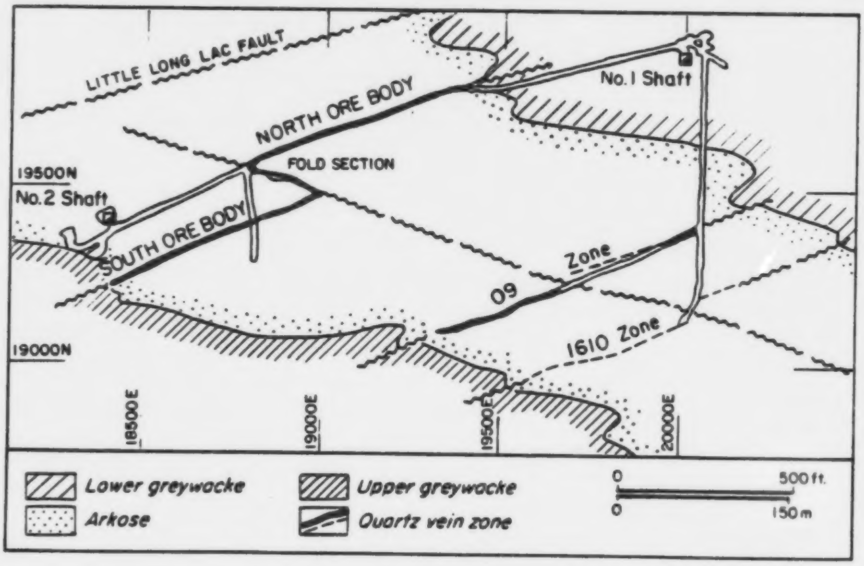
LITTLE LONG LAC FAULT
NORTH ORE BODY
No. 1 Shaft
FOLD SECTION
19500N
No.2 Shaft
SOUTH ORE BODY
09 Zone
1610 Zone
19000N
18500E
19000E
19500E
20000E
Lower greywacke
Arkose
Upper greywacke
Quartz vein zone
0
500 ft.
0
150 m

Figure 15 : Relationship between Mineralisation and Stratigraphy, Little Long Lac Mine. Redrawn from Horwood and Pye (1951).

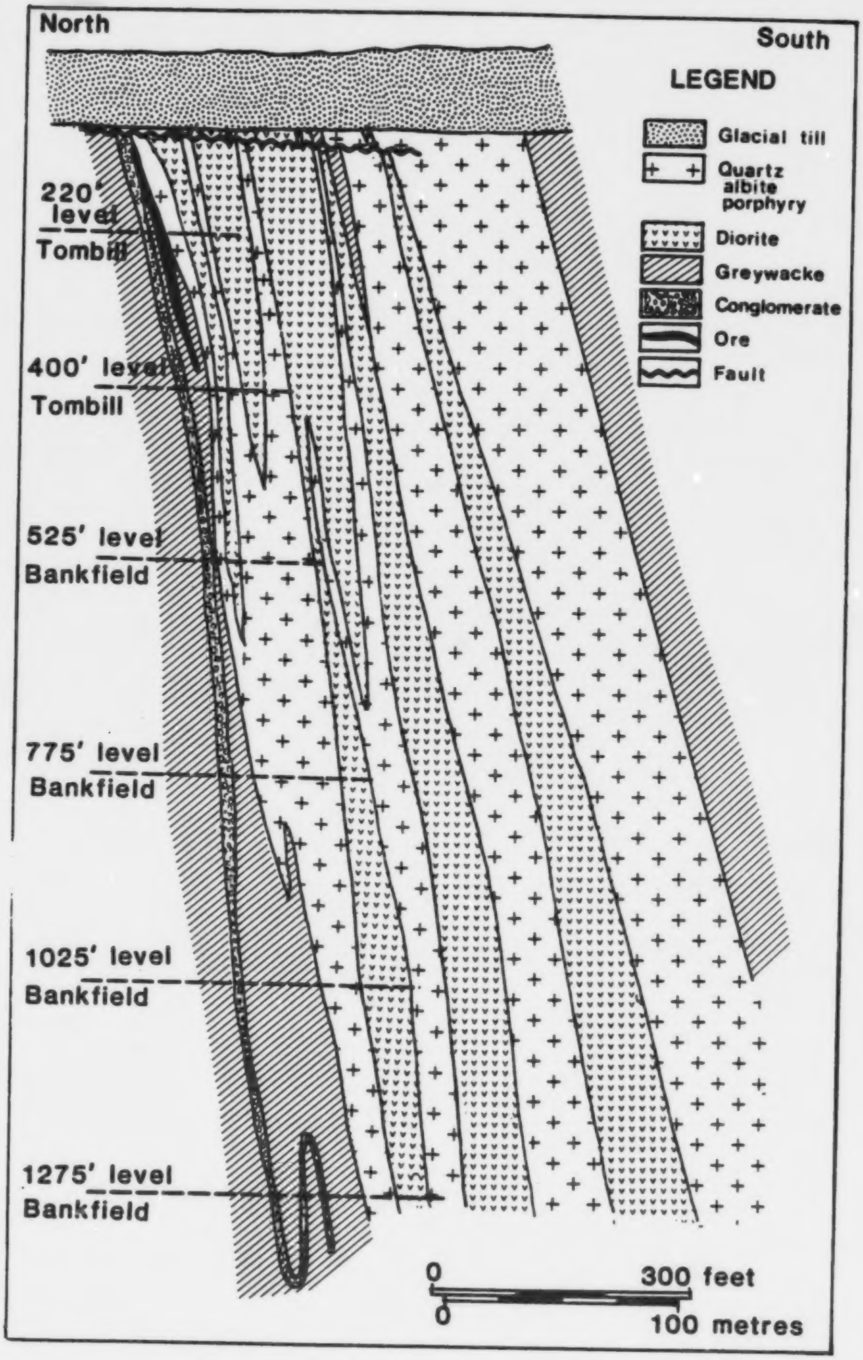
North
South
LEGEND
Glacial till
Quartz albite porphyry
Diorite
Greywacke
Conglomerate
Ore
Fault
220' level Tombill
400' level Tombill
525' level Bankfield
775' level Bankfield
1025' level Bankfield
1275' level Bankfield
0 300 feet
0 100 metres

Figure 16 : Section through the Bankfield Mine, re-drawn from Pye (1951).

The Little Long Lac Mine produced approximately 1.6 million tonnes at a grade of 11.7 ppm for a gold content of approximately 19 tonnes. Horwood and Pye (1951, p.43) report, interestingly, that many small, scattered, quartz stringers are found throughout the Little Long Lac Mine and "that these stringers become increasingly more auriferous as the assumed located of the Little Long Lac fault is approached".

6.4 **Saddle veins:** Saddle vein structures (Hodgson, in press) were encountered both in deformed wacke (Hard Rock Mine) and albite porphyry (MacLeod-Cockshutt Mine), in both cases within antiformal structures. The zone consists of a *leader* vein, parallel smaller, branching veinlets in the hanging and footwalls by . In wacke-hosted saddle veins, bedding commonly controls vein location for much of its length although veins locally follow east-striking shear fractures. The saddle reef zones also tend to plunge westerly at between 10^o and 25^o.

6.5. **Zones in the vicinity of sheared lithological contacts:** Horwood and Pye (1951) described several different contact-related deposits, of which the F Zone (described in Section 6.1) is the most significant. Of less economic importance, and also subtly different from the F Zone, are mineralized wacke-albite porphyry contacts where up to 10% of the ore is massive sulphide, chiefly pyrite with subordinate arsenopyrite, sphalerite and chalcopyrite. The sulphides are located within wacke and BIF where thin tongues of albite porphyry project upward and westward from the main intrusive mass. Where the tongues are narrowest, sulphides are also present within the intrusive rock. Horwood and Pye (1951, p.37) infer that the sulphides replace their host rock. Quartz veins are also localized along narrow zones at contacts between two intrusive rocks, hornblende diorite/gabbro and albite porphyry, as, for example, on the Roche Long Lac property, in the eastern portion of Ashmore Township (Figure 3). Here, mineralization is confined to quartz veins within narrow, sheared and fractured zones and has not, to date, proved to be economic.

At the Bankfield Mine, ore was hosted by a thin sliver of brecciated and sheared wacke adjacent to an intrusive complex, consisting of hornblende-diorite, intruded by albite porphyry (Figure 16). The zone had a strike length of 650 metres and ranged in thickness from 30 cm to 6.5 m, averaging 3 metres.

6.6. **Zones wholly within extrusive rocks**: A number of subeconomic auriferous zones are hosted solely by quartz veins within sheared volcanic rocks. Most tend to be lenticular or boudinaged, ranging in thickness from a few centimetres to two or three metres, and persistent along strike: some veins of this type have been traced in excess of 350 m. These veins have, to date, not been of economic significance.

6.7. **Zones wholly within intrusive rocks**: On the Mosher Long Lac property a zone 600 m long and approximately 2.5 m wide is wholly hosted by a sill-like body of albite porphyry. The low gold content rendered the zone uneconomic in the early 1930's (Pye 1951). On the Talmora property, quartz veins and stringers of two generations, based upon crosscutting relationships, are hosted by hornblende diorite or gabbro. Mineralized zones generally consist of a *main* or *leader* vein 1 metre thick, flanked by narrow stringers of limited lateral and vertical extent (Pye 1951, p.54).

6.8. **Zones within major faults**: As mentioned previously in the section on structural geology of the Geraldton Camp, the Barton Bay Lithotectonic Zone, in which all known significant mineralization is hosted, is bounded in general terms, to the north by the Little Long Lac Fault and to the south by the Bankfield-Tombill Fault Zone (Figure 3). No ore has been found in either fault, although grades in veinlets increase toward the Little Long Lac fault (see section 6.3). On the McLellan Property, gold mineralization is hosted by the BTF (Figure 17). Gold is associated with pyrite in sheared wacke, slate and, as revealed by recent trenching (1983, Roxmark Mines Ltd.), deformed gabbro. Diamond drilling in the 1930's suggested that gold mineralization is present along a strike length of at least 650 m, but only to a depth of 30 m. Underground development substantiated this assessment, and mineralization proved to be sub-economic (Pye 1951, p.118).

In summary, gold mineralization in the Geraldton Camp is present within every rock type in the area, in sediments and volcanics that comprise the supracrustal component of the greenstone belt, and in to intrusive rocks, both gabbro and younger felsic intrusions. The only exce[tions are diabase dikes, which are not found to host gold mineralization. The style of each zone is controlled by a combination of host rock *reactivity*, both physical and chemical, and the characteristics of the stress field that prevailed during the mineralizing event(s), as recognized by Pye (1951) and Horwood and Pye (1951) in their attempts to classify the Geraldton deposits.

The reaction of rocks to deformation is controlled by a number of variables, which in turn determine the ability of a rock to accept mineralization within a zone of rocks subject to a protracted, complex deformational history, many local heterogeneities will be present which will affect the degree and type of strain, and style and degree of deformation. For example, fabrics formed within a specific unit will depend upon the strain rate and the rheology of the rock, and as a result, ore bodies can be lithology specific; for example at the Little Long Lac Mine (Figure 15) where the *arkose* is mineralized by veins and the surrounding greywacke is relatively barren, brittle failure of the arkose, which permitted vein formation has localized fluid flow and resulting mineralization. A regime of relatively ductile deformation in the enclosing wacke did not permit dilational fracturing and the wacke is therefore, not, in this particular case, mineralized.

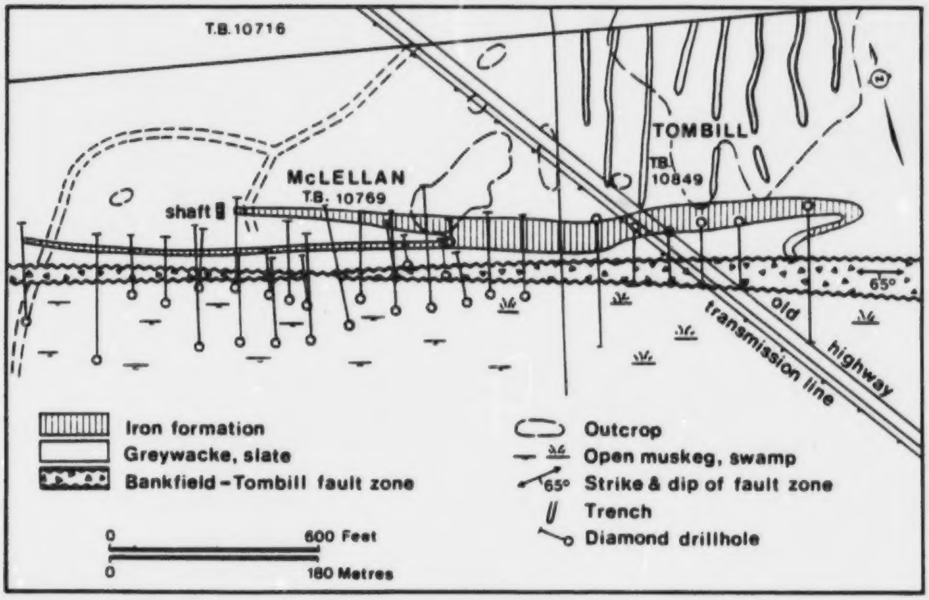
T.B. 10716
McLELLAN
T.B. 10769
shaft
TOMBILL
T.B. 10849
65°
old highway
transmission line
Iron formation
Greywacke, slate
Bankfield-Tombill fault zone
Outcrop
Open muskeg, swamp
65° Strike & dip of fault zone
Trench
Diamond drillhole
0
600 Feet
0
180 Metres

Figure 17 : Mineralisation hosted by major fault (Bankfield-Tombill), McLellan Property, redrawn from Pye (1951).

In each mineralized zone described above, the host rocks commonly differ from their barren counterparts in unmineralized zones by being more sheared and/or fractured, i.e., veined. The repercussions of this observation will be considered at later stages in this report, although it suffices to say that there is a direct relationship between degree of fracturing in a rock and amount of fluid that can flow into and through the rock. Indeed, the permeability of a rock is a function of the third power of the fracture width and is inversely proportional to the spacing of fractures (Snow 1969).

7.0 Timing of Mineralization

From the foregoing it is possible to erect a paragenetic sequence of geologic events which gave rise to gold mineralization at Geraldton. Pye (1951) and Horwood and Pye (1951) describe detailed mineralogical parageneses based upon petrographic analysis. These vary somewhat from deposit to deposit and are not considered here. Detailed mineralogy of the Hard Rock North Zone is described in a later section.

The geologic history of the Geraldton camp commenced with formation of the supracrustal pile, comprising volcanic and sedimentary rocks. Mafic and possible minor ultramafic intrusions are the first mappable units to intrude the supracrustal rocks. Pye (1951) noted that the mafic intrusions are localized by hinges of isoclinal folds in the volcano-sedimentary package. He suggests, therefore, that intrusion was in part guided by already deformed rocks. Lavigne (1983) emphasised the spatial association between one apophysis of the mafic body and the BTF, implying localization of the intrusion along the fault zone. The alternative hypothesis, that fold wavelength and localization of a major structure would both be controlled by the presence of mafic intrusive rocks, receives little support from field evidence. Consequently, in establishing a paragenetic sequence, Figure 18 (from Macdonald 1984a), folding and regional dextral shear are hypothesized to have commenced prior to mafic intrusion. Pye (1951) and Horwood and Pye (1952) provide evidence for pre-, syn- and post mineralization motion on the BTF, for which therefore continual deformation is shown in Figure 18, with the implication that the dominant deformation style is dextral shear.

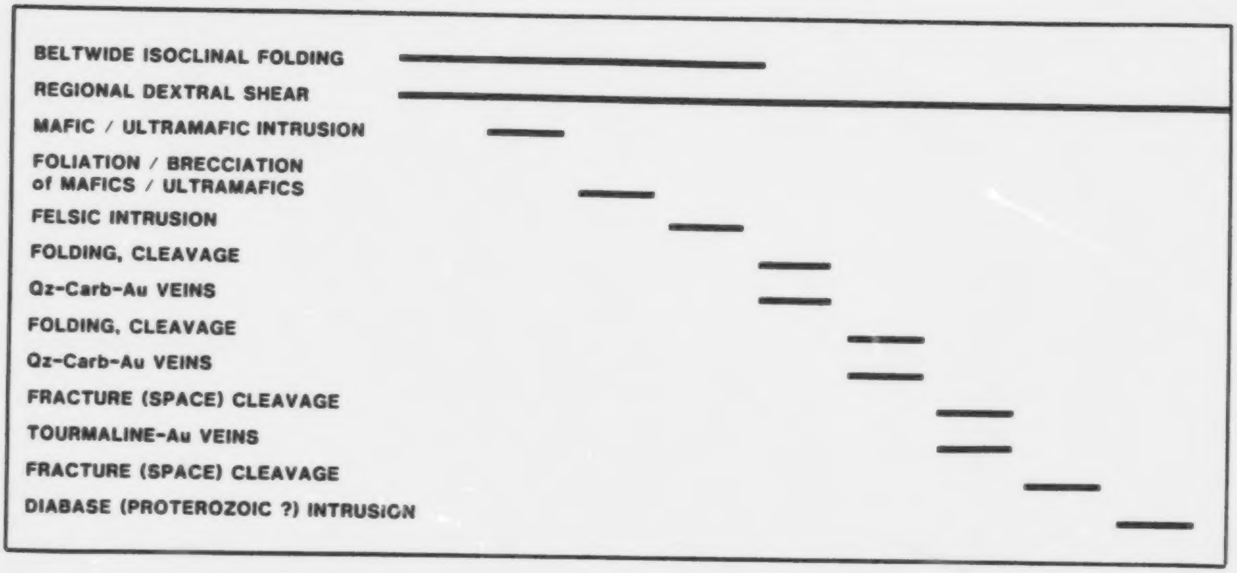

Figure 18 : Post-Sedimentation/Volcanism Paragenetic Sequence of geological events in the Geraldton Camp (Macdonald, 1984a).

Anglin (M.Sc. candidate, Memorial University, oral communication 1983) demonstrated the presence of clasts of gabbro in dikes of felsic intrusive rock (albite and albite-quartz porphyry). Strain fabrics in the two rocks were not identical. Field mapping by Anglin suggested that the gabbro had experienced some deformation prior to being included within the felsic rocks. Felsic intrusive rocks contain at least two penetrative fabrics, visible in exposures with vertical faces are exposed, e.g. underground, and in thin section (Figure 19). Problems with mapping these fabrics are compounded for the field geologist by the fact that they tend to be subparallel or have a small acute angle between one another, generally within 10^{o} to 15^{o}. Only where an earlier fabric has been folded and the hinge of the folded fabric is visible, are cross-cutting relationships observed. At least two fabrics are also observed in wacke in the Geraldton Camp (Figure 20), subparallel to, and therefore possibly related to, those in the porphyry. Locally the youngest penetrative fabric displays a prominent pressure solution texture (e.g. Figure 10) axial planar to minor intrafolial folds and best developed within silty horizons.

Each fabric may also host auriferous quartz + carbonate veins, indicating that the fabric was dilated either during or after development and filled by vein material. Earliest veins are folded and cut by younger veins. These relationships are indicated, in simplistic form, in the paragenetic sequence, Figure 18. The final auriferous vein set consists of tourmaline + quartz fracture filling a fracture (space) cleavage that cuts obliquely across earlier quartz-carbonate veins. Figures 21 and 22 demonstrate the relationship between three auriferous vein sets at Porphyry Hill on Hard Rock property.

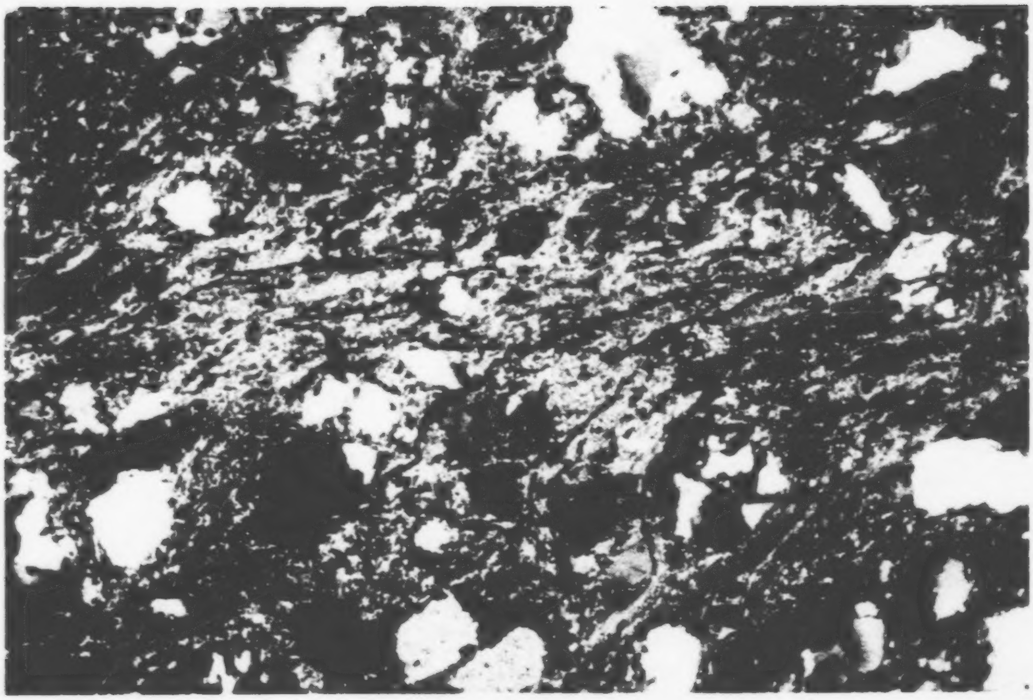

Figure 19 : Photomicrograph of porphyry with two penetrative fabrics, Magnet Mine, Geraldton. Field of View is 5 mm.

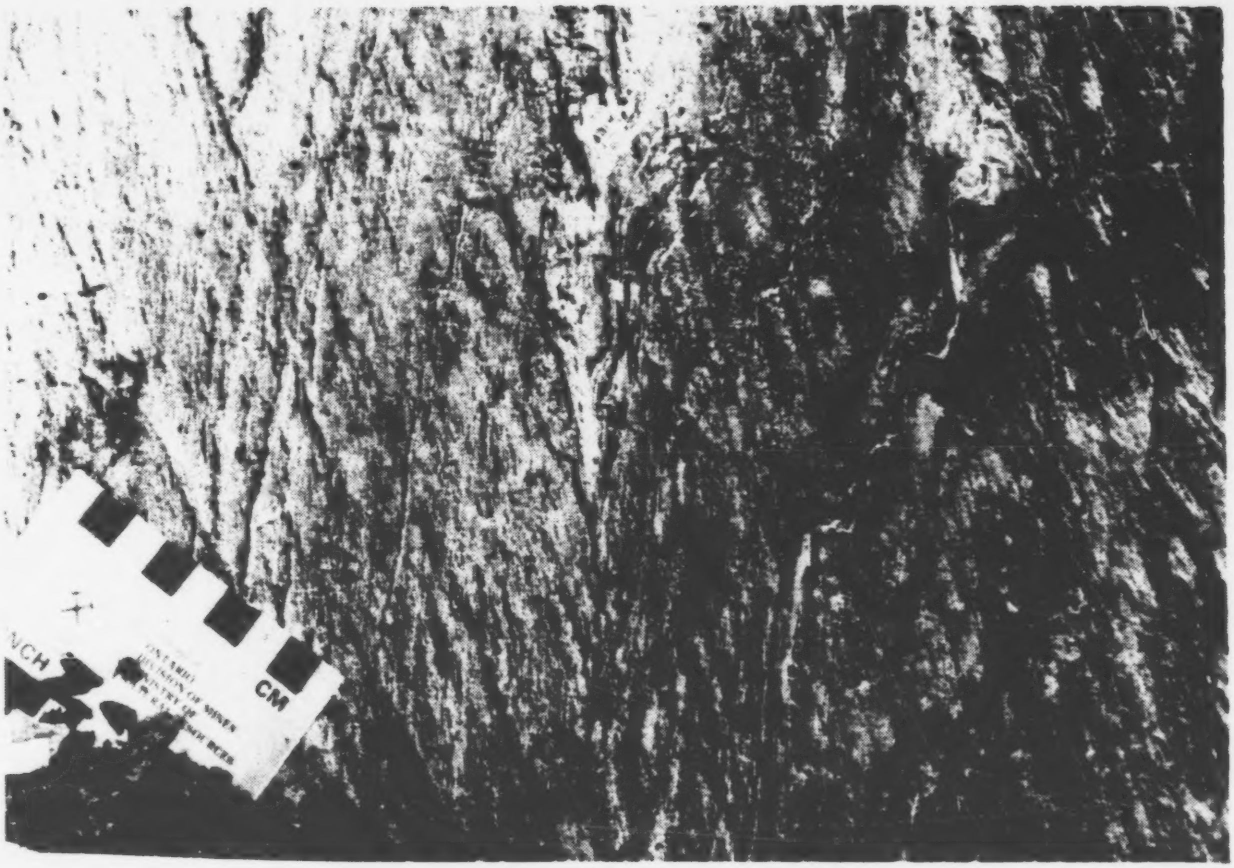
NCH
CM
ONTARIO
DIVISION OF MINES

Figure 20 : Two fabrics in wacke, Mosher Property, Geraldton.

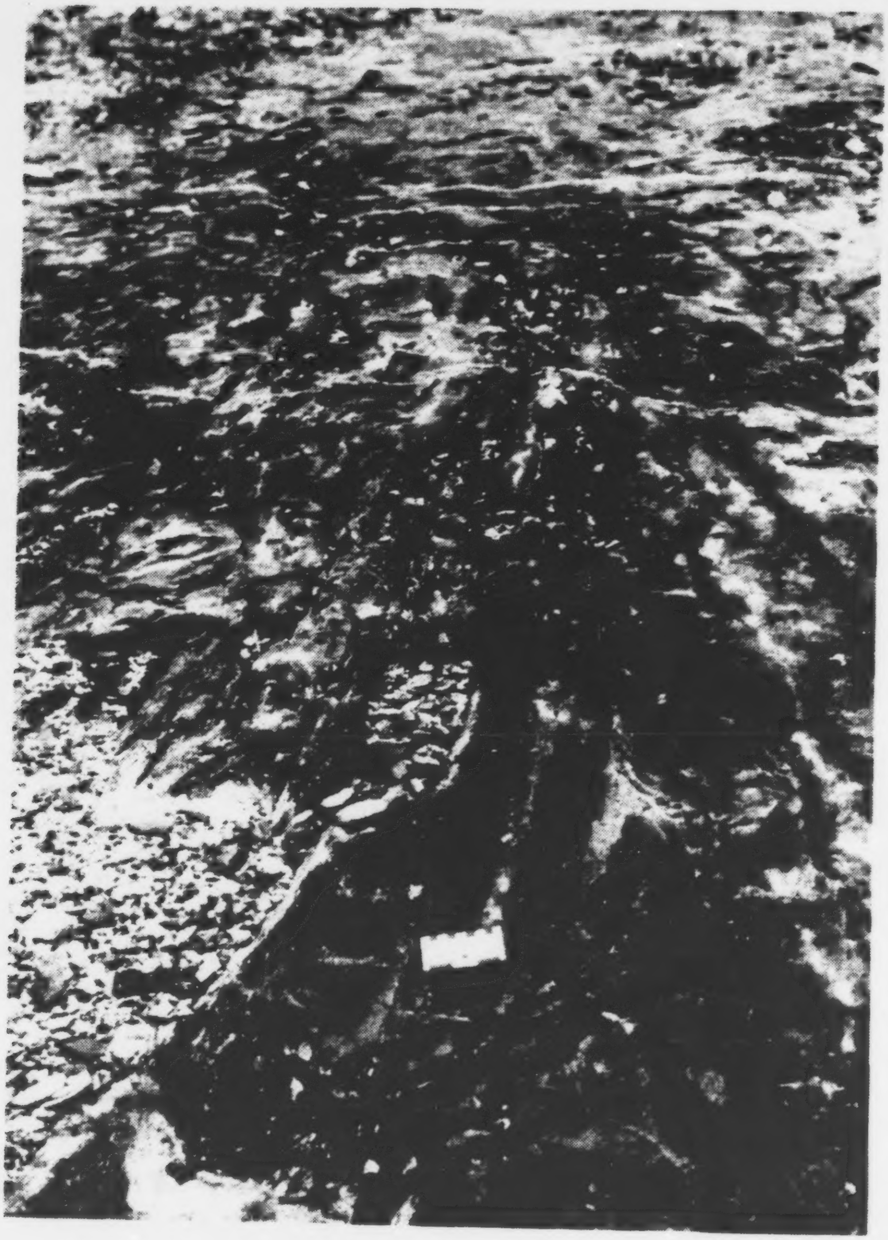

Figure 21 : Early, folded quartz-carbonate vein (foreground), cut by non-folded quartz-carbonate vein, Porphyry Hill, Hard Rock Mine, Geraldton.

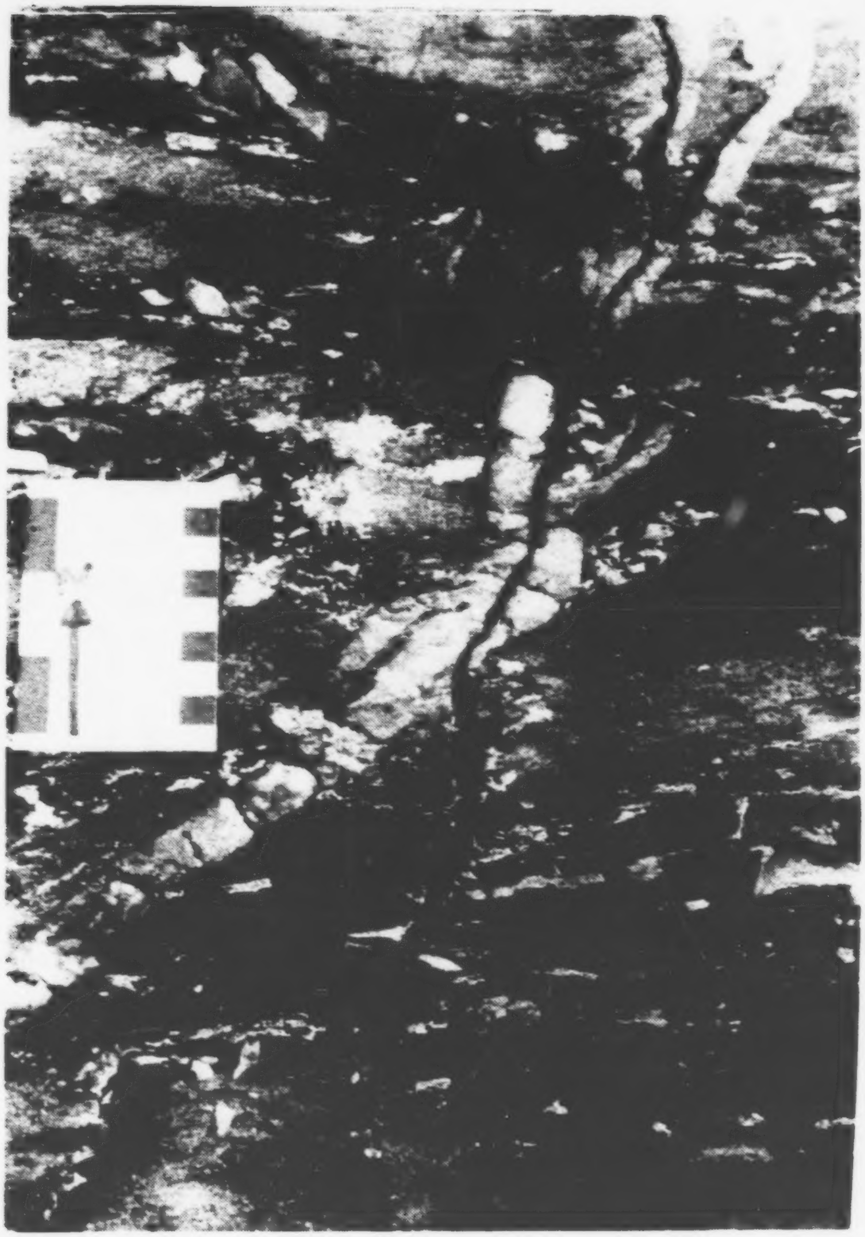

Figure 22 : Tourmaline veinlet cutting non-folded quartz-carbonate vein (Figure 21), Porphyry Hill, Hard Rock Mine, Geraldton.

The gold-bearing veins are, in turn, cut by fracture cleavages which are locally filled by barren quartz + carbonate veins. Diabase dikes, striking generally north are the last rock types to be introduced. Even the late dikes, probably Proterozoic, are offset by some of the final movements along the Bankfield-Tombill Fault (See Maps in Pye 1951; Horwood and Pye 1951). In the Bankfield Mine, a diabase dike deviates from its north strike intruding along the fault zone in excess of 800 m until resuming its more characteristic north strike. This may suggest that the fault was active during dike emplacement as well as afterwards.

The paragenetic synopsis given here is, of necessity, brief, being the subject of other ongoing studies (Lavigne, in preparation; Anglin, in preparation; Buck, in preparation).

In summary, therefore, not only is mineralization at Geraldton hosted by all available lithologies, it also appears to be localized in structures that developed during a protracted period of deformation and intrusive activity. This observation is by no means unique to the Geraldton Camp. At Red Lake, for example, ore structures transect both extrusive (2990 Ma) and intrusive rocks (2718 Ma); at Timmins, similarly, ore zones are hosted by, and cut, extrusive rocks (older than 2725 Ma) and intrusions (2685 Ma) (Marmont 1984, Colvine 1985). An important question that has to be addressed at these gold camps in general, and particularly at Geraldton, is whether field evidence supports either (a) multiple periods of mineralization over several tens of millions of years or longer, or (b) one period of mineralization during the latter stages of the geological evolution of the greenstone belt. In addition, gold originally resident in one site, may also be remobilized episodically into subsequent sites.

8.0 Hard Rock Open Stope - Geology

In early 1982, the Mineral Deposits Section of the Ontario Geological Survey commenced a comprehensive and directed effort to evaluate the factors controlling gold mineralization in Ontario. One gold mineralization type included in this for investigation was the gold-BIF association. It had been asserted elsewhere that various BIF facies contained inherently elevated gold values, i.e. synsedimentary gold which could serve as a protore for an economic deposit (e.g. Ridler 1970, 1976; Karvinen 1981). The Geraldton gold camp was considered to contain mineralization that showed a prominent association with BIF (e,g. Boyle 1979) and Geraldton was selected as the initial site to test hypotheses regarding the Au-BIF relationship (see Figure 2).

Accordingly, in June 1982, the author visited the Geraldton area and was introduced to the geology by J.K. Mason, Resource Geologist, Thunder Bay, MNR (now Resident Geologist, Geraldton, MNDM). Based upon an initial overview of the Geraldton Camp, it was considered that an Open Stope on the Hard Rock property afforded the best potential for addressing the BIF-Au problem. Less than 1 metre of silty and clayey overburden had to be removed, using a D3 Caterpillar tractor and a Wajax Mark III power pump.

BIF at Geraldton is comprised of 1-5 cm beds of magentite and, locally, hematite, alternating with rare beds of silica chert) and/or fine grained clastic sediments (shale to wacke; Horwood and Pye 1951). The chert is most commonly dark in colour but is locally red (jasperitic). The BIF in the Geraldton area is found within a wacke package, contrasting with BIF hosted by volcanics in the Pickle Crow deposit (Corking 1948). Detailed petrographic descriptions of BIF are given in Horwood and Pye (1951). The chert component of BIF is relatively rare in the Geraldton area, contrasting with typical

"Algoman": type BIF which are characterized as"thin-banded chert or quartz and iron oxides, silicates, carbonates and sulphides" (Gross 1965, p.74).

Barrett and Fralick (1985) described three measured sections of BIF in the Beardmore Geraldton Belt: (a) the Leitch Mine at Beardmore; (b) Boston Bay Island at Geraldton (Figure 3); (c) the Hutchinson Lake area, approximately 10 km northeast of Geraldton (Beakhouse 1984). They observed that the BIF consists of "dark, laminated magnetite (chemical component) with common intercalations of siltstone/sandstone (clastic component) which range in thickness from sub-millimetres to tens of centimetres" (Barrett and Fralick 1985). Sedimentary structures in the clastic rocks suggest deposition of the strata, together with some magnetitic material, by turbidity currents. A grain size analysis suggested that variations in coarseness and thickness of clastic beds in different sections within the BIF reflected proximity to sediment source. Figure 23 shows photomicrographs of BIF from the Hutchinson Lake area at various magnifications. The microlaminations visible within meso-bands of magnetite-rich material are similar to those of the Hammersley Basin in Western Australia, attributable to annual varving (Trendall and Vlackly 1970). Barrett and Fralick (1985) suggest that the microlaminations in the Geraldton BIF may also be a result of annual sedimentary processes. Some caution must be exercised in measuring sections in areas of intense bedding transposition and grain size reduction, as seen in portions of the Geraldton area. This point will be addressed further below. The reader who requires further details of the petrography of BIF in the Beardmore-Geraldton greenstone belt, in general, can refer to Barrett and Fralick (1985) and in the Geraldton area, in particular, to Pye (1951), Horwood and Pye (1951), Beakhouse (1984) and Anglin (in preparation).

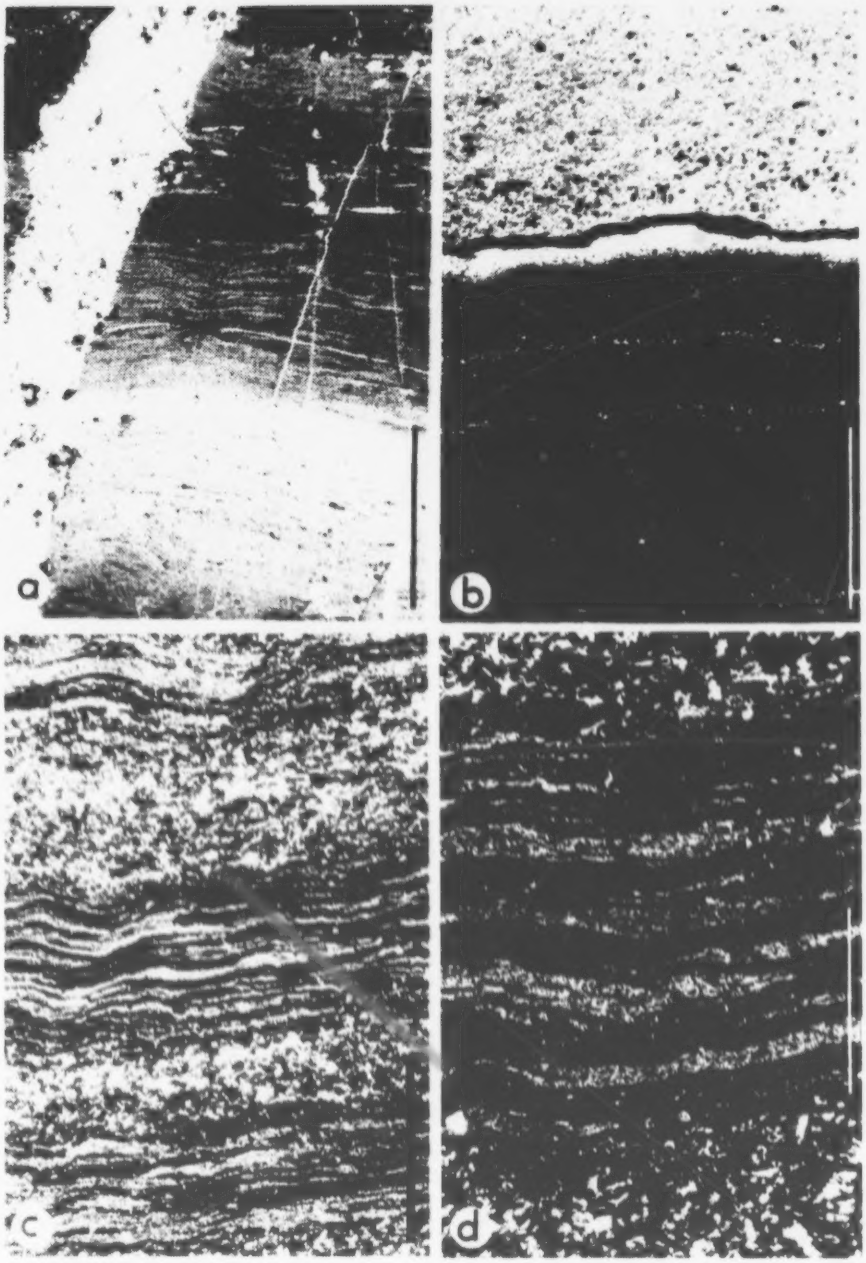

Figure 23 : Photomicrographs of Banded Iron Formation from Barrett and Fralick (1985); see text for details.

8.1 Field Relationships in the Hard Rock Open Stope

The following section describes observations made from mapping the Hard Rock open stope in 1982 and 1983. This information is also summarized in Macdonald (1982, 1984a and in press). The interested reader may also wish to refer to geological descriptions, plans and sections in Horwood and Pye (1951) and sections in Ferguson (1967, Map. P. 437).

The Hard Rock open stope (HRos) is located at the western margin of the Hard Rock property (Figure 24) approximately 150 m south of Highway 11.

A geological map of the HRos is included with this report (Map, back pocket). The map shows the geology around the stope rim and on the upper surface of available pillars within the stope. Also shown are outcrop sketches and drawings from photographs illustrating some of the key geological relationships. These are referred to in the text.

Figure 25 is a sketch of the HRos geology (Map, back pocket) superimposed upon the low altitude air photograph of the HRos (Figure 24). The iron formation unit (IF), defined here in field terms as a mixed clastic-chemical sediment (magnetite) where the iron oxide component comprises greater than 25% of the rock, is approximately 15 m in width at the eastern and western extremities of the stope. The unit is thicker, up to 30 m, in the central region, and defines a crude Z shape, easily visible in Figure 24. Contacts to the north and south with wacke and siltstone are relatively sharp. Within 5 m of the contact, the wacke unit may locally contain up to 20% magnetite. The contact between the two units tends to be highly disrupted and is described in further detail below.

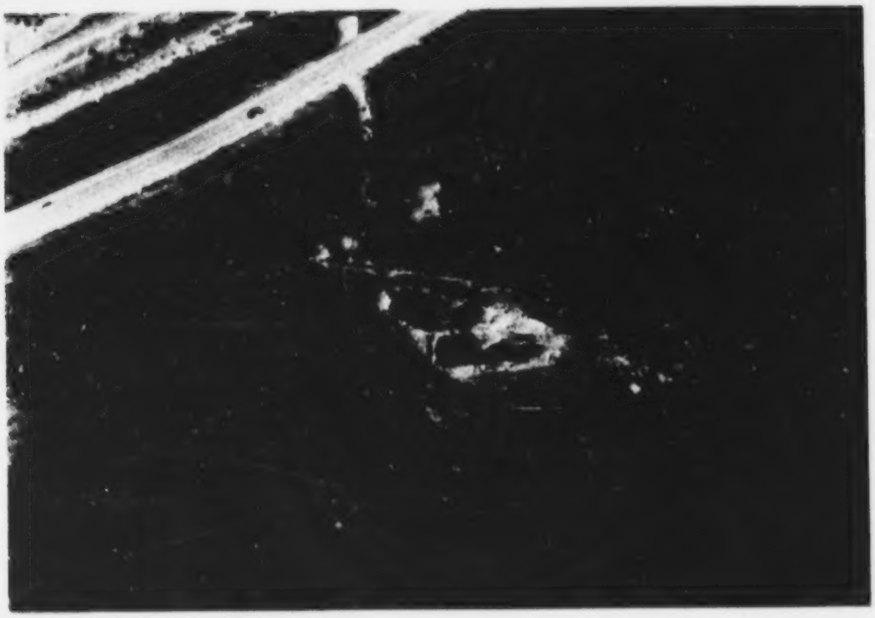

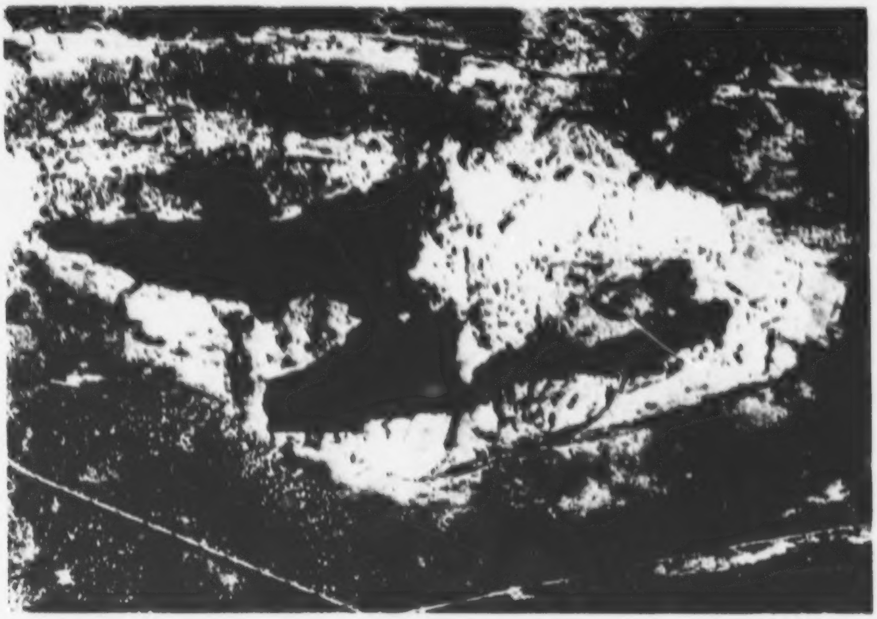

Figure 24a, b : Hard Rock Open Stope, Geraldton, South of Highway 11, automobile for scale. Property boundary with MacLeod-Cockshutt Mine is located approximately 50 m west of open stope (Photographs aligned with north up). Ore body plunged to the west.

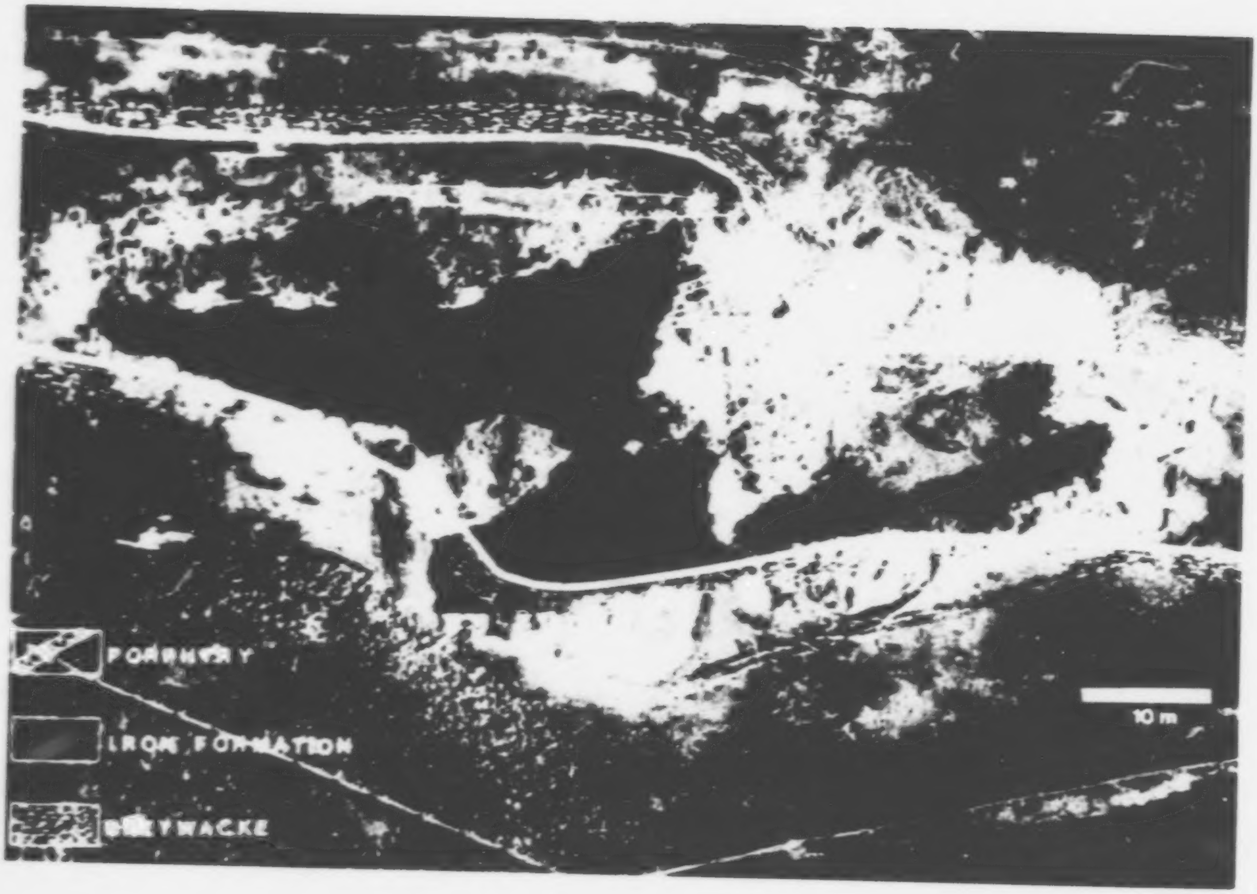
PORPHYRY
IRON FORMATION
GREYWACKE
10 m

Figure 25 : Geological Sketch Map, Hard Rock Open Stope, overlain upon Figure 24b.
See map in back pocket for more detail.

Within the IF are highly folded rocks described in Figure 25 as *porphyry*. While the rocks exhibit a porphyritic (*sensu lato*) texture of relict plagioclase and amphibole in a fine grained altered matrix, no genetic origin for the rock is implied at this stage. The porphyritic rock unit is described in further detail below.

8.1.1. Iron Formation

Figure 26 shows a typical ice-polished outcrop of IF at the HRos. The rock consists of alternating mesobands of magnetite-rich material (dark) and clastic material, variably altered by ankerite (buff colour). In this case note that the mesobands, generally 0.5 cm thick, tend to be thicker in fold hinges. An adjacent IF unit with alternating mesobands that are thinner, 0.1 to 0.2 cm, displays folds of considerably smaller amplitude and wavelength (Figure 27).

A second, but minor, component of IF exposed in the HRos consists of red chert mesobands interbedded with magnetite and containing little clastic material. In outcrop, the unit is highly deformed (Figure 28), even where in stratigraphic contact with IF containing a clastic component and exhibiting apparently more coherent strain; for example the exposures in Figures 27 and 28 are in stratigraphic contact. The effects of stress upon different lithological components of the IF, and the contrasting strain shown by other units in the HRos will be emphasized below.

No attempt has been made in this study to produce a stratigraphic section of the IF from exposures in this location, due to the degree of deformation. For example, Figure 29 shows the hinge region and one flank of a minor fold in IF. In the apical region of the fold below the scale card, approximately 15 mm-thick magnetite microbands are easily visible. On the flank of the fold, however, the microbands merge into only three microbands. One metre further along the fold flank, only one magnetite microband is present. Thus, while the rock apparently may be a well-preserved "bedded" unit, strain has been manifested as intense bedding-plane parallel transposition or stretching, destroying all vestiges of original bedding. A detailed sedimentological study in this location is therefore not considered appropriate.

Table III lists representative samples of relatively unaltered BIF, based upon field criteria, such as absence of veins or other secondary features. All BIF in the immediate vicinity of Geraldton contains a small amount of red-weathering carbonate, of ankerite to ferroan dolomitic composition. Carbonate is most prominent in siltstone bands and in fractures cutting all bands in the IF (Figure 30). Rocks some distance from the mineralized Barton Bay Lithotectonic Zone (BBLZ) contain considerably less red-weathering carbonate, and Pye (1951) noted that on approaching mineralization, secondary carbonate and other minerals replace the wallrock. While it is possible that minor iron-bearing carbonate constituted an original synsedimentary component of the BIF, the demonstrable secondary nature of the bulk of the Fe-carbonate requires consideration that perhaps all of the red-weathering carbonate in the immediate vicinity of Geraldton is secondary. As a result, all the rocks from the Geraldton area, may have experienced some degree of alteration. If all the carbonate is secondary, the degree of alteration may be monitored by comparing $CO_3^{=}$ content in Table III. Notable features from Table III include the high iron contents of the rock, generally >20%, low sulphur (<1%), low arsenic (<50 ppm), low antimony (<30 ppm), and low gold (<10 ppb).

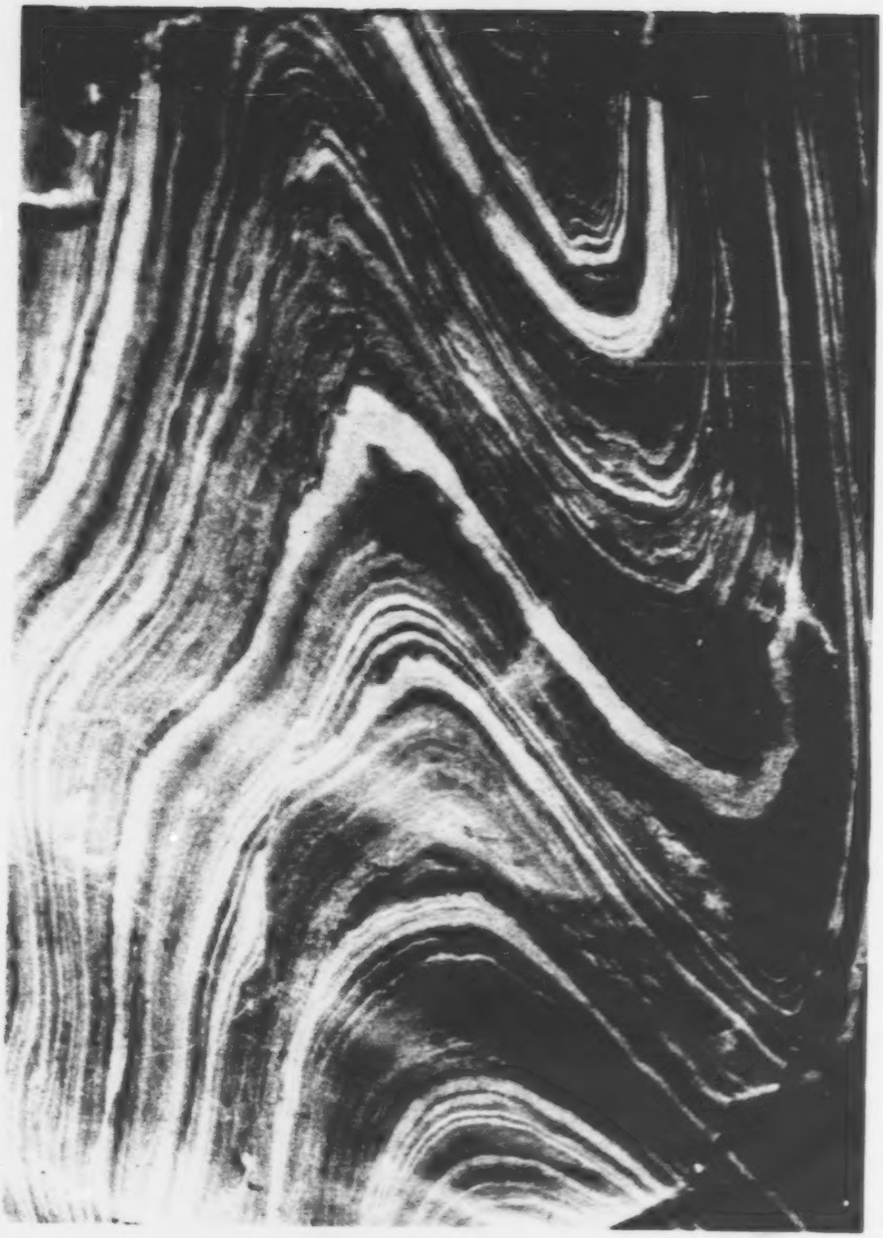

Figure 26 : Ice polished surface of iron formation, Hardl Rock Open Stope, Geraldton. Long field of view is 20 cm. Light bands are silt-rich, dark bands are magnetite-rich.

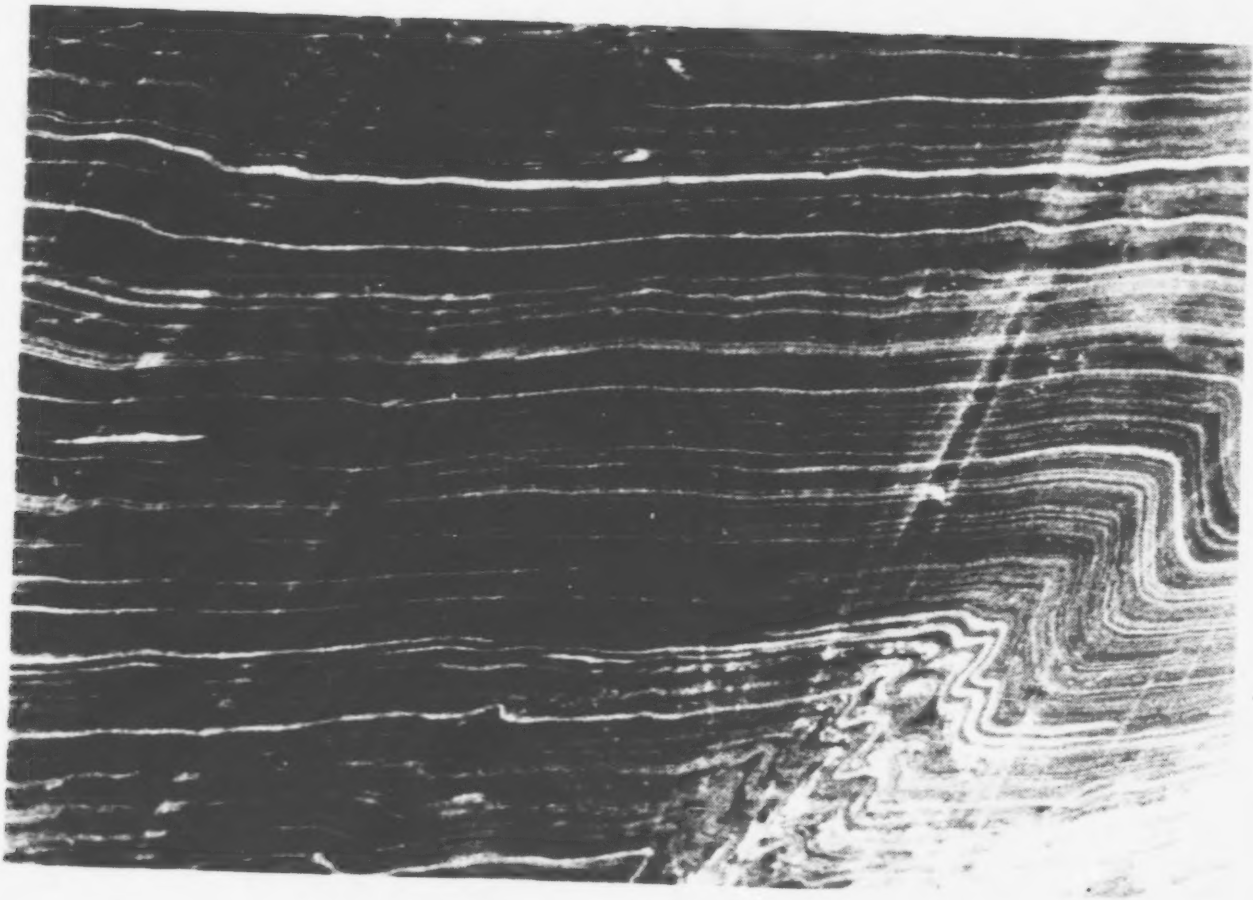

Figure 27 : Thin, alternating bands of silt and magnetite, Hard Rock Open Stope, Geraldton. Field of view 20 cm.

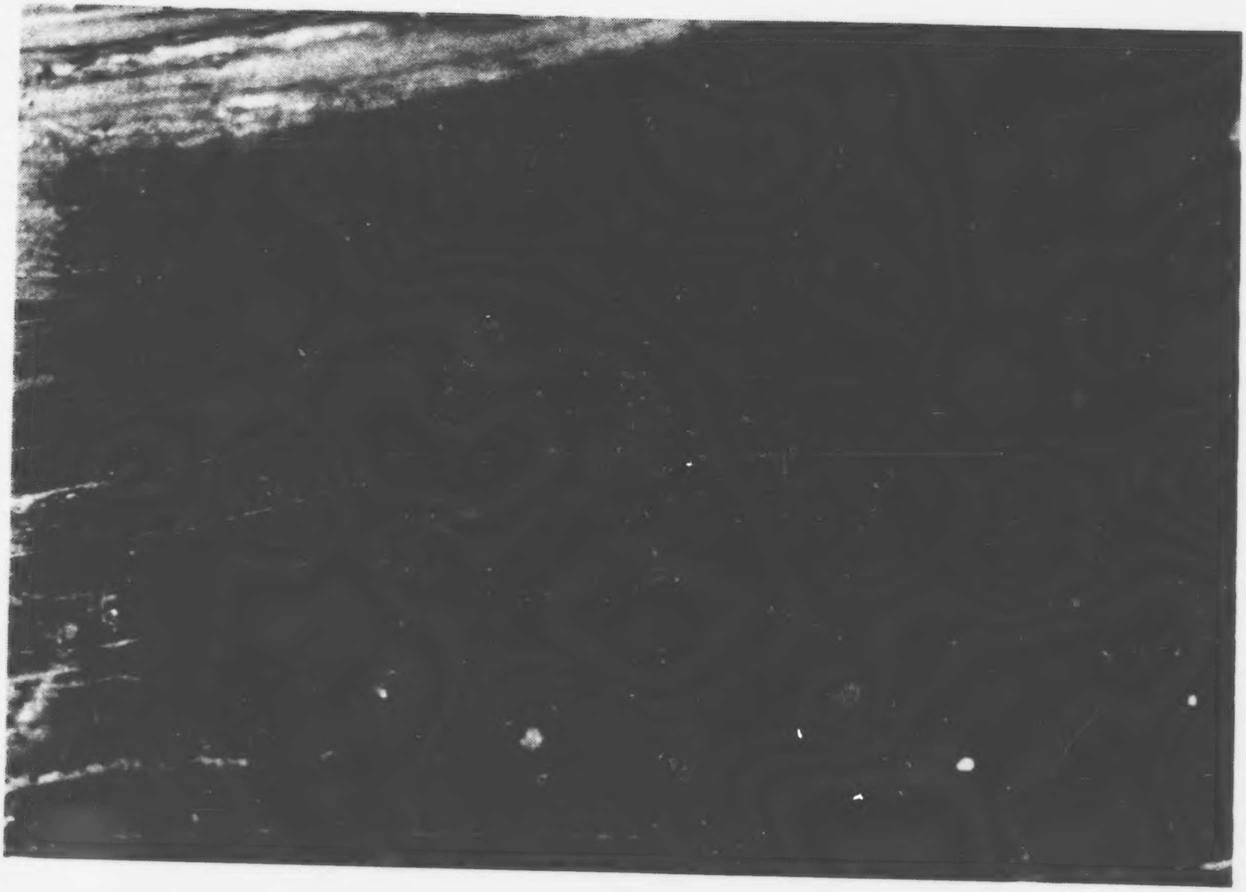

Figure 28 : Contact between silt/magnetite iron formation and red chert/magnetite iron formation, Hard Rock Open Stope, Geraldton. Field of view 20 cm.

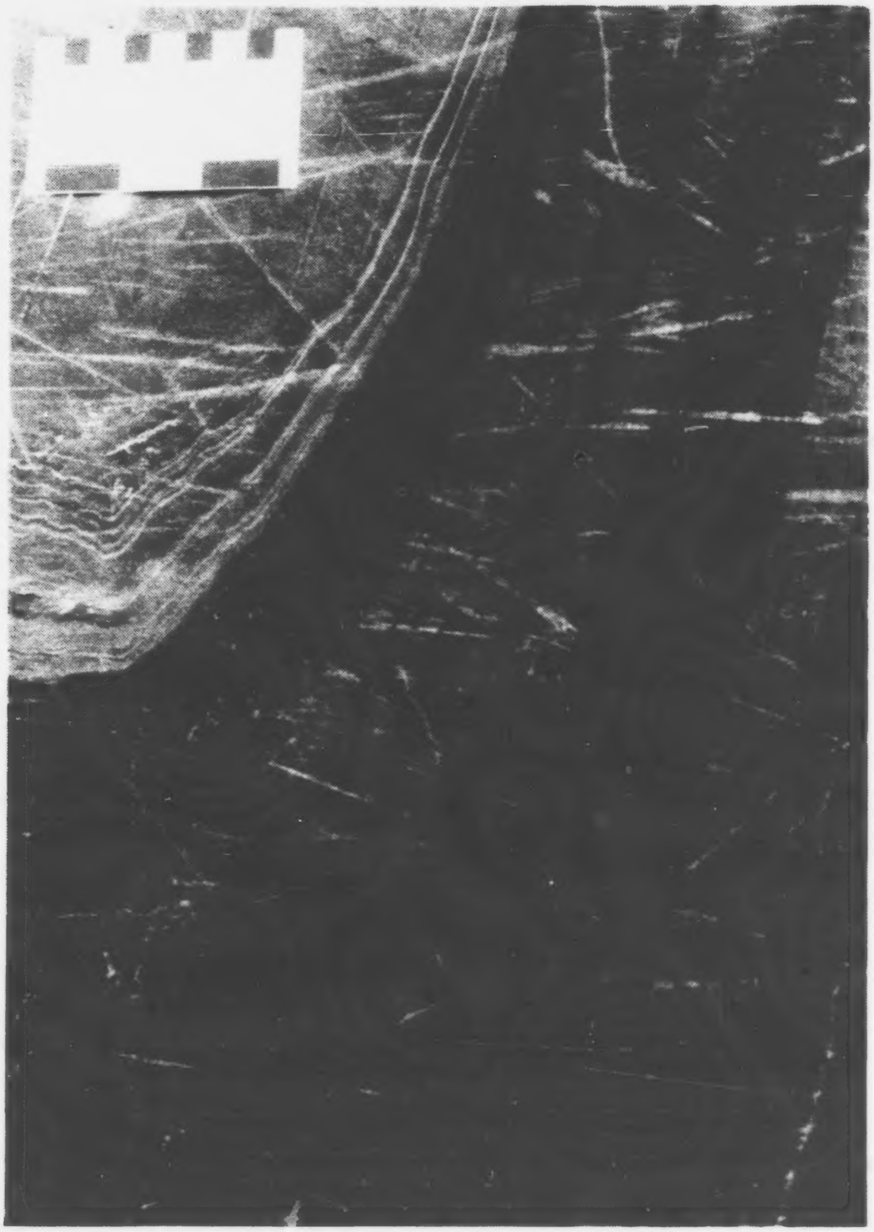

Figure 29 : Folded silt-rich iron formation, Hard Rock Open Stope, Geraldton. Note millimetre-wide magnetite beds in fold nose suffering considerable attenuation on fold limbs.

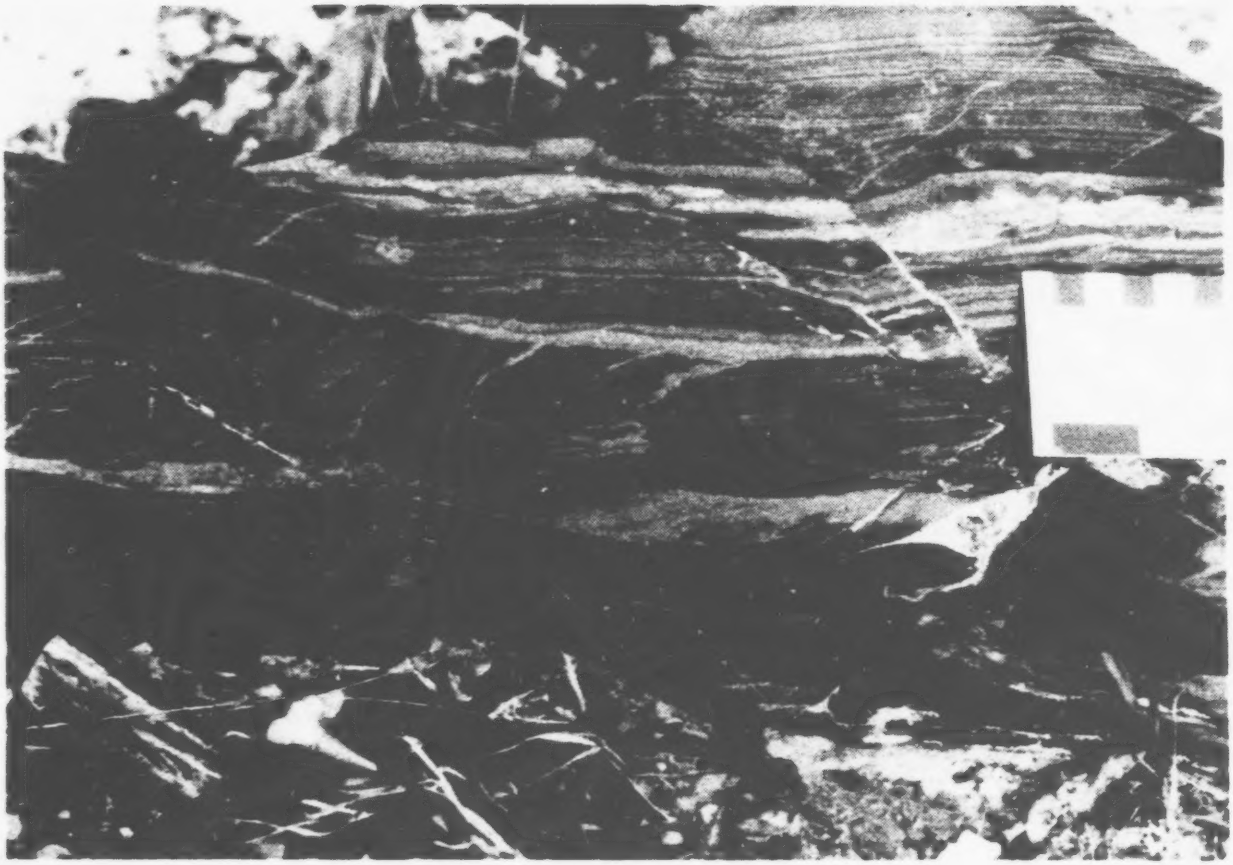

Figure 30 : Iron carbonate veinlets in iron formation, Hard Rock Open Stope, Geraldton.

TABLE III : CHEMISTRY OF RELATIVELY UNALTERED IRON FORMATION, HARD ROCK OPEN STOPE

	005	031	032	033	037	075	076
SiO_2	36.9	39.2	49.3	35.3	29.5	46.3	41.0
TiO_2	0.0	0.0	0.41	0.29	0.0	0.06	0.1
Al_2O_3	1.82	1.87	9.54	7.60	1.81	2.19	3.94
Fe_2O_3	35.4	40.5	10.9	25.9	43.5	45.3	36.1
FeO	16.3	12.1	10.7	16.7	20.6	2.96	13.5
MnO	0.05	0.04	0.08	0.09	0.03	0.05	0.05
MgO	1.24	0.54	2.17	1.73	0.0	0.04	1.35
CaO	2.94	1.41	3.83	1.51	0.71	0.41	1.01
Na_2O	0.6	0.07	2.64	3.29	0.64	0.00	0.39
K_2O	0.12	0.37	1.44	0.24	0.0	0.5	0.25
P_2O_5	0.22	0.2	0.2	0.2	0.25	0.08	0.16
CO_2	3.73	1.61	8.03	6.13	0.30	0.22	0.86
S	0.08	0.08	0.02	0.2	0.13	0.02	0.02
H_2O^+	0.19	0.48	0.67	1.36	0.98	0.79	1.13
H_2O^-	0.05	0.07	0.07	0.07	0.1	0.05	0.05
LOI	(1.6)	(0.3)	(8.0)	(5.5)	(0.7)	(0.3)	(0.2)
TOTAL	99.6	98.5	100.0	100.6	98.6	99.0	99.9
As	49	20	37	12	29	27	28
Au (ppb)	6	6	2	5	5	3	5
B	3	5	30	24	3	17	30
Co	7	8	17	16	7	6	11
Cr	20	21	102	75	15	20	33
Cu	8	16	25	24	6	18	11
Hg(ppb)	<dl	30	<dl	<dl	<dl	40	30
Ni	30	35	55	60	40	30	45
Pb	<dl	<dl	16	14	10	10	<dl
Sb	10	29	15	9	10	22	13
Sc	5	5	15	13	6	5	8
Sr	50	35	150	105	35	20	60
V	80	85	95	125	100	75	115
Zn	24	21	35	85	25	2	30

All samples from 82AJM series

Trace elements in ppm, unless specified otherwise.

dl : detection limit

8.1.2. Porphyritic Rock

Of minor importance in terms of outcrop percentage in the HRos, but of great interest with regard to mineralization, described below, is a unit termed "porphyry" (see map, back pocket and Figure 31). The unit consists of elongate grains of relict feldspar (aspect ratio of 5:1:1), amphibole, and rare quartz grains in a fine grained matrix of dominantly chlorite, sericite and carbonate. Figure 31 shows a photograph of the rock in outcrop, while Figure 32 is a photomicrograph showing relict (?) plagioclase phenocrysts. The porphyry unit is generally concordant, although on Boston Bay Island low angle cross-cutting relationships are present (Figure 33). A slab of the outcrop in Figure 33 shows (?) rip-up clasts at the contact between IF and the porphyry (Figure 10 in Macdonald 1984a). One outcrop in the HRos showed a grain size variability within a porphyry unit in which a fine grained, 10 cm wide portion of the rock graded, over less than 1cm, into material more typical of the porphyritic rock. The fine grained portion was mapped as a "chilled-margin" in 1982, although it can be argued that it reflects synsedimentary graded bedding. Figure 34 is a photomicrograph of the fine grained "porphyry", consisting of small (0.1 mm) feldspar grains in a sericite and carbonate matrix.

The information presented here does not provide unequivocal support for an intrusive, extrusive or sedimentary origin for the porphyritic unit. Horwood and Pye (1951), in their plan and section of the North zone of the Hard Rock Mine label the rock "diorite" and "quartz diorite" (Figure 35). The quartz diorite in Figure 14 clearly cuts stratigraphy; the diorite in Figure 35, less obviously so. Although referred to as quartz diorite in Figure 14 and diorite in Figure 35, the sequence of plans provided by Horwood and Pye indicates that the rocks are one and the same unit. Thus, although definitive field relationships are absent, geometric relationships available from mine plans down to a depth of 1571 ft, approximately 500 m, support an intrusive nature for the porphyritic rock.

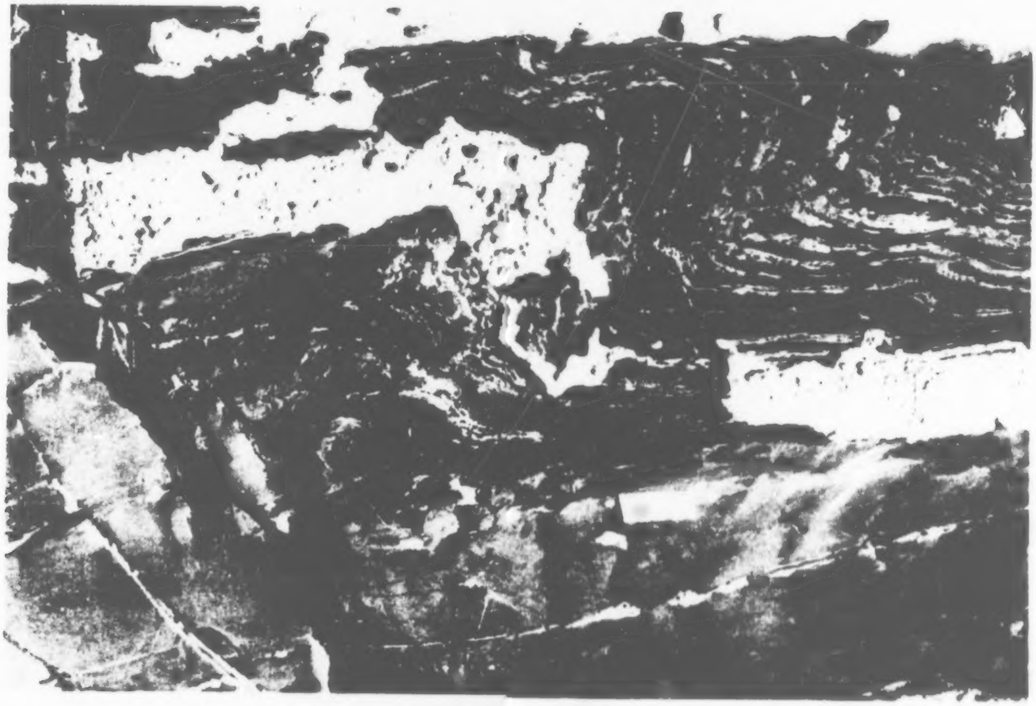

Figure 31 : Porphyritic Rock in contact with banded iron formation, Hard Rock Open Stope, Geraldton.

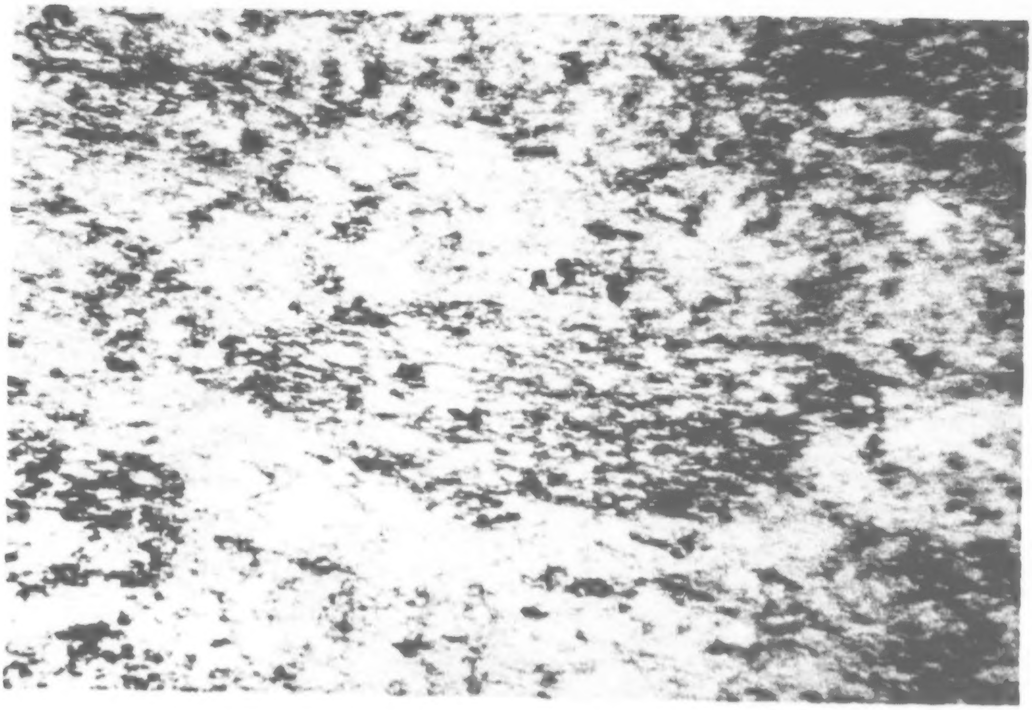

Figure 32 : Photomicrograph of highly altered porphyritic rock, Hard Rock Open Stope, Geraldton. Phenocryst in centre of field of view is 3 mm in long dimension and is relict (?) plagioclase.

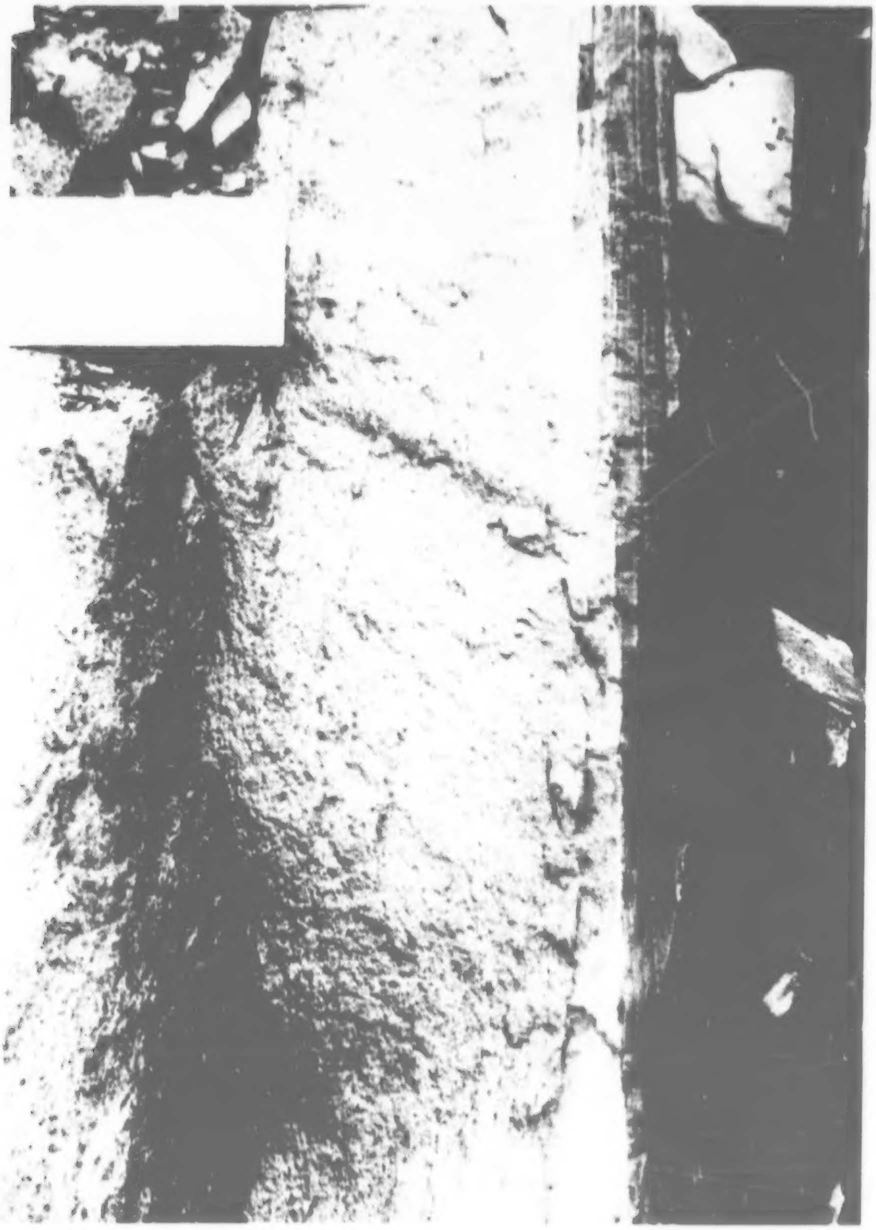

Figure 33 : Contact of Porphyritic unit and banded iron formation, Barton Bay Island. Contact is discordant, either erosional or intrusive.

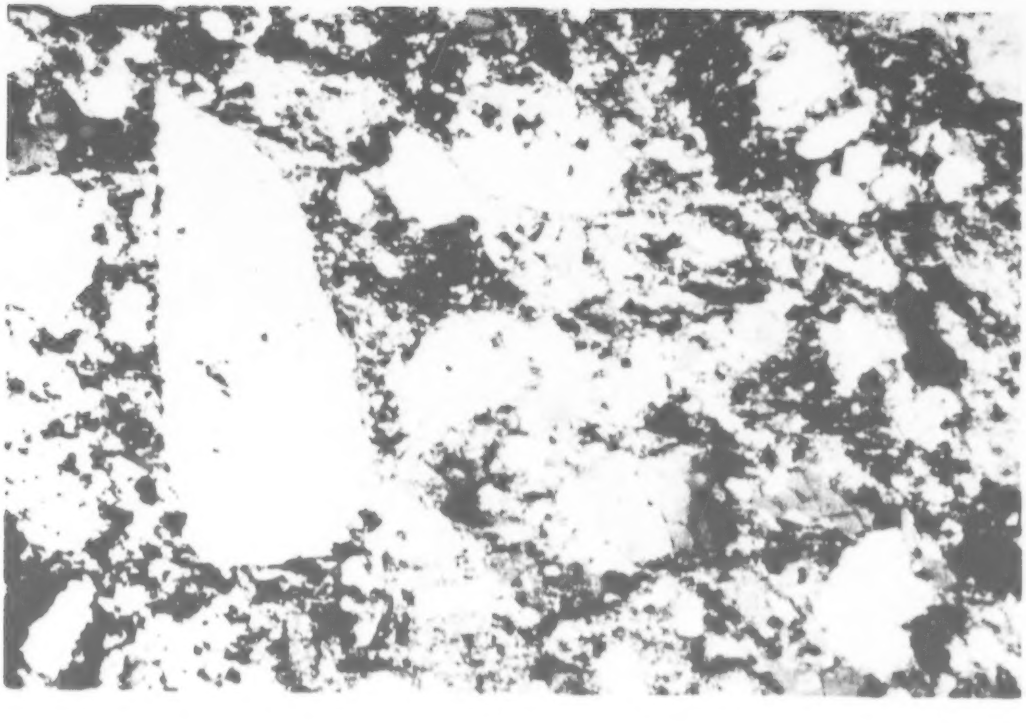

Figure 34 : Photomicrograph of margin of porphyritic unit. Field of view is 2 mm.

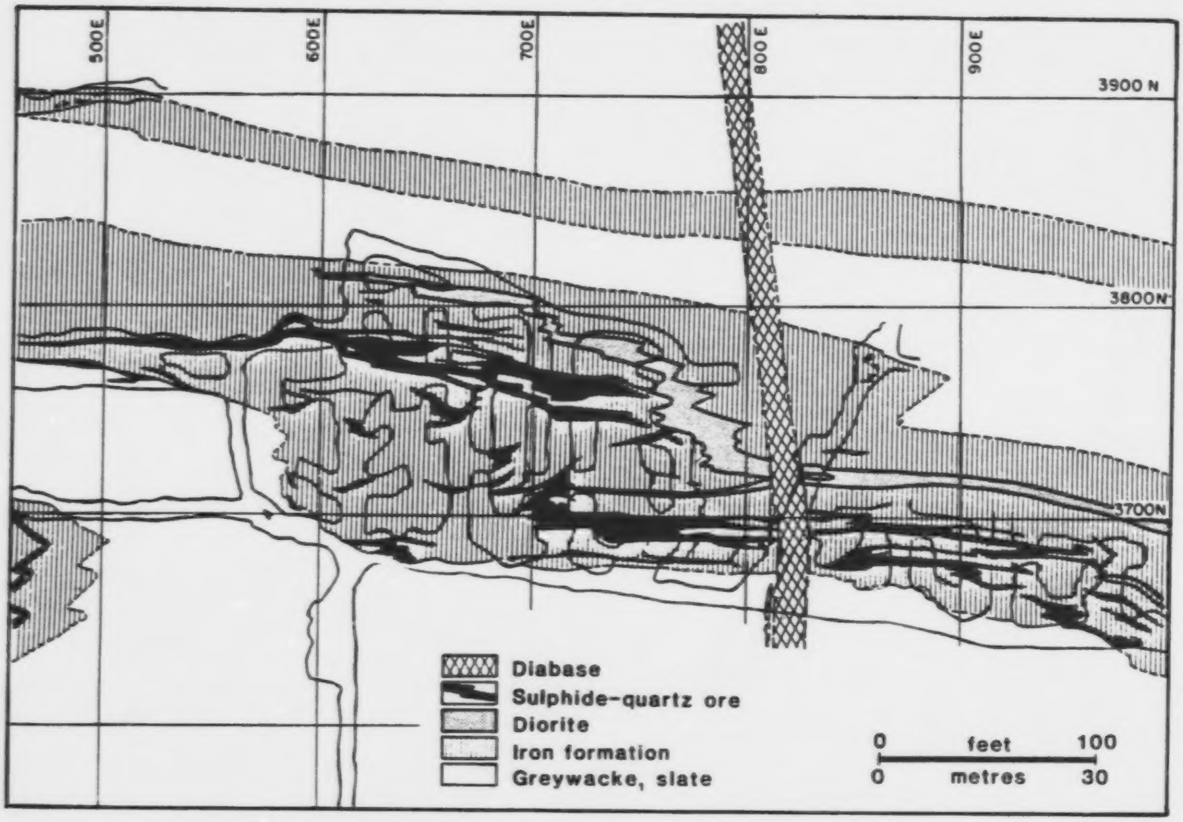
500E
600E
700E
800E
900E
3900 N
3800N
3700N
Diabase
Sulphide-quartz ore
Diorite
Iron formation
Greywacke, slate
0 feet 100
0 metres 30

Figure 35 : Geological map of North Zone subsurface, redrawn from Horwood and Pye (1951)

TABLE IV : CHEMISTRY OF PORPHYRY, HARD ROCK OPEN STOPE.

	001	010	012	017	020	040	042
SiO_2	34.5	34.2	36.3	28.0	44.6	37.5	70.00
TiO_2	0.65	0.64	0.43	0.58	0.5	0.68	0.52
Al_2O_3	11.7	13.5	11.4	11.8	13.3	10.1	13.8
Fe_2O_3	1.5	1.6	7.59	2.8	10.1	1.31	1.32
FeO	9.49	8.4	9.64	5.4	14.8	8.25	3.58
MnO	0.17	0.16	0.16	0.17	0.31	0.16	0.05
MgO	7.09	6.38	3.98	7.4	4.5	10.6	2.16
CaO	11.3	11.2	9.04	14.0	0.7	7.73	0.74
Na_2O	0.36	0.57	0.0	0.54	0.14	0.49	3.57
K_2O	2.52	3.19	2.64	3.14	1.52	1.8	1.8
P_2O_5	0.07	0.74	0.05	0.03	0.14	0.07	0.05
CO_2	16.9	16.6	12.1	21.2	1.32	17.1	0.6
S	0.14	0.15	2.33	1.74	6.94	0.15	0.21
H_2O^+	2.62	2.44	3.45	1.94	6.03	2.21	1.67
H_2O^-	0.08	0.06	0.1	0.06	0.12	0.1	0.08
LOI	(17.1)	(17.3)	(11.4)	(20.0)	(8.1)	(9.43)	(1.9)
TOTAL	99.09	99.83	99.21	98.8	105.02	98.25	100.15
As	170	176	280	350	1140	500	56
Au (ppb)	115	240	1423	390	1623	120	64
Ba	790	860	770	710	220	330	460
Co	39	34	32	40	24	48	15
Cr	390	304	260	530	166	765	137
Cu	44	26	96	63	8	74	34
Li	16	16	12	11	28	29	38
Nb	16	15	13	12	13	13	8
Ni	84	66	75	78	63	280	35
Pb	dl	dl	dl	dl	dl	dl	13
Pd (ppb)	5	5	5	4	2	4	dl
Pt (ppb)	5	5	5	5	2	4	dl
Sb	10	9	9	9	9	19	2
Sc	25	22	25	30	14	18	8
Sr	235	375	205	430	35	275	275
V	230	220	195	195	115	175	90
Y	5	5	5	4	8	4	5
Zn	90	78	115	52	39	46	57
Zr	40	40	30	30	115	40	120

All Samples {82AJM} Series

dl : detection limit (Pb=10 ppm, Pt,Pd=1 ppb)
All trace elements in ppm unless stated otherwise.

Lithogeochemistry has provided little to assist in diagnosing the origin of the rock, which is highly susceptible to alteration and may, in the HRos, commonly contain up to 30% combined H_2O and CO_2. Table IV gives geochemical analyses for the rock, most from the porphyritic phase and one from the "chilled margin" (sample 82AJM-42). In comparing sample 82AJM-42 with the others, note the following in the coarser grained rocks: (1) elevated CO_2 and H_2O; (2) depleted SiO_2; (3) elevated MgO and CaO (4) elevated Au, As and Sb, (5) elevated Co, Cr, Ni, Pd and Pt. No attempt is made here to estimate quantitative gains and losses of species in the alteration event following the method of Gresens (1967) for the following reasons: (1) the HRos is within a high strain portion of the BBLZ and may have suffered considerable volume change which cannot be quantified; (2) No species can be arbitrarily considered to have been immobile in the alteration process. Alumina, for example was mobile, contributing to secondary sodium feldspar; titanium was also mobile, forming as hydrothermal ilmenite in the Geraldton area (X-Ray Diffraction Identification, W.D. Hicks, Mineralogist, Ontario Geological Survey, written communication, 1985).

Many of the above alteration phenomena are typical of lode gold deposits (Colvine et al. 1984). The presence, however, of elevated MgO, Co, Cr, Ni, Pd and Pt is enigmatic. These elements are only elevated in rocks that are highly altered, suggesting that they constitute part of the elemental suite involved in the alteration process.

8.1.3. Wacke and Siltstone

In the immediate vicinity of the HRos, the clastic sediments are intensely deformed. Little remains of original sedimentary features, which have been rotated into the east-trending fabric. In some cases, microbands of magnetite reflect the original bedding (Figure 36), there being no such indicators in the bulk of the rock. The siltstone component is most obviously susceptible to deformation, developing a highly penetrative pressure solution fabric (described in section 8.2.3.2 and Figure 10) which may also destroy bedding. M.W. Kehlenbeck (Professor, Lakehead University, Thunder Bay, personal communication, 1984) has also noted local pervasive pressure solution in wacke.

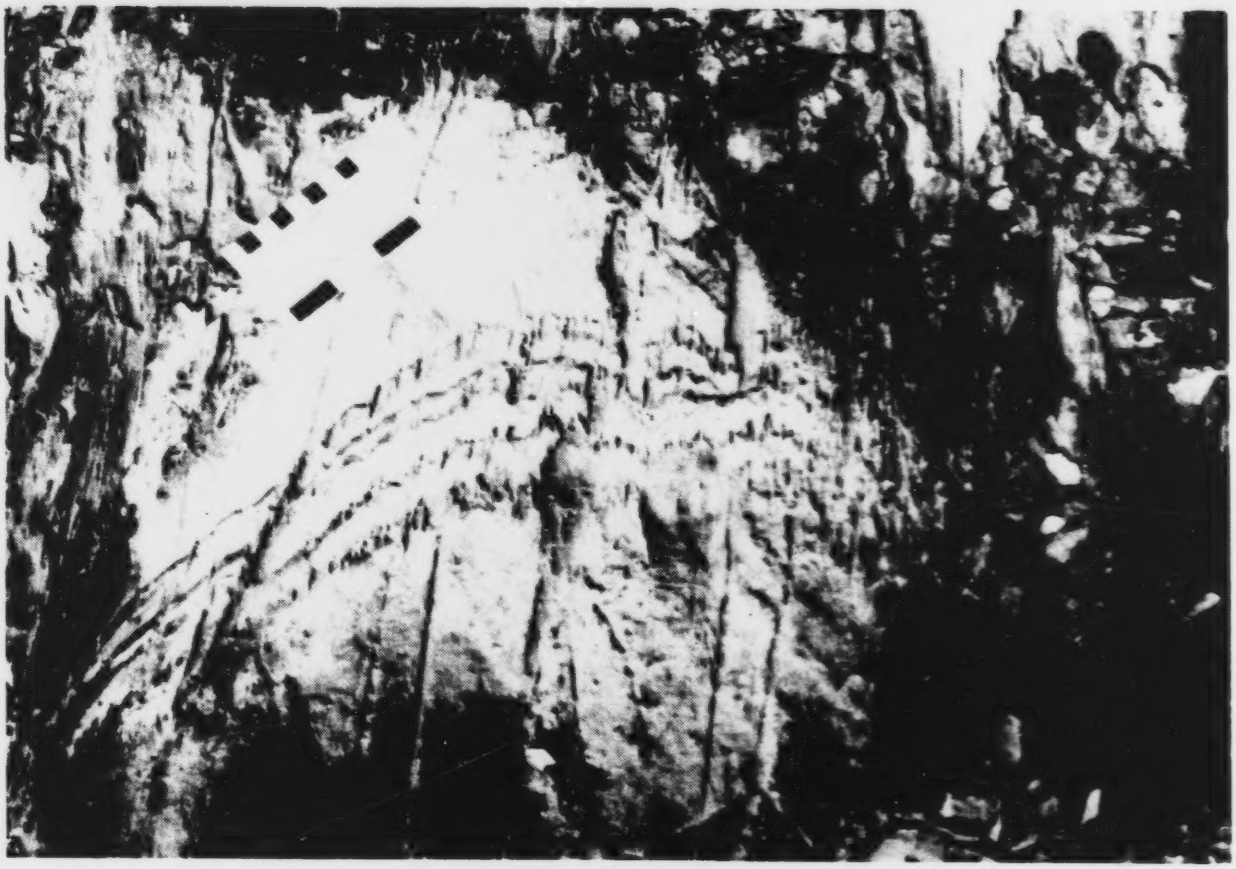

Figure 36 : Magnetite layers within highly deformed wacke, MacLeod-Cockshutt Property, Geraldton.

8.2. Structure in the Hard Rock Open Stope

8.2.1. Soft Sedimentary Structures

Many geologists visiting the HRos during mapping by the author in 1982 commented on the apparent proclivity of IF to develop soft sedimentary, slump folds, an origin proposed for the minor folds in, for example, Figure 27. While soft sediment, slump folds commonly occur in water-charged muds and silts, the minor folds in the HRos are dominated by Z-shapes plunging at 20^{o} to 30^{o} to the west, as do many of the larger structures in the area. In addition, cleavage in wacke units associated with folded BIF or siltstone is also folded around the minor folds (Figures 9 and 37), as pointed out by K.H. Poulsen (Geologist, Geological Survey of Canada, oral communication, 1983). As cleavage development in a sediment is a process either accompanying or subsequent to lithification, the observation that cleavage is folded around the minor folds precludes the origin of the folds as a pre-lithification, soft sediment structure.

The IF at HRos does contain however, spectacular examples of clastic, or Neptunean dikes, cutting BIF (Figure 38). The unit in Figure 38 was erroneously mapped, in 1982, as an igneous felsic dike (Macdonald 1982). More detailed mapping in 1983 revealed that the dike passes with continuity into a clastic horizon.

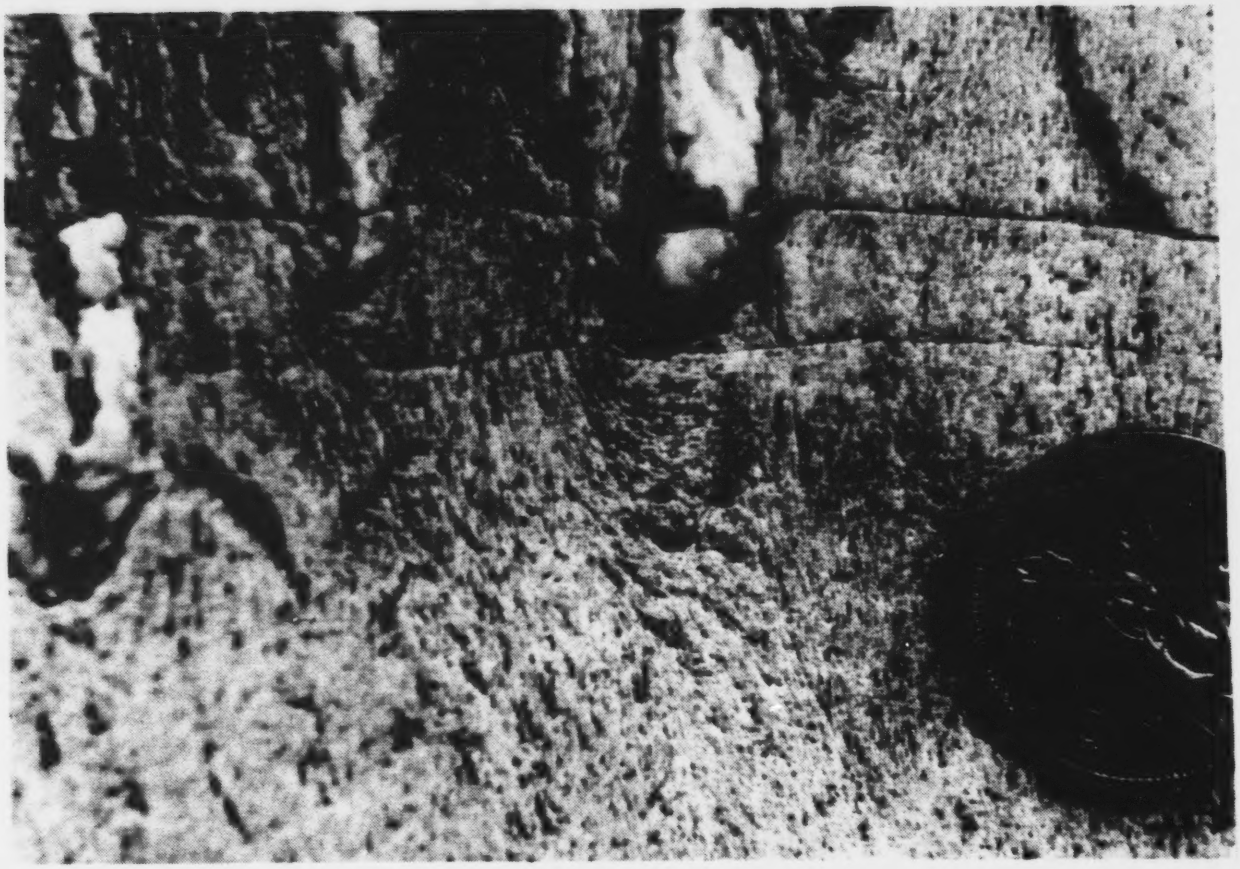

Figure 37 : Folded cleavage and quartz veins in wacke, McLellan Property, Geraldton.

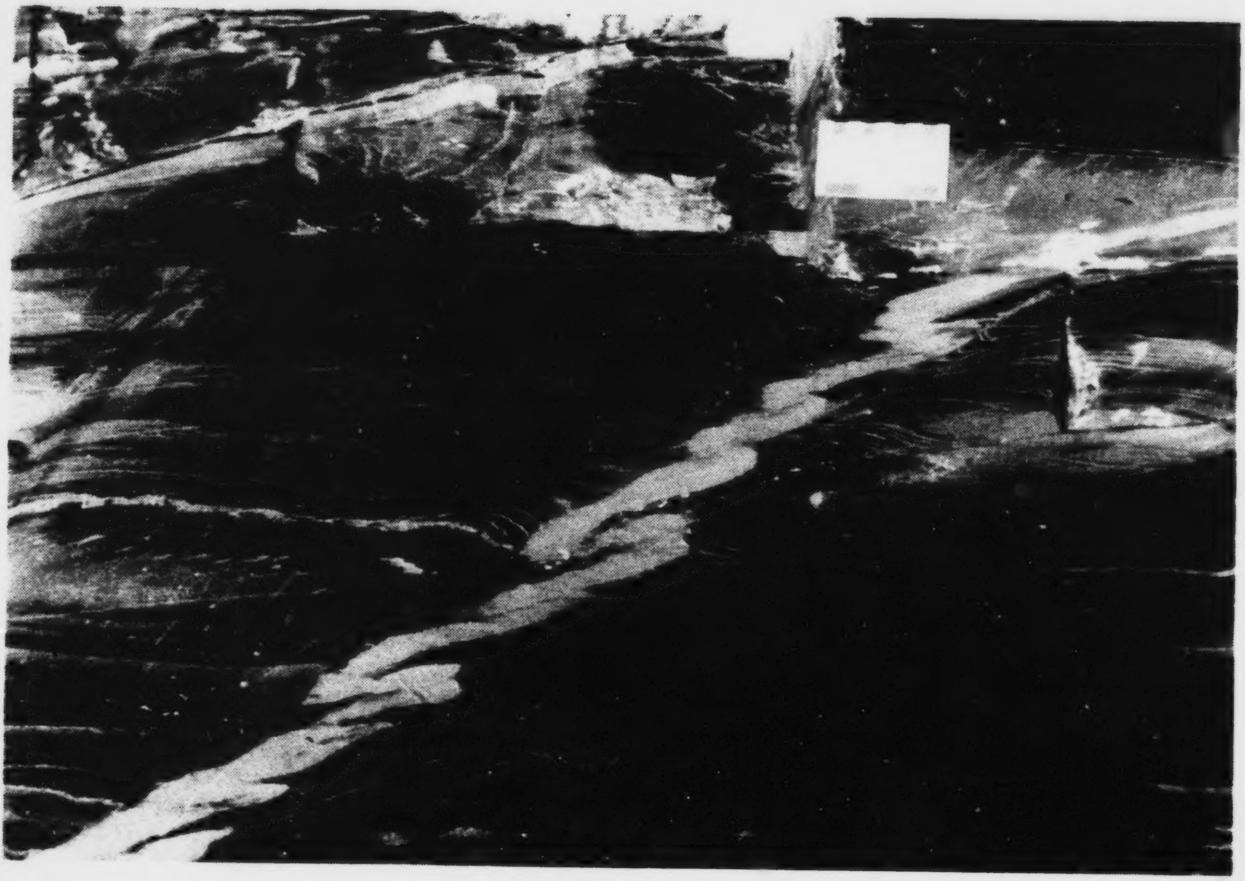

Figure 38 : Deformed clastic dike, Hard Rock Open Stope, Geraldton.

Clastic dikes form in response to disequilibrium experienced by water-charged sediments, subdivided by denser sediments; in this example, silts between iron oxide layers. In response to density instability, a sand dike erupts upward, perpendicular to bedding, i.e. parallel to the pressure gradient. The original 90^{o} angle between a sand dike and surrounding beds can therefore provide a useful strain indicator if the rocks are subsequently deformed (Borradaile et al. 1982). For example, Figure 39 shows a small clastic dike at a high angle (80^{o}) to bedding from the apical region of relatively large wavelength (tens of metres) fold exposed in Barton Bay Island, west of the Little Long Lac Mine (Figure 3). Figure 40 shows a clastic dike at a more acute angle to bedding on the flank of the same fold. The obliquity is a measure of the degree of homogenous flattening that has occurred on the fold flank during folding. These relationships are shown diagrammatically in Figure 41. In this particular case, the amount of deformation parallel to bedding is not extreme (c.f. Figure 29) retaining the integrity of the original stratigraphy. Care must be taken, however, in a deformed sequence when interpreting finely laminated rocks whose original sedimentary features are highly susceptible to transposition during deformation.

The more intense deformation experienced by clastic dikes in the HRos (Figure 38) will be addressed in Section 8.2.3.3.

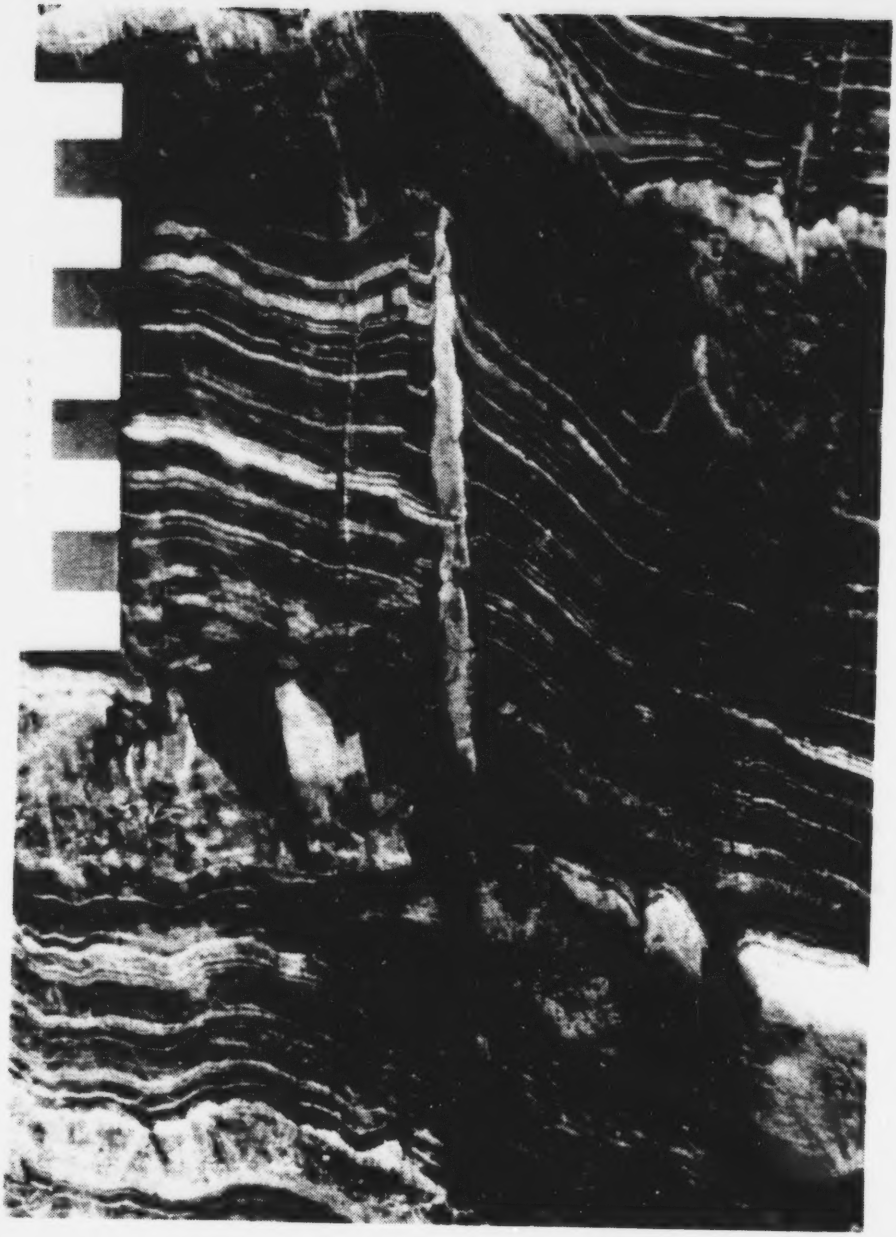

Figure 39 : Clastic dike in iron formation, in apical region of fold, Barton Bay Island, Geraldton.

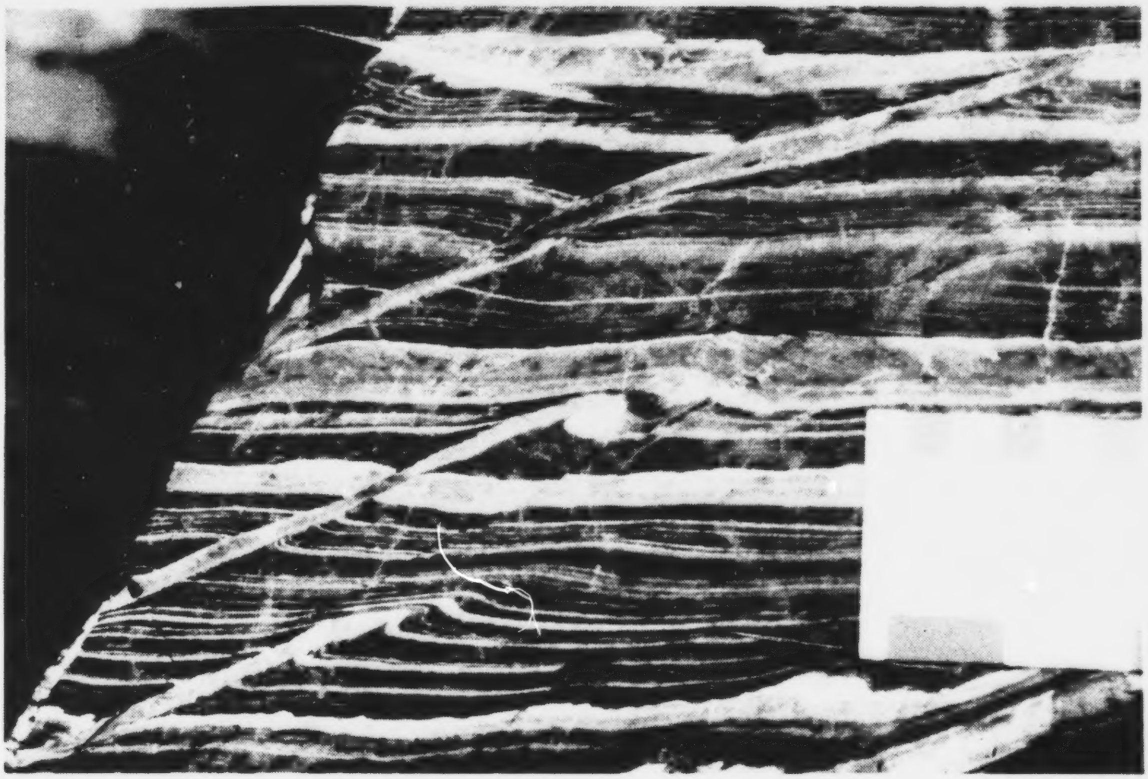

Figure 40 : Clastic dikes in iron formation on flank of fold, Barton Bay Island, Geraldton.

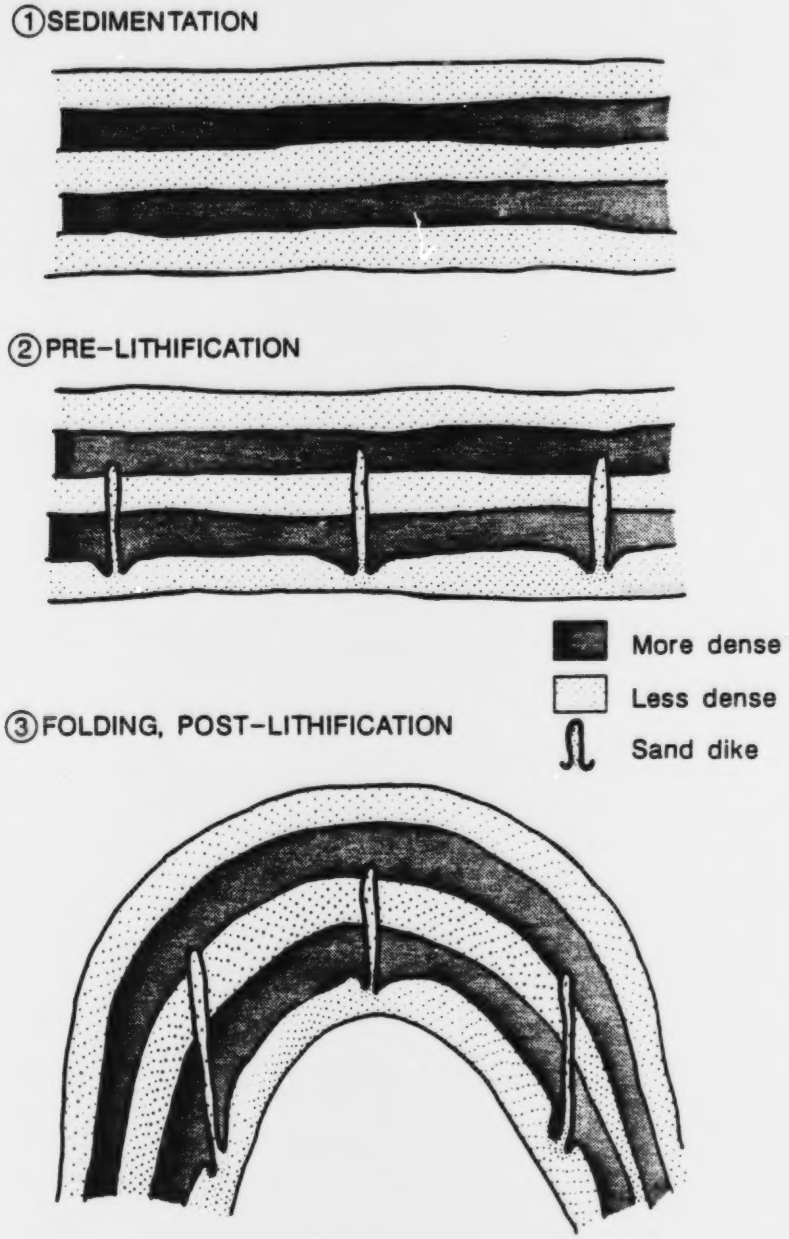
①SEDIMENTATION
②PRE-LITHIFICATION
More dense
Less dense
Sand dike
③FOLDING, POST-LITHIFICATION

Figure 41 : Sketch showing relationships between clastic dikes and folds.

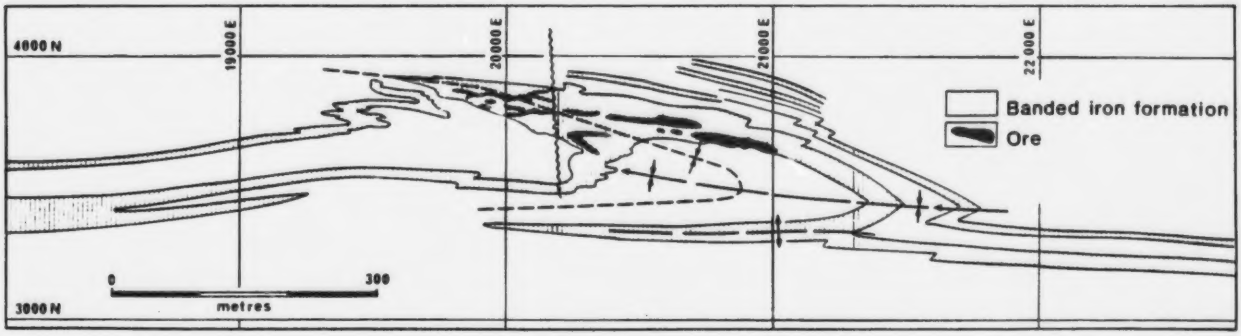
4000 N
19000 E
20000 E
21000 E
22 000 E
Banded iron formation
Ore
0
300
metres
3000 N

Figure 42 : Level plans, North Zone, Hard Rock and MacLeod-Cockshutt Mines (from Horwood and Pye, 1951).

8.2.2. Structural Geology of the North Zone, Hard Rock and MacLeod Cockshutt Mines

In the Geraldton Camp, IF has responded to regional stress by folding to produce structures on all scales. Figures 24 and 25 illustrate the Z fold (in plan) of wavelength 45m and amplitude nearly 100 m. While this study focused upon the open stope, plans and sections available from the Hard Rock and MacLeod-Cockshutt Mines and summarized in Horwood and Pye (1951) are most illuminating and relevant to the study. A portion of the level plans is reproduced in Figure 42. Ore is hosted within IF in a structurally complex zone (Figure 42). Aside from wacke and diabase (not shown), the only other rock type in the North Zone is the enigmatic "quartz diorite" of controversial origin (see above). The plans of Horwood and Pye (1951) indicate, quite clearly, that quartz diorite transects IF units on both the 502 ft and 1571 ft levels, supporting evidence for an intrusive origin for this rock type, termed "porphyry" by Macdonald (1982).

Horwood and Pye (1951) show the locations of measured synforms and antiforms. All plunges are either 28^{o} or 29^{o} to the west. Figure 43 is a section through the North Zone, showing the plunge of the mineralized zone. Horwood and Pye (*ibid*) also show that folded albite porphyry units plunge at 20 - 25^{o} to the west, indicating a cross-cutting relationship with enclosing stratigraphy. In Figure 42, two additional antiform axes are shown on the northern side of the ore host structure and to the east of the No. I shaft to rationalize the mapped distribution of the IF unit. In addition, a proposed folded fold axis is shown on Figure 42 to accommodate the cuspate geometry of the IF. The plans of Horwood and Pye (1951) indicate (1) with depth, the southernmost antiform passes transitionally from a tight to isoclinal structure with juxtaposed, subparallel limbs and no intervening wacke, to a more open fold whose limbs diverge, in plan, at approximately 30^{o}; (2) mapped fold axes are curvilinear (3) the outcrop distributions on the 356 ft level describe crude "canoe" or "dome and basin" morphology; and (4) the large cuspate structure, hosting the north zone near surface, contracts with depth from (greater than 2000 ft by 500 ft to 800 ft by 200 ft on the 1571 ft level.

Unpublished company records indicate that below the 1571 ft level, the Z-fold structure that hosts ore contracts further to a simple, steeply dipping, monoclinal, east-striking BIF unit with no antiforms or synforms. Where the Z-fold structure has not been superimposed upon steeply dipping IF, the unit is devoid of economic mineralization. An isometric diagram of the Z fold exposed at surface and unfolding with depth is given in Figure 44. IF material sampled during the course of this study along strike from the HRos is also barren, containing a conspicuous absence of carbonate, sulphides and quartz-carbonate-tourmaline vein (e.g. analysis for sample 82AJM-076 in Table III).

The geometry of the folded IF hosting the North Zone (Figure 42) does not reflect a simple, single stage of deformation, which would be expected to induce relatively simple folds, e.g. cylindrical folds such as Types 1, 2, 3 of Ramsay (1967). Ramsay (1967, Chapter 10) also describes the characteristic geometries of re-folded folds, and de Sitter (1964) has described dome and basin structures that may be produced by two superimposed folding events. Apparent re-folded folds are visible in outcrop at Geraldton, although infrequently: Figure 45 shows an isoclinally folded fold axis on the Consolidated Mosher Long Lac property. While it is not the objective of this study to describe the overall structure of the Geraldton Camp (see Buck, 1986; Lavigne in preparation; Kehlenbeck 1986), the following observations are pertinent to an understanding of the fold style in the North Zone of the Hard Rock and MacLeod-Cockshutt deposits:-

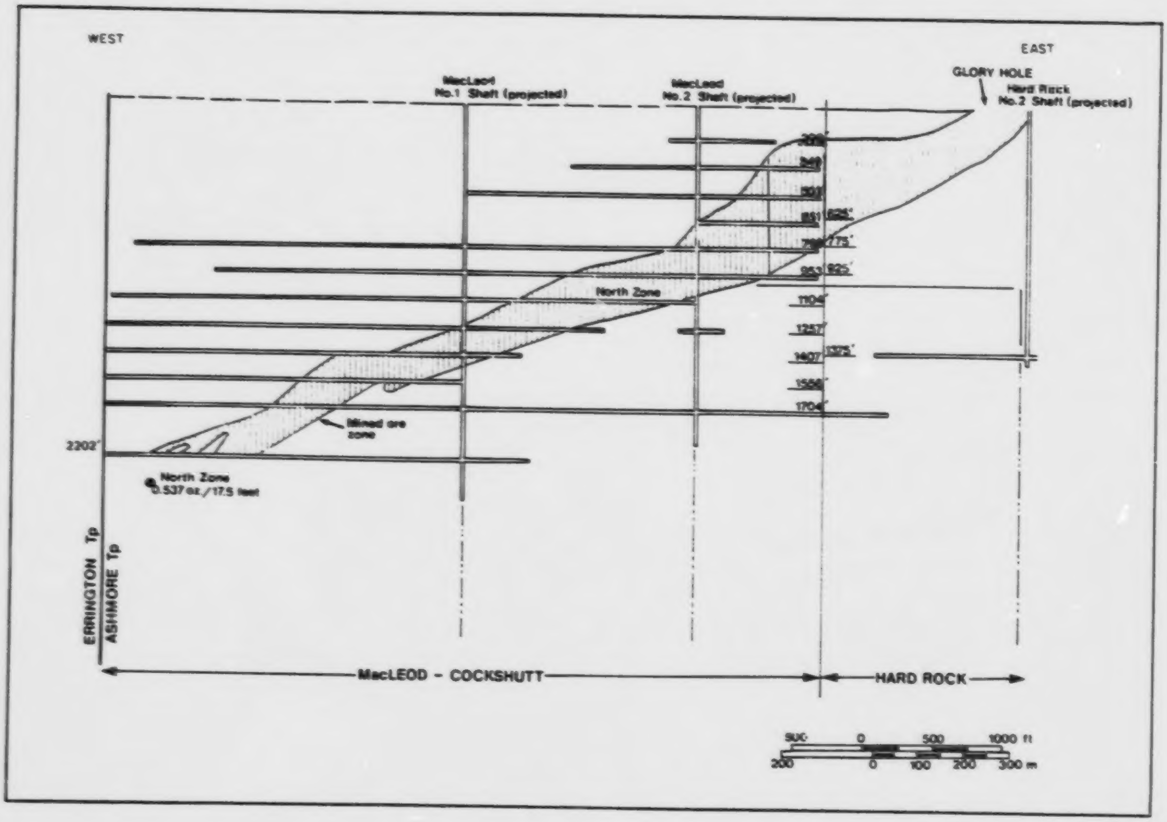
WEST
EAST
MacLeod No.1 Shaft (projected)
MacLeod No.2 Shaft (projected)
GLORY HOLE
Hard Rock No.2 Shaft (projected)
200'
348'
503'
651'
625'
798'
775'
953'
925'
North Zone
1104'
1257'
1407'
1375'
1556'
1704'
Mined ore zone
2202'
North Zone
0.537 oz./17.5 feet
ERRINGTON Tp
ASHMORE Tp
MacLEOD - COCKSHUTT
HARD ROCK
500 0 500 1000 ft
200 0 100 200 300 m

Figure 43 : North Zone, Hard Rock and MacLeod-Cockshutt Mines, Longitudinal Section (Ferguson 1967).

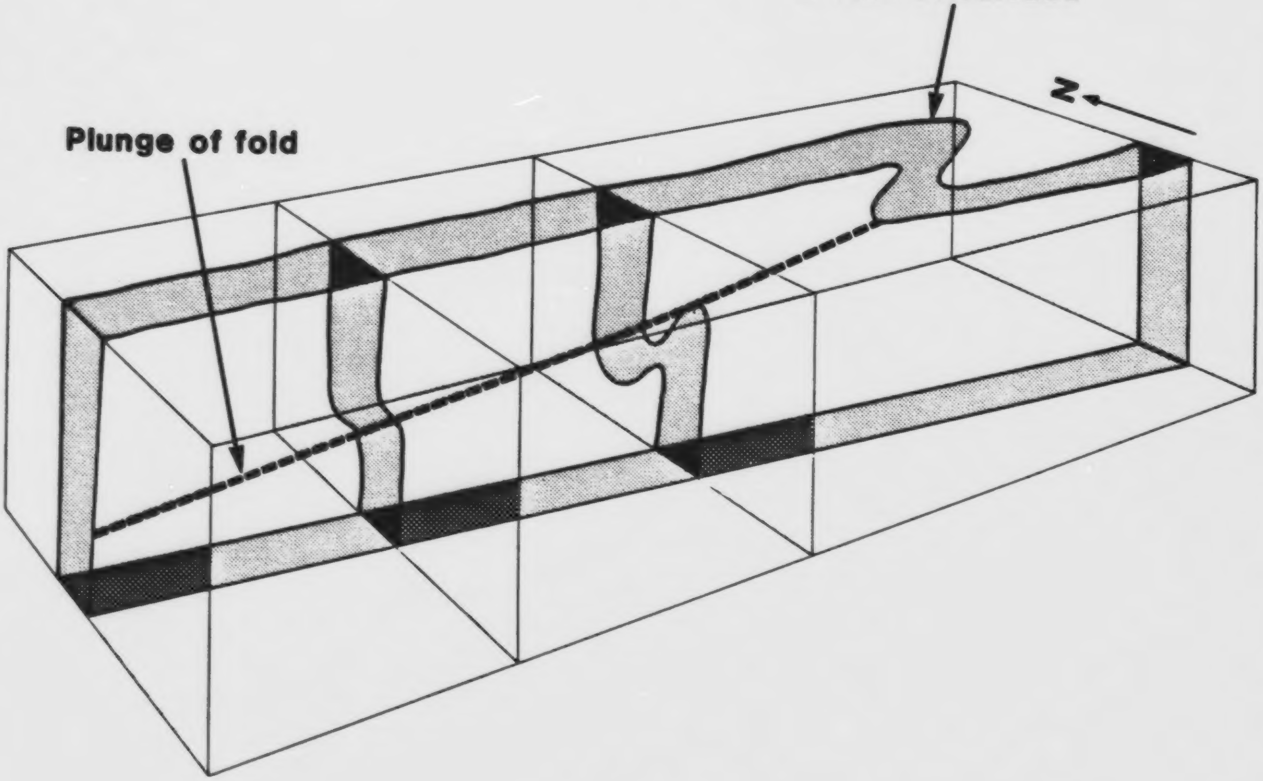
Z-fold at surface
Plunge of fold
N

Figure 44 : Isometric perspective projection of the North Zone, showing the Z fold "unwinding" with depth (Macdonald, in press).

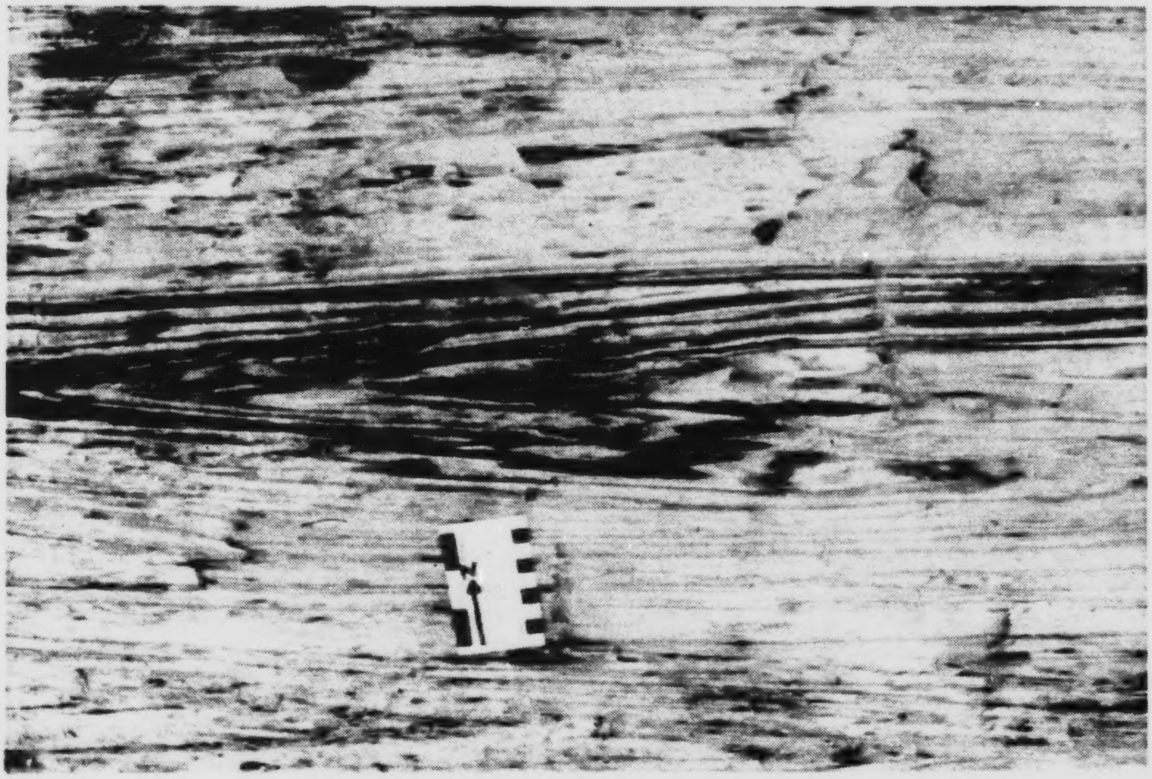

Figure 45 : Refolded, folded magnetite bands in wacke, Consolidated Mosher Property, Geraldton.

(i) In the Geraldton Camp, at least two penetrative fabrics are present, most obviously visible in porphyry (Figure 19) and wacke (Figure 20).

(ii) The two fabrics are generally subparallel, except in the hinge zones of minor folds that deforms the older of fabrics.

As the two fabrics tend, in most outcrops, to be subparallel, distinguishing between them in the field is often difficult. This parallelism of fabrics, coupled with the subparallelism of fold axes in apparent refolded folds (Figure 45) is consistent with the hypothesis that the deformation regime was cotinuous or episodic, with no evidence of a major change between the events. M.J. Lavigne (Resident Geologist, Ministry of Northern Development and Mines, Red Lake, Ontario, personal communication, 1983), has suggested that the apparent superposition of structures may simply reflect a protracted, but uniform, deformational event, which locally, may produce further deformation of previously formed folds. This hypothesis receives theoretical support from the work of Cobbold and Quinquis (1980), who have described the experimental generation of non-cylindrical, sheath-like folds, possessing curved fold axes within their axial planes, and exhibiting basin and dome structures. Their experiments were performed in shear boxes, where laminated plasticine is subjected to abnormally high strain rates to produce sheath folds. A typical set of fold structures produced in their experiments is shown in Figure 46 Cobbold and Quinquis (1980) also describe the formation of non-cylindrical folds in the Ile de Croix blueschists of France and the Valdres district of Norway. They suggest that fold styles such as these are found in areas experiencing progressive simple shear and high strain rates, such as diapir margins, nappe bases or shear zones. Earlier in this report (section 4.2), it was suggested that the Barton Bay Lithotectonic Zone (Figure 3) may have been subject to one period of transpression (oblique compression). Recognition of areas within the BBLZ exhibiting non-cylindrical folds may support this hypothesis and suggest, further, that "folds may be generated episodically throughout history of progressive shearing, as a result of episodic instability of the flow. Successive refolding of metamorphic fabrics is also likely" (Cobbold and Quinquis 1980). One repercussion of this hypothesis is that refolded folds and folded cleavage, both observed in the Geraldton Camp (Macdonald 1984a) but not apparently extant beyond the BBLZ (Kehlenbeck 1986), need not necessarily reflect an isolated, additional folding event in one locality when compared to an adjacent one. Rather, the field observations may be interpretable in terms of localized progressive shearing and resultant generation of non-cylindrical folds. This hypothesis has been addressed by Lavigne (in preparation) and Buck (1986).

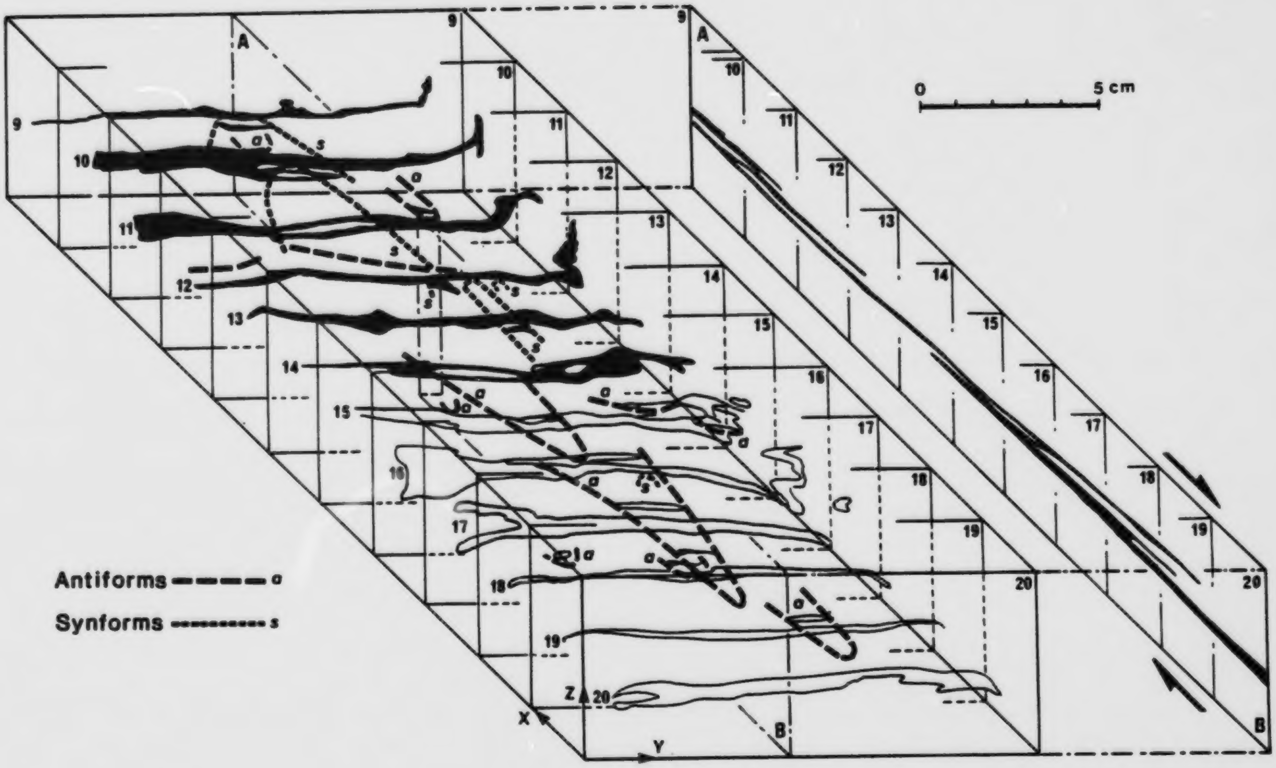
A
B
X
Y
Z
0
5 cm
9
10
11
12
13
14
15
16
17
18
19
20
a
s
Antiforms
Synforms

Figure 46 : Experimentally-produced sheath folds during progressive simple shear with high strain rate (Cobbold and Quinquis 1980).

8.2.3. Structural Geology of the Hard Rock Open Stope

As mentioned in foregoing lithological descriptions, each discrete rock type exposed in the HRos has reacted to stress as a function of its individual physical properties. The following section describes the strain exhibited by each rock type and subsequently considers foliation and vein attitudes throughout the HRos.

8.2.3.1. Banded Iron Formation

The bulk of the unit marked iron formation on the Map 1 (back pocket) and Figure 25 consists of alternating thin bands of magnetite and clastic sediment - wacke or siltstone depending upon grain size. During ductile deformation the mixed magnetite-wacke unit (e.g. Figures 27 and 28) undergoes folding with some accompanying bedding plane transposition in fold limbs (e.g. Figure 29). Fold style is a close approximation to Ramsay Class 2, also known as *similar* folds (Ramsay 1967), as shown in Figure 47.

In detail, the folds are somewhat more complex. Figures 48 and 49 are tracing of the folds shown in Figures 26 and 29, respectively. Dip isogons are shown for the apical portions of the folds. Note that in Figure 48, the isogons diverge from the outer curve to the inner curve; i.e. the rate of change of the slope of the outer core exceeds that of the inner one. This is a Class 3 fold (Ramsay 1967, p. 365). The fold in Figure 49 exhibits further complexity: dip isogons range from subparallelism to both convergent and divergent forms. The subparallel isogons are a characteristic of similar (Class 2) folds, while convergent isogons indicate Class 1 folds (Ramsay 1967). Note in Figure 48 that convergent isogons (Class 1 folds) are found in the lighter coloured units, those containing the highest percentage of clastic sediment.

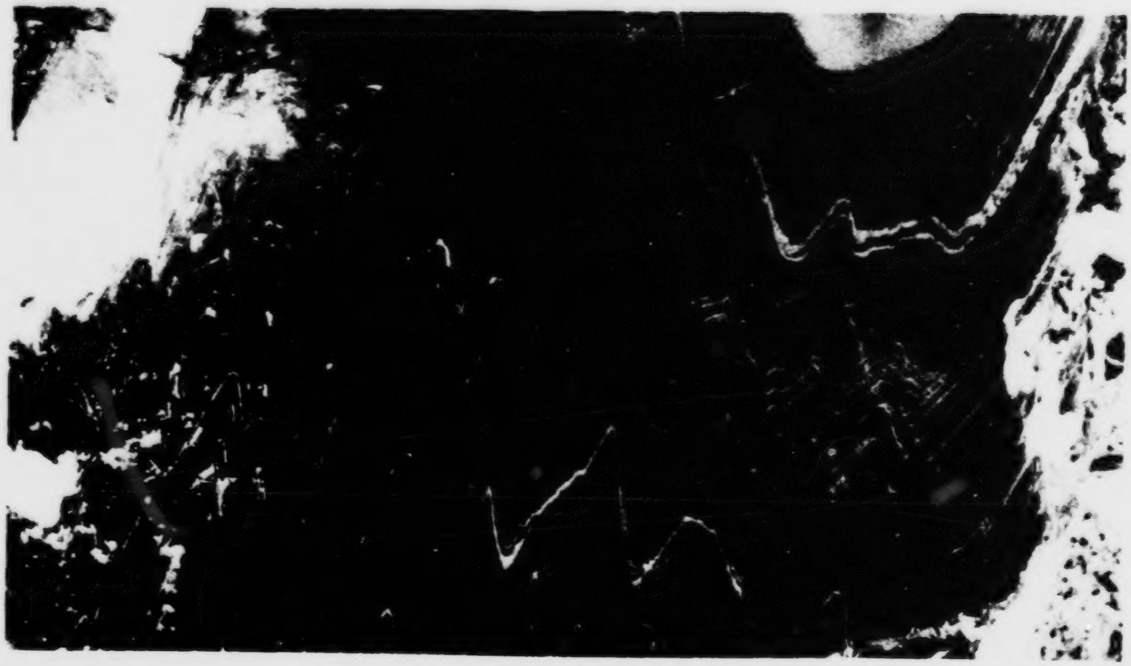

Figure 47 : Similar folds in banded iron formation, Hard Rock Open Stope, Geraldton.
Field of view is 20 cm.

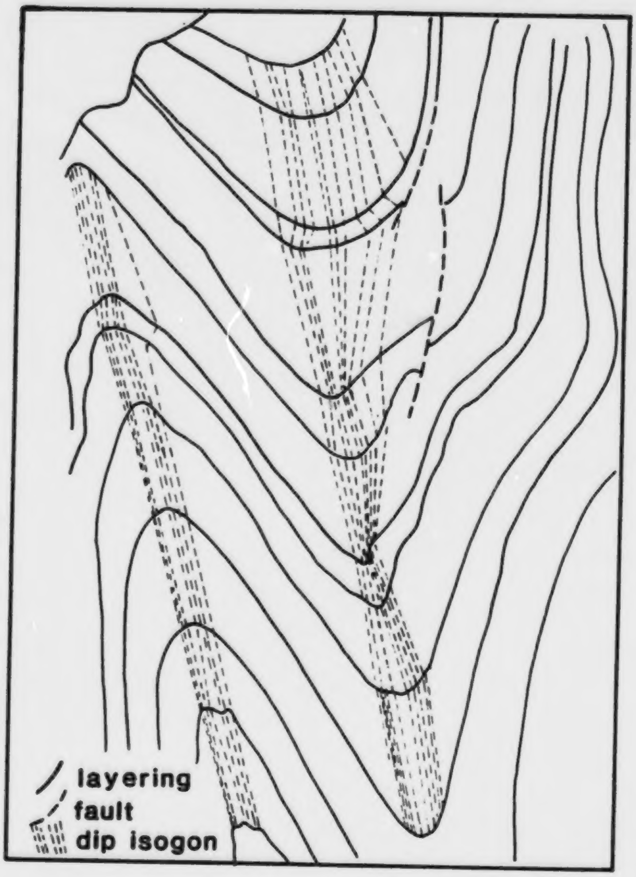
layering
fault
dip isogon

Figure 48 : Dip isogons constructed on tracing of fold in Figure 26.

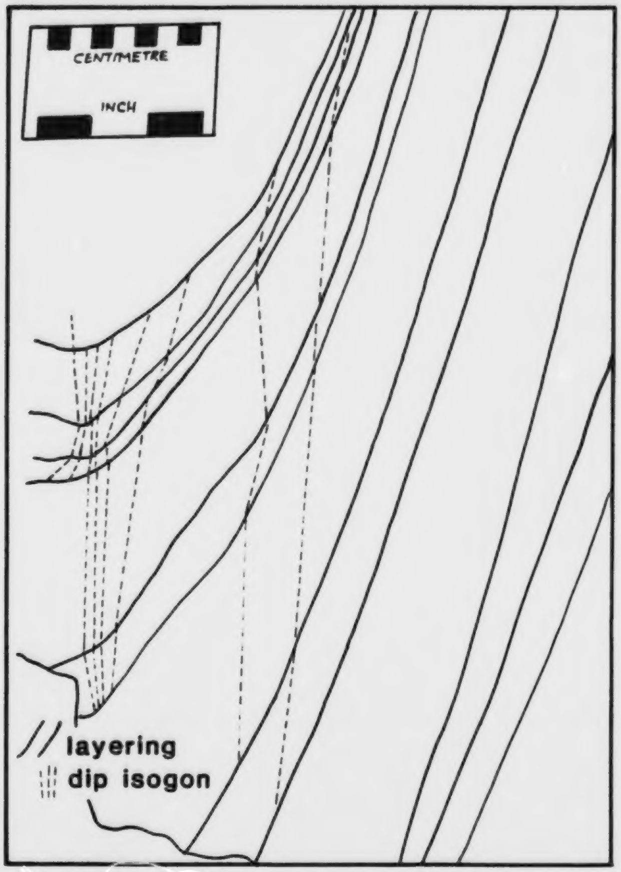
CENTIMETRE
INCH
layering
dip isogon

Figure 49 : Dip isogons constructed on tracing of fold in Figure 29.

Class 1 folds occur in rocks containing units of greatest rheological contrast. Class 2 folds form in rocks containing units with little rheological contrast. Class 3 folds, however, form in rocks that have experienced considerable inhomogenous, post-fold flattening (H. Williams, Geologist, Ontario Geological Survey, personal communication 1987).

These observations warrant a brief discussion. Ramsay (1967, p. 371) notes that certain fold types are unable to affect an unlimited number of successive layers without altering their geometry, i.e. where dip isogons either converge or diverge toward the inner fold arc, they cannot do so in perpetuity or they will come into contact with each other or with the axial surface, which is geometrically and dynamically unacceptable. Thus folds of Classes 1 or 3 must alternate from layer to layer, either with each other, or with Class 2 folds. Buckling behaviour in the coarser clastic layers results in ductile flow in intervening lithologies giving rise to a mixture of Classes 1 and 3 within a dominantly Class 2 regime. This is seen to some extent in Figure 48. Alternatively, the geometric adjustment necessary to accommodate divergent or convergent isogons may manifest as limb thrust faults, shears, bedding transposition, etc. These features are observed in folded BIF in the HRos: Figure 29, from which Figure 49 is traced, exhibits extreme transposition, effectively eradicating original stratigraphy; at least two limb thrust faults are visible in Figure 26 and are shown in the tracing, Figure 49. The faults sinistrally offset units and merge with bedding as bedding parallel faults.

Ramsay (1967, p.421) considers that similar folds (Class 2) result from "a very ductile state during fold formation". Also, with reference to Figure 47, if there is a range of size of similar folds of various amplitudes and wavelengths, which probably represent different stages in the development of the fold model, then "there are only two possible processes that can account for the formation of the folds:

1) progressive, inhomogeneous, simple shear, and

2) a uniform homogeneous strain throughout the region together with a progressive, inhomogeneous simple shear." (Ramsay 1967, p.422).

In either case, progressive, inhomogeneous, simple shear is an integral component of the deformation process. These folds are formed by a variable component of shear acting across the layering and transposing layers as passive markers; hence the folds may be called shear folds (Ramsay 1967). This phenomenon will be addressed further in this report and the interested reader is referred to work by Kehlenbeck (1986), Lavigne (in preparation) and Buck (1986).

The volumetrically less significant, magnetite-jasperite chert component of the BIF reacted to stress in a different manner. Figure 28 displays folds in the jasper-bearing unit that can be described as convolute, or disharmonic, using the terminology of Hobbs et al. (1976), to indicate that axial planes do not pass from layer to layer. Ramsay (1967) suggests that this phenomenon can occur if rheological properties, such as viscosity of adjacent layers, differ.

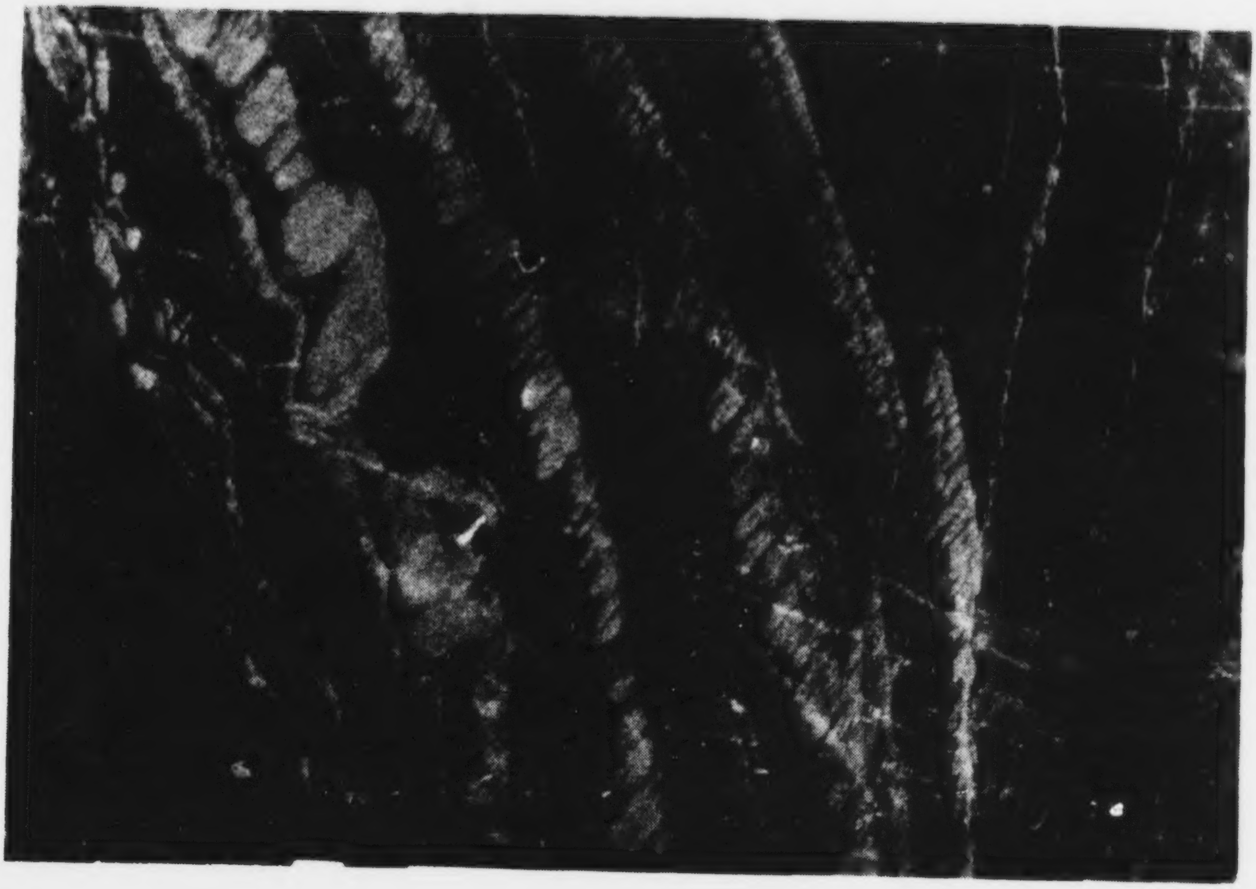

Figure 50 : Carbonate-rich layers in siltstone, Hard Rock Open Stope, Geraldton. Layers segregated into ovoids by cleavage development. Field of view is 20 cm.

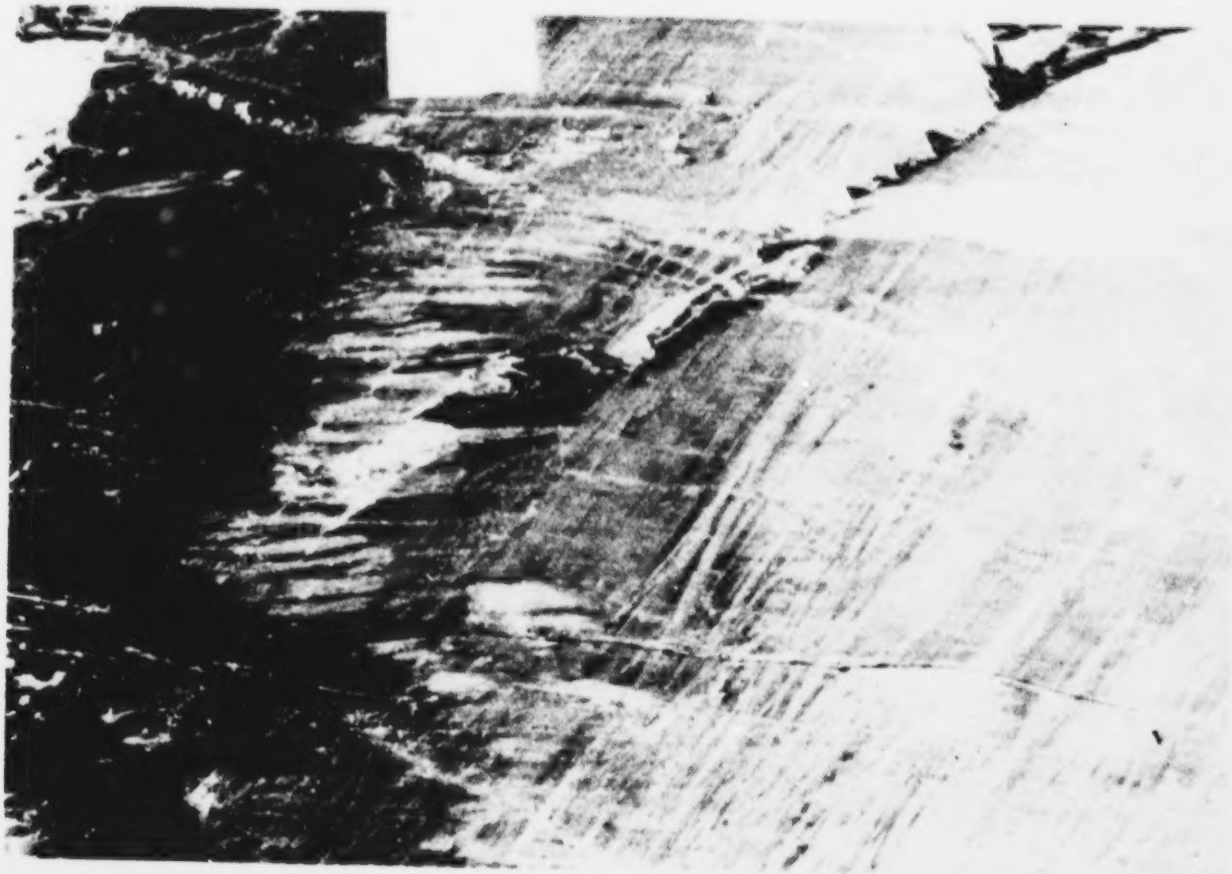

Figure 51 : Folded carbonate layer in siltstone; lozenges become disaggregated in fold nose, Hard Rock Open Stope, Geraldton. Scale card is 9 cm long.

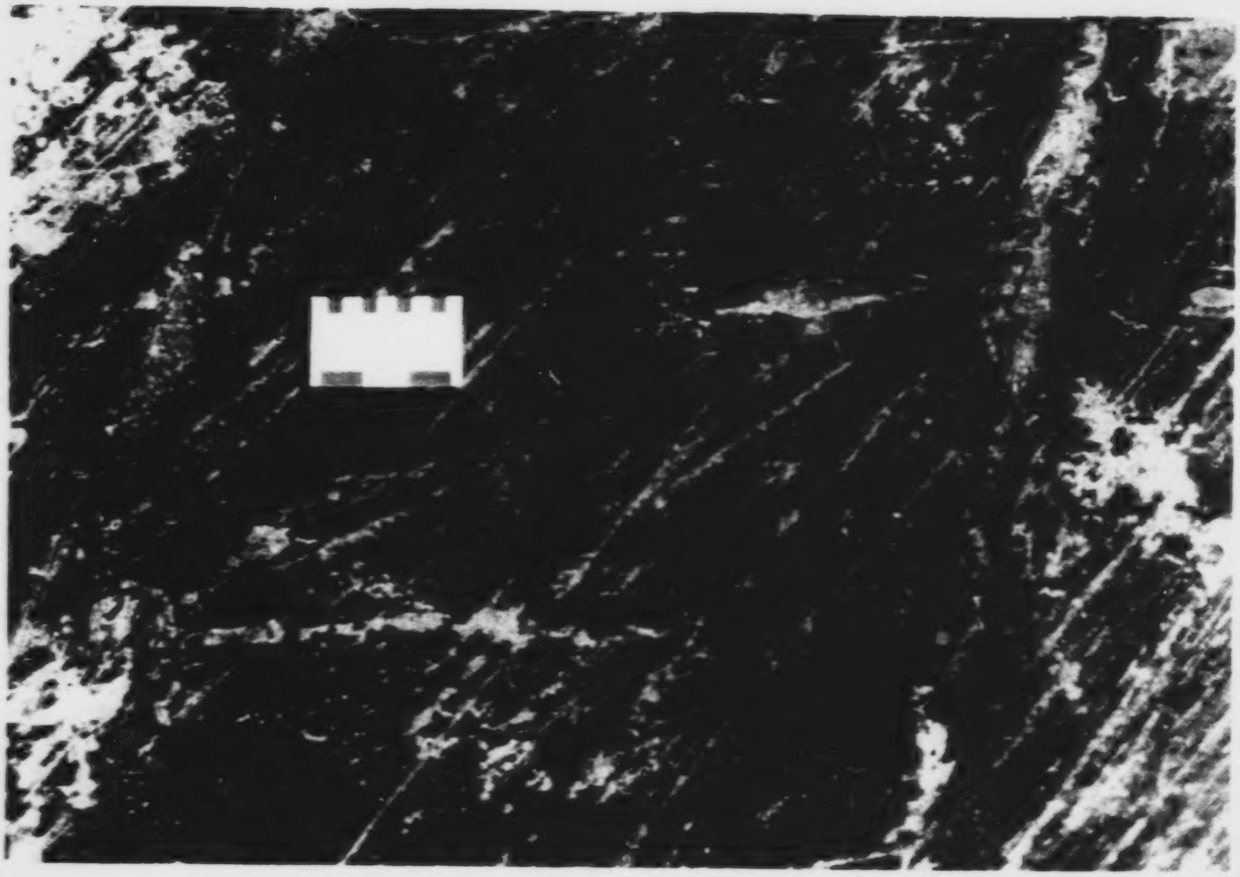

Figure 52 : Completely disaggregated carbonate layers in siltstone, with ovoids of carbonate "floating" in the clastic sediment, Hard Rock Open Stope, Geraldton.

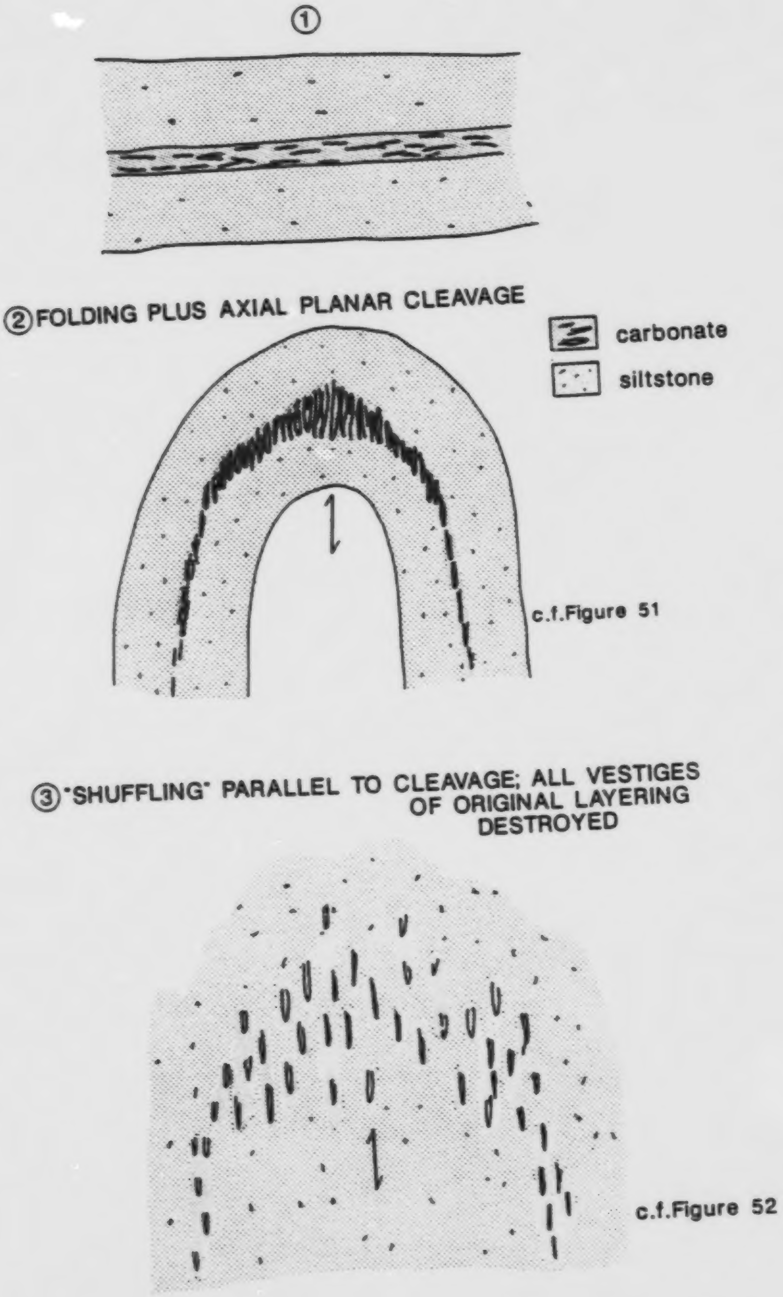
①
② FOLDING PLUS AXIAL PLANAR CLEAVAGE
carbonate
siltstone
c.f.Figure 51
③ "SHUFFLING" PARALLEL TO CLEAVAGE; ALL VESTIGES OF ORIGINAL LAYERING DESTROYED
c.f.Figure 52

Figure 53 : Schematic representation of the disaggregation of carbonate layers in siltstone during folding, Hard Rock Open Stope, Geraldton.

8.2.3.2. Wacke and siltstone

In the vicinity of the HRos, original sedimentary features of the fine to medium grained clastic rocks are highly deformed (e.g. Figure 36) and often obscured. Figure 50 shows deformed wacke in which lighter coloured beds are disrupted by a non-penetrative cleavage development, forming elongate shapes. Further deformation of this style is exhibited in Figure 51, where the wacke contains a light coloured, stratiform, but folded carbonate-bearing unit (of unspecified origin). An axial planar cleavage is well developed; which in the hinge zone of the carbonate unit in Figure 50 is dissected into discrete, prolate, ellipsoidal shapes. Adjacent to the outcrop in Figure 51 is wacke containing an apparently random distribution of carbonate ellipsoids (Figure 52) which may be interpreted to be derived by further deformation of ellipsoids such as those in Figure 51. While adequate strain markers are not present to define precisely the mode of strain within wacke, an interpretation is shown in Figure 53.

At contacts between wacke and BIF, deformation is more extreme than seen within the bulk of the BIF (e.g. Figures 26, 27) reflecting the differing rheological properties of the two rock types, as proposed above to account for disharmonic folding in jasper-rich bands. Figure 54 shows intensely deformed magnetite-rich bands within wacke. Apparent disconformities are present between bedding in the magnetite-rich bands and adjacent wacke. Such disconformities are nowhere seen in relatively undeformed rocks and are considered to be the result of bedding plane transposition, resulting from differences in strain exhibited by the two rock types. In addition, the upper part of Figure 54, shows a fold limb that has been dismembered and is not further traceable in outcrop. Wacke appears to have "flowed" into the void left by the tectonic rupture of a fold limb.

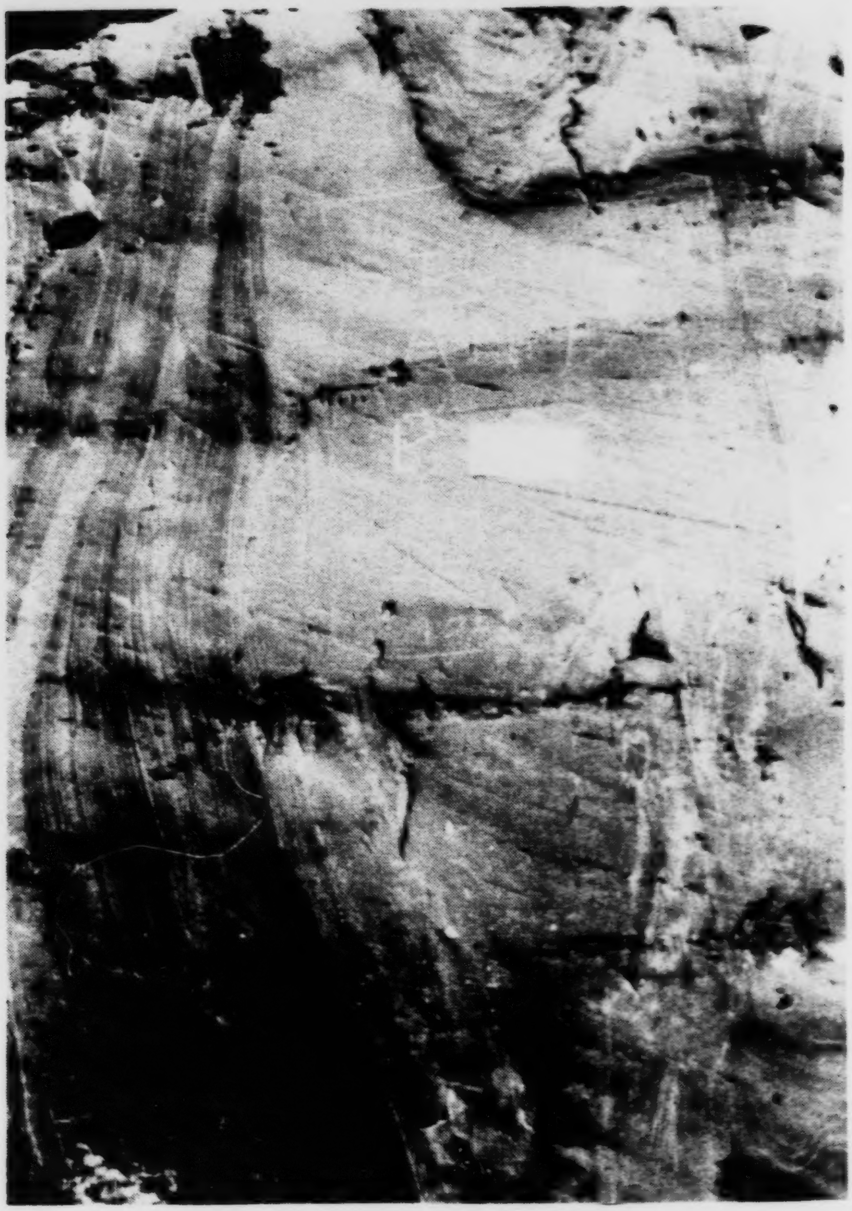

Figure 54 : Dismembered magnetite bands within siltstone, Hard Rock Open Stope, Geraldton.

Although siltstone is a minor component of the clastic sediments, where present it exhibits yet another strain style, that of well-developed pressure solution, as shown in a photomicrograph in Figure 55. The relationship between this spaced cleavage and remnants of original bedding is only visible in fold hinges; on the flanks of the tight, low amplitude folds characteristic of the HRos, fabric and bedding are subparallel and the former overprints and obscures the latter.

8.2.3.3. Soft Sedimentary Structures

Clastic dikes in the HRos may show some spectacular folds (e.g. Figure 38). As these soft sedimentary features are generally accepted to have formed during early diagenesis of the units due to density disparity between adjacent layers (Borradaile et al. 1982), and were originally perpendicular to bedding, they are excellent strain markers. The fold style exhibited in Figure 38 seemed initally enigmatic: it consists of a sequence of S shaped folds, whereas the bulk of the minor folds observed in BIF throughout the stope are Z shaped; for example in Figure 38, Z shaped folds are present in BIF adjacent to the S shaped folds of the clastic dikes. Hugon and Schwerdtner (1985) and Andrews et al. (1986) have demonstrated how early buckle folds of a Z shape may undergo passive amplification during homogenous simple shear (Figure 56). Thus, an originally Z folded feature (the expected fold morphology in a dextral shear) at a high angle to the shear zone margin may develop into S folds at late stages of intense dextral shear.

Close inspection of Figures 38 and 56, however, reveal geometric differences which suggest that this hypothesis is inapplicable: the short limbs of the buckle folds in Figure 38 are attenuated when compared to the longer limbs. The model of Hugon and

Schwerdtner (1985) in Figure 56 would suggest exactly the opposite. H. Williams (Geologist, Ontario Geological Survey, personal communication, 1987) has suggested that the observed geometry is produced by simple buckling of the dike, due to compression and shortening perpendicular to layers followed by layer parallel, dextral shear.

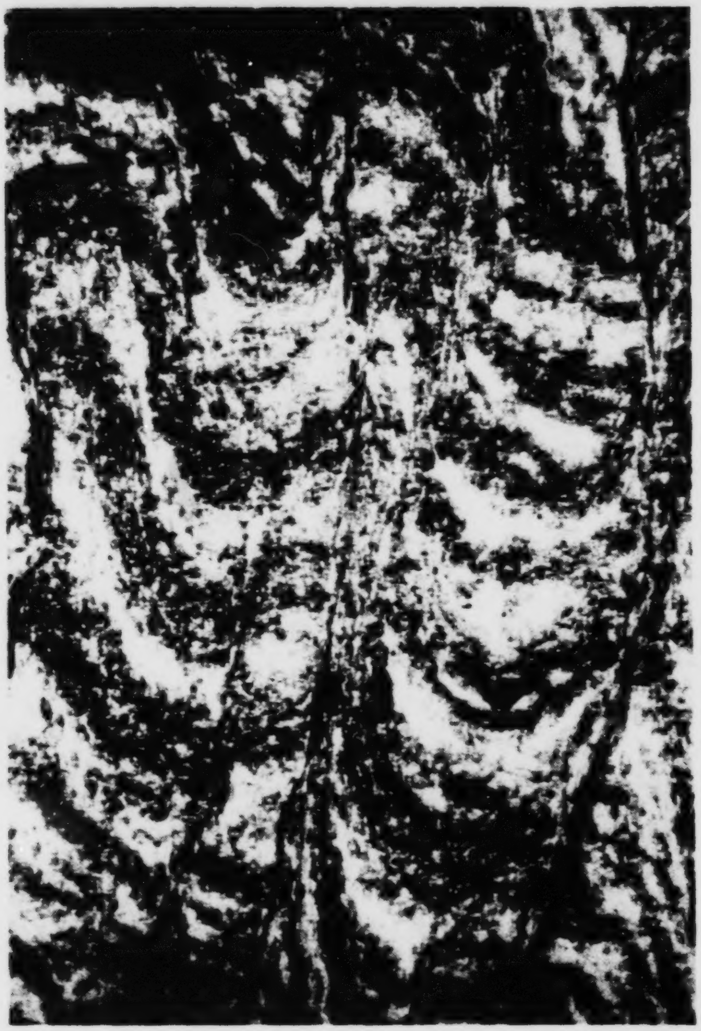

Figure 55 : Spaced, pressure solution cleavage in siltstone, Hard Rock Open Stope, Geraldton. Field of view is 1mm.

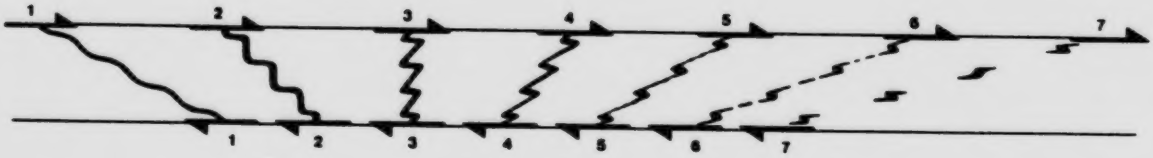
1
2
3
4
5
6
7
1
2
3
4
5
6
7

Figure 56 : Transformation of Z to S Folds through progressive shear (after Hugon and Schwerdtner 1985).

8.2.3.4. Porphyry

The "porphyry" units serve as excellent indicators of minor folds within the HRos (refer to Map, back pocket and Figure 25). Figure 57 and a tracing, Figure 58 show one of the minor folds at the southeastern corner of the exposure. As described earlier, the unit contains prominent phenocrysts (?) or grains of suspected original quartz, feldspar and amphibole, in variable proportions. The grains show a prominent stretch or elongation lineation (Figure 59) that is sub-parallel to axial traces of folds such as seen in Figures 57 and 58. Aspect ratios of the elongate grains are approximately 5:1:1. The lineation was not observed to be folded.

In thin section, at least one prominent foliation can be seen in the rock, sub-parallel to the elongation of relict (?) amphibole and plagioclase (Figure 60). The foliation is defined by fine grained foliae of white mica, chlorite and carbonate.

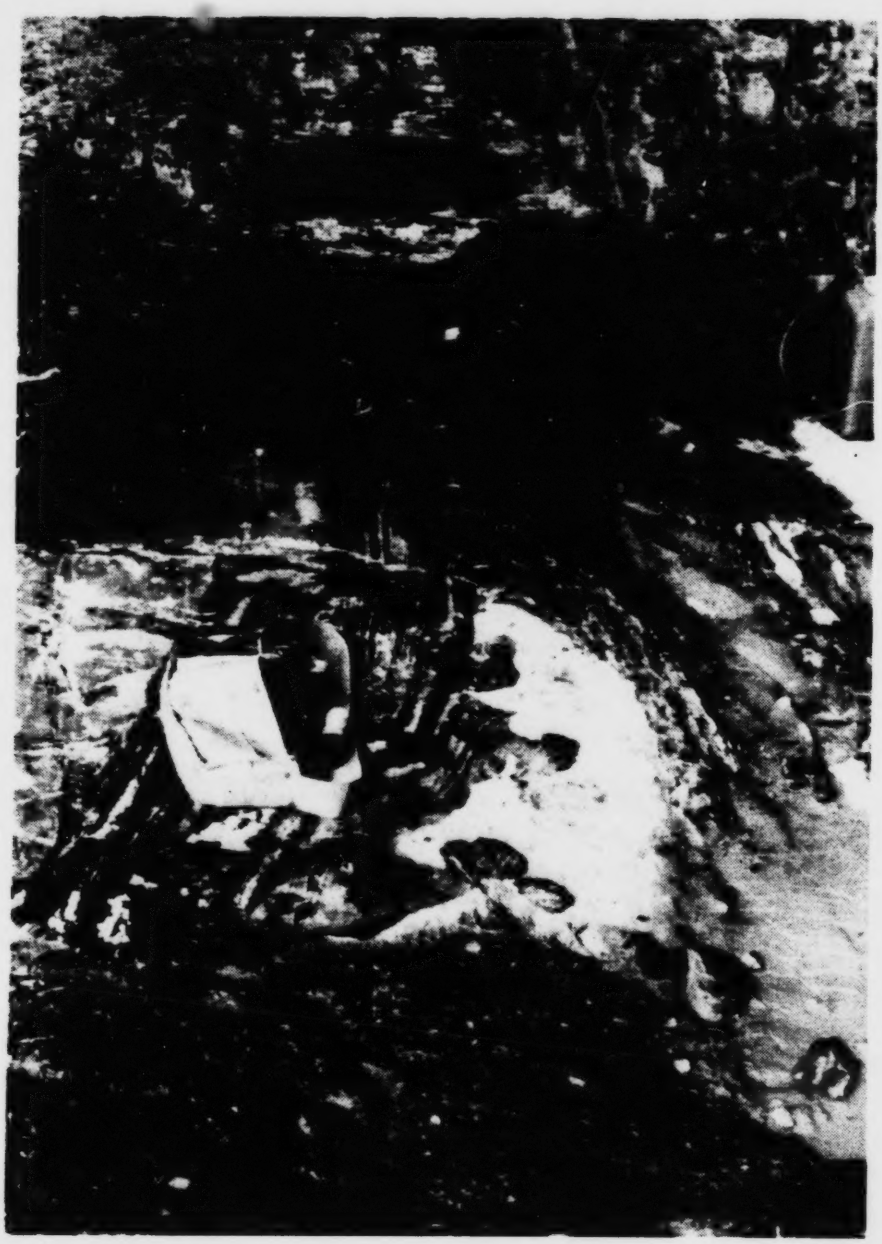

Figure 57 : Folded porphyry/banded iron formation contact, looking west, Hard Rock Open Stope, Geraldton. Bag is 30 cm long.

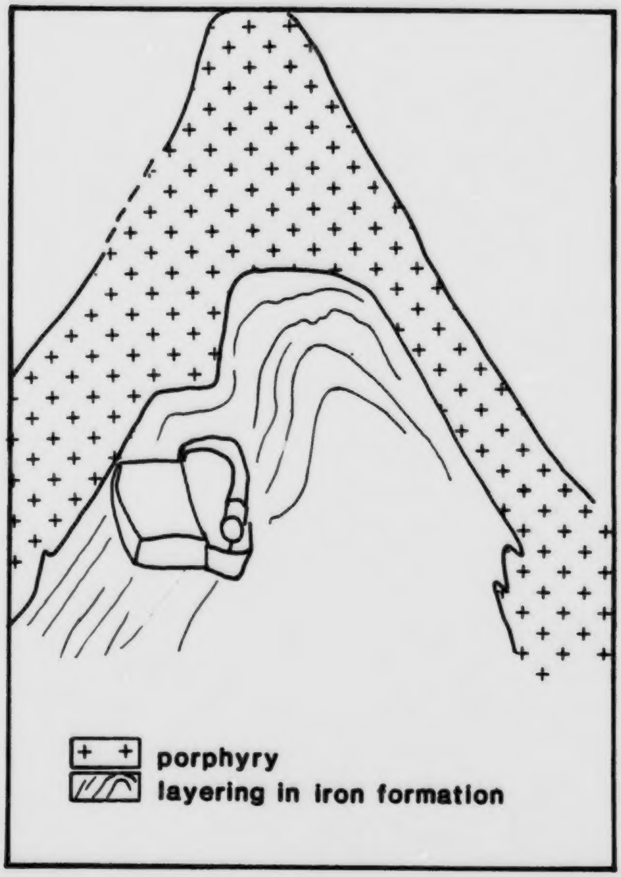
porphyry
layering in iron formation

Figure 58 : Tracing of photograph in Figure 57.

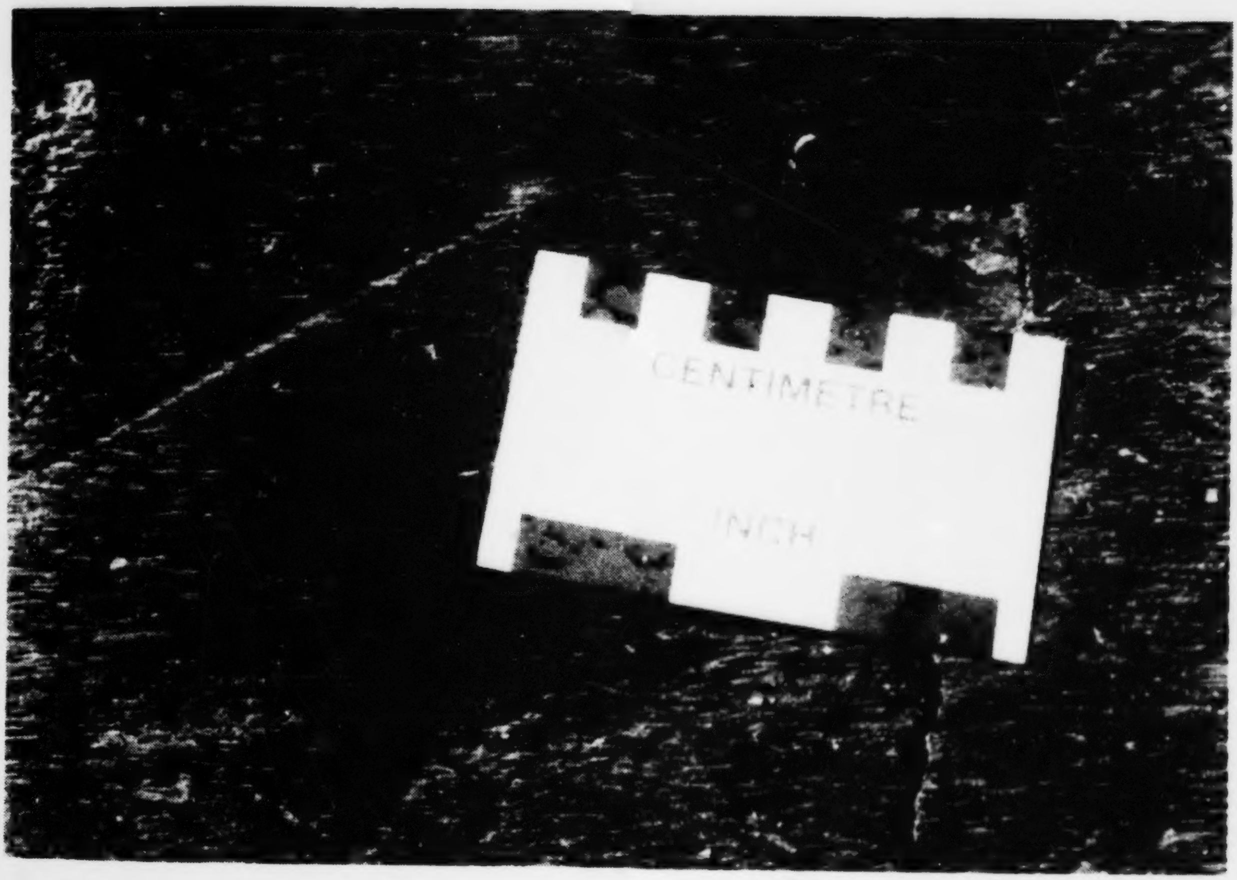
CENTIMETRE
INCH

Figure 59 : Outcrop of Porphyry, Hard Rock Open Stope, Geraldton. Note elongate phenocrysts.

Figure 60 : Foliae of white mica, chlorite and carbonate, and altered phenocrsts of (?) plagioclase and amphibole, Porphyry unit , Hard Rock Open Stope, Geraldton. Field of view is 1 mm.

9.0 Mineralization in the Hard Rock Open Stope

9.1 Veins and Selvages

Several vein types and generations are exposed within the HRos. Vein morphology and style and degree of alteration are, to some extent, host rock dependent and will be described accordingly. In general terms, 3 principal vein sets are recognized in the HRos and, from oldest to youngest, are:

(1) Carbonate veins and veinlets
(2) Quartz-carbonate + tourmaline + sulphide veins
(3) Quartz-carbonate + tourmaline + sulphide veins.

Relative age of vein sets is based upon observed cross-cutting relationships. Vein set 3, while containing an identical mineralogy, cuts and is therefore younger than set 3.

9.2 Carbonate Veins in BIF

Red weathering carbonate fills fractures in BIF (Figure 30), which are typically less than 1 cm thick and are ubiquitous throughout the HRos exposure. Staining of rocks with a 2% HCl and potassium ferrocyanide solution gives a deep blue colour, confirming the presence of ankerite or ferroan dolomite. Relative timing between carbonate fractures and other veins in the BIF is not well constrained as critical cross-cutting relationships are obscured by voluminous alteration selvages that accompany quartz veins in this rock type (see below). Careful examination of slabs of BIF (Figure 61) reveals that carbonate veinlets cut stratigraphic layering, and are folded where the IF beds are folded into asymmetric folds. This provides two pieces of information:

1) that asymmetric folds are a post-lithification phenomenon, and
2) that carbonate veinlets pre-date asymmetric folding in IF,

Interpretation (1) supports the conclusion reached earlier, that asymmetric folds in the IF do not represent a pre-lithification, "soft-sedimentary" slump folding, as an unlithified rock is, by definition, unable to undergo brittle failure.

9.3 Quartz veins in BIF

Quartz-carbonate + tourmaline + sulphide veins show a close spatial and temporal relationship with asymmetric folding. In a typical exposure, such as that shown in Figure 62, IF is folded into asymmetric folds which exhibit a decreasing wavelength towards the vein; alternatively the folds can be considered to be "tighter", with a smaller interlimb angle, closer to the vein. Quartz-bearing veins are not folded by the asymmetric folds, unlike carbonate veinlets (Figure 61). Therefore quartz-bearing veinlets do not predate asymmetric folding. The relationship between decreasing fold wavelength of the asymmetric folds and quartz veins is suggestive of cause-and-effect relationship. Tightening of folds reflects increased ductile strain, which may increase to the point where brittle failure occurs, allowing a fracture to develop, filling to form a vein. The quartz veins are themselves formed internally, as indicated by strained quartz in thin section, consistent with syn-deformational vein formation.

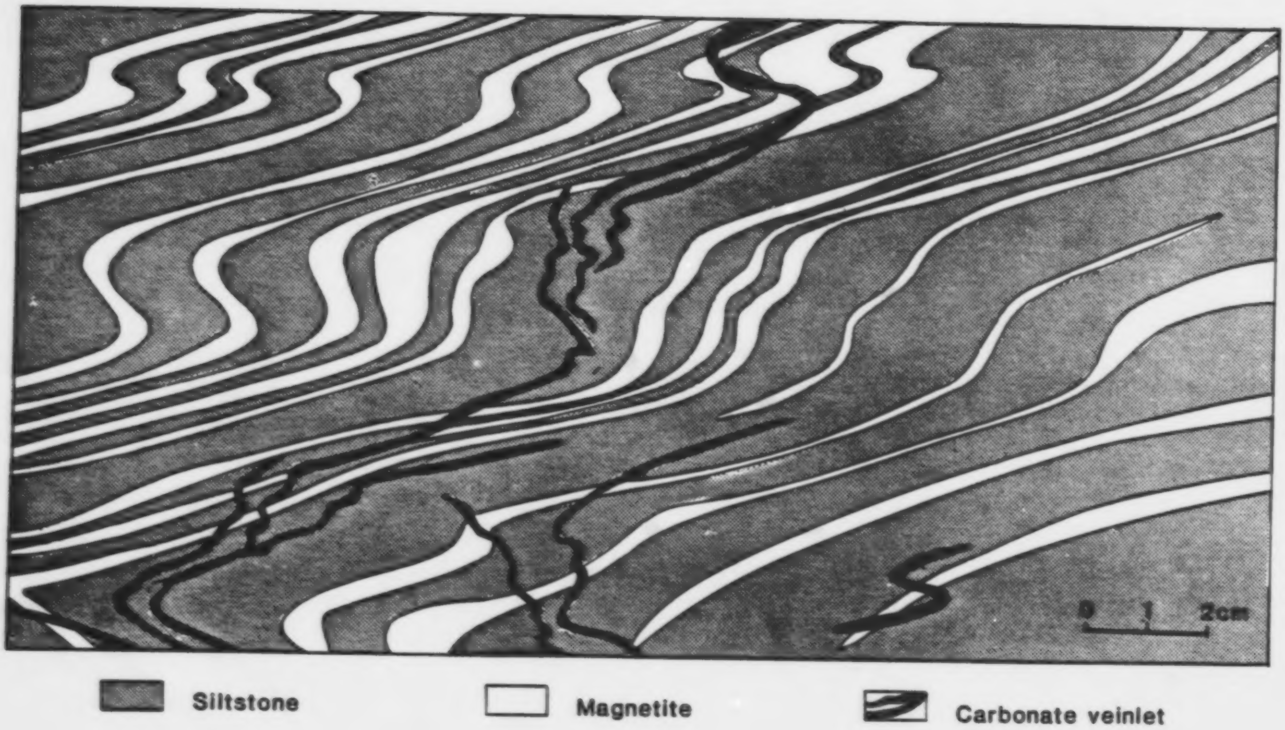
0 1 2cm
▨ Siltstone
☐ Magnetite
Carbonate veinlet

Figure 61 : Sketch of iron formation slab, Hard Rock Open Stope, Geraldton. Note carbonate veinlets cutting stratigraphy and folded by S folds.

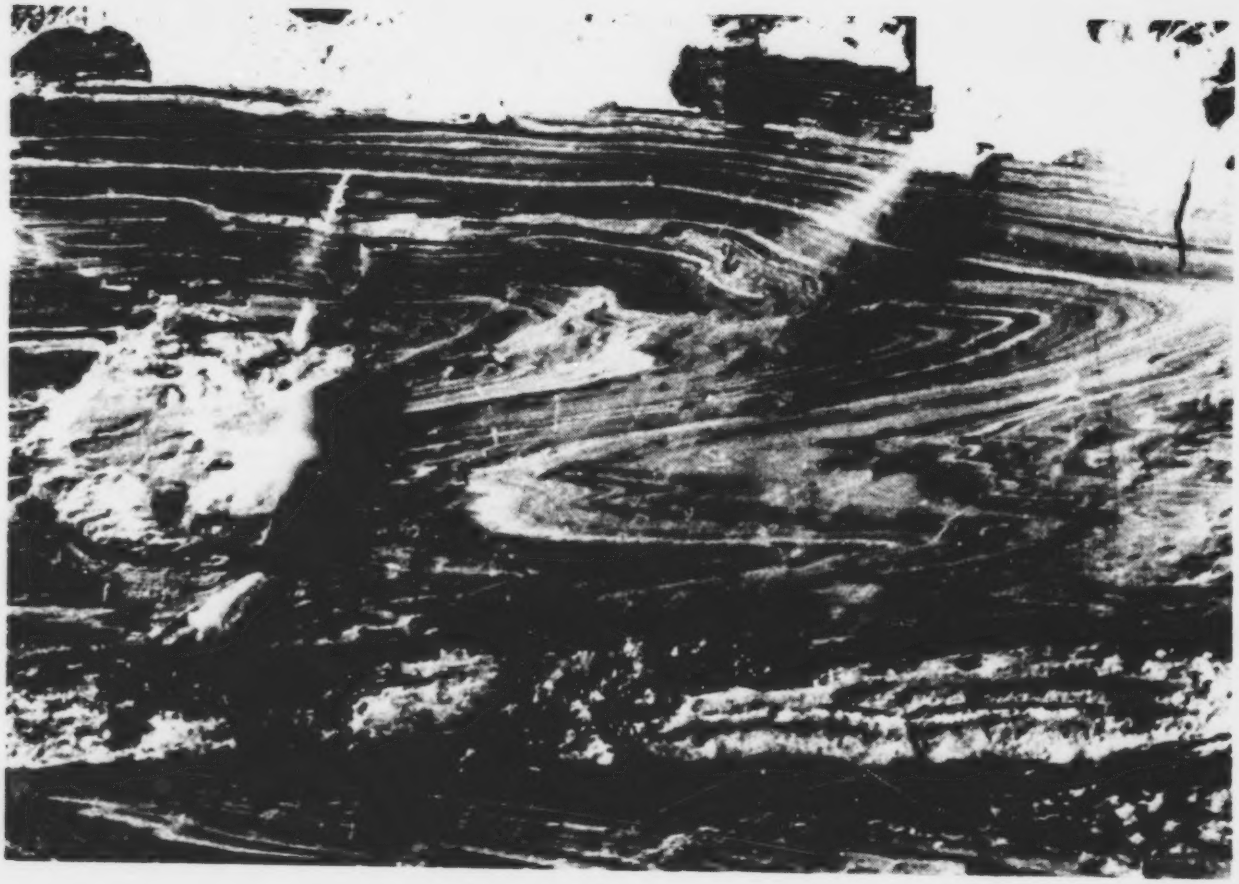

Figure 62 : Quartz-carbonate-sulphide vein cutting folded, banded iron formation, Hard Rock Open Stope, Geraldton. Field of view is 30 cm.

Horwood and Pye (1951, p.38 to 45) describe vein mineralogy and paragenesis in detail. The junior author. who was responsible for writing the report, noted (p.34) that the senior author proposed an early, pre-mineralization, silicification of the BIF:" This mineralization occurred along the bedding planes in both the iron formation and greywacke bands to produce narrow quartz stringers and narrow seams of cherty quartz. In the iron formation the chert is coloured dark-greyish red since it has apparently incorporated some iron oxide. Some recrystallization of the magnetic *(sic)* in these bands has also taken place, as the rock has a coarser grain close to the stringers." This observation is not supported by the current study, which considers the red cherty material (e.g. Figure 28) to be an integral component of the mixed clastic/chemical sedimentary rock. There is no field evidence to suggest that the red chert has been introduced subsequent to sedimentation and/or re-sedimentation in the HRos (c.f. Barrett and Fralick 1985). In other locations, however, red chert may be a secondary alteration product product after darker coloured chert (c.f. Temagami BIF, D.H. Watkinson, Professor, Carleton University, personal communication, 1987. The author has, however, observed secondary red chert, restricted to fold hinges on Barton Bay Island, to the west of the Little Long Lake Mine (Figure 3).

Linear arrays of coarser magnetite, and locally specularite, are observed adjacent to microfractures cutting BIF. These microfractures, which may or not not be filled by quartz + red weathering carbonate, are often bedding-parallel and appear to be equivalent to the features observed by Horwood and described above by Horwood and Pye (1951, p.39). Quartz veins in BIF also contain a red-weathering carbonate - shown by Horwood and Pye (1951, p.41) to be intermediate in composition between dolomite and ankerite and is best referred to as ferroan dolomite - tourmaline, minor calcite, and the following sulphides in decreasing order of abundance: pyrite, arsenopyrite and pyrrhotite plus rare sphalerite, galena and chalcopyrite. Iron oxides are also locally present in veins but, as suggested by Horwood and Pye (1951), appear to represent wall rock inclusions. In polished section, magnetite adjacent to quartz veins is seen to be coarser than in wall rock distant from veins, suggesting some recrystallization, and grains may be observed passing from wallrock BIF into quartz veins. Small quantities of scheelite and tellurides have been reported from elsewhere in the camp (Armstrong 1943). The reader requiring more detailed description of mineralogy throughout the Geraldton camp is referred to Pye (1951), Horwood and Pye (1951) and Armstrong (1943). The last author erected a complex paragenetic sequence to account for many of the apparently contradictory relationships observed microscopically throughout the several mines described in his study.

Gold within quartz veins is located in a variety of sites:

(1) intimately associated with sulphides, either as inclusions (Figure 63) or in fractures cutting sulphide (Figure 64),

(2) associated with gangue in veins, either with quartz or carbonate (Figure 65) or in quartz-carbonate threads cutting earlier formed gangue (Figure 66).

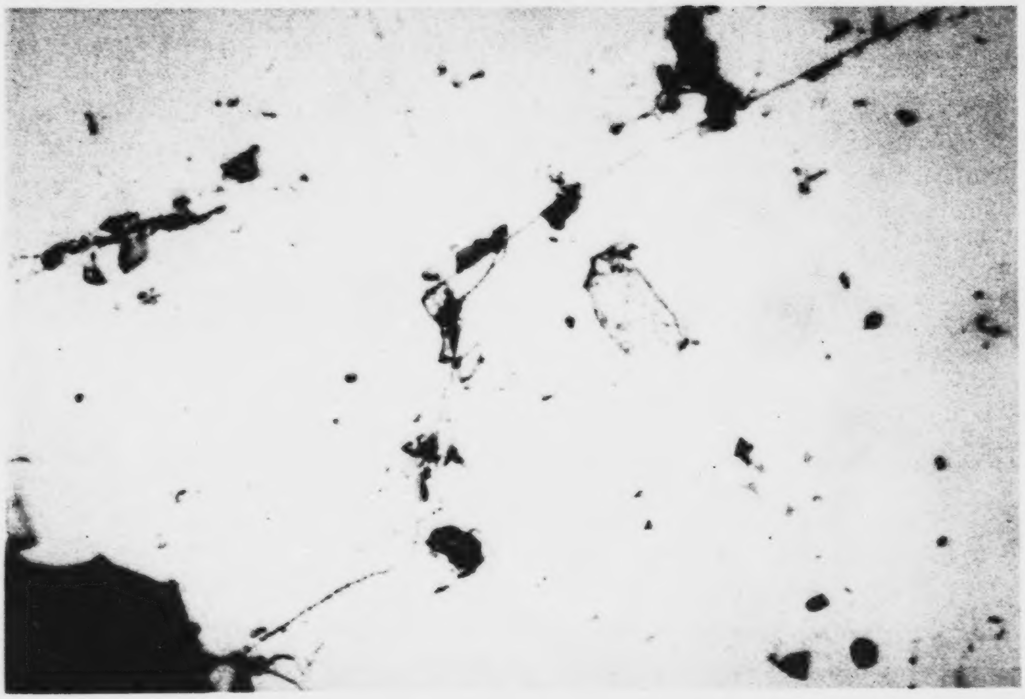

Figure 63 : Grain of gold (100 microns) wholly enclosed within vein pyrite, Hard Rock Open Stope, Geraldton.

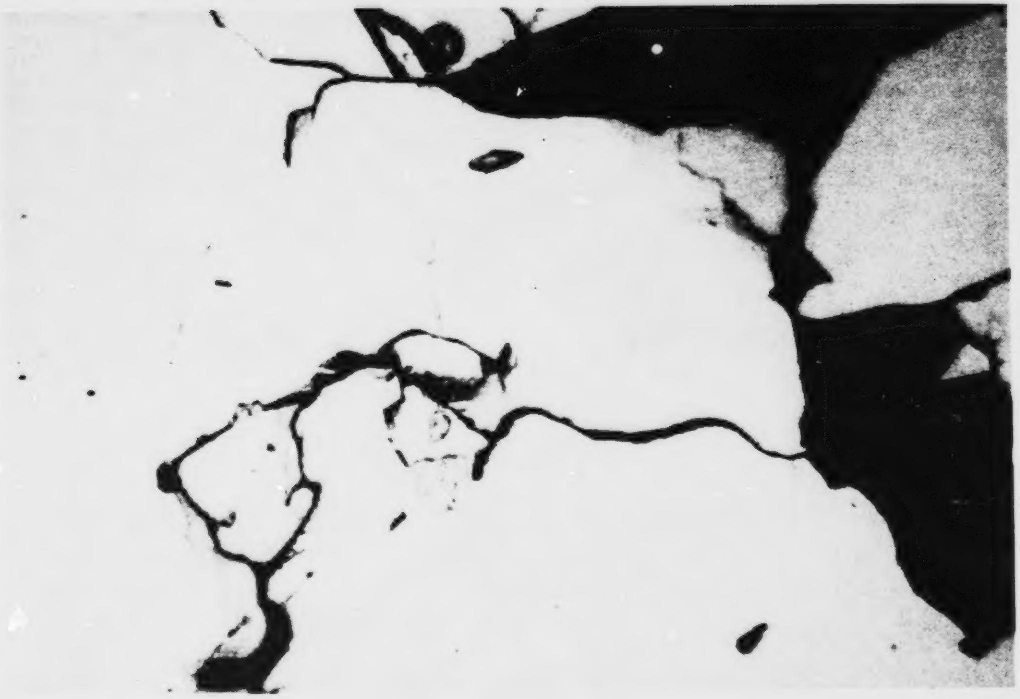

Figure 64 : Gold grains (10 and 50 microns) in fracture within vein pyrite, Hard Rock Open Stope, Geraldton.

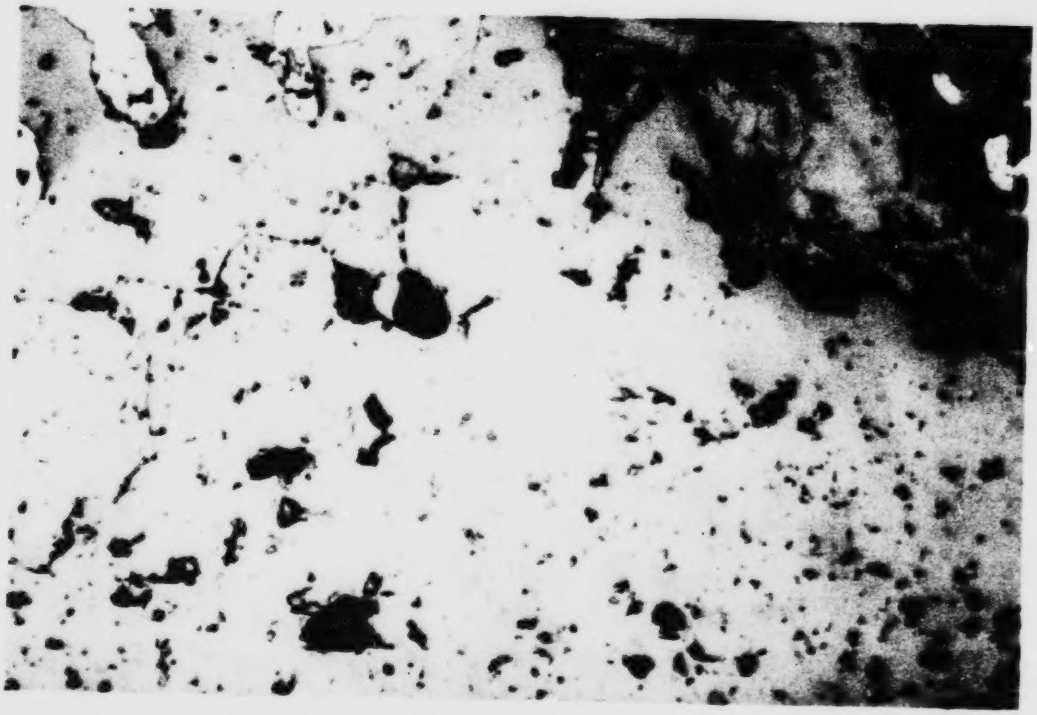

Figure 65 : Gold grain (100 microns) wholly within vein quartz, Hard Rock Open Stope, Geraldton.

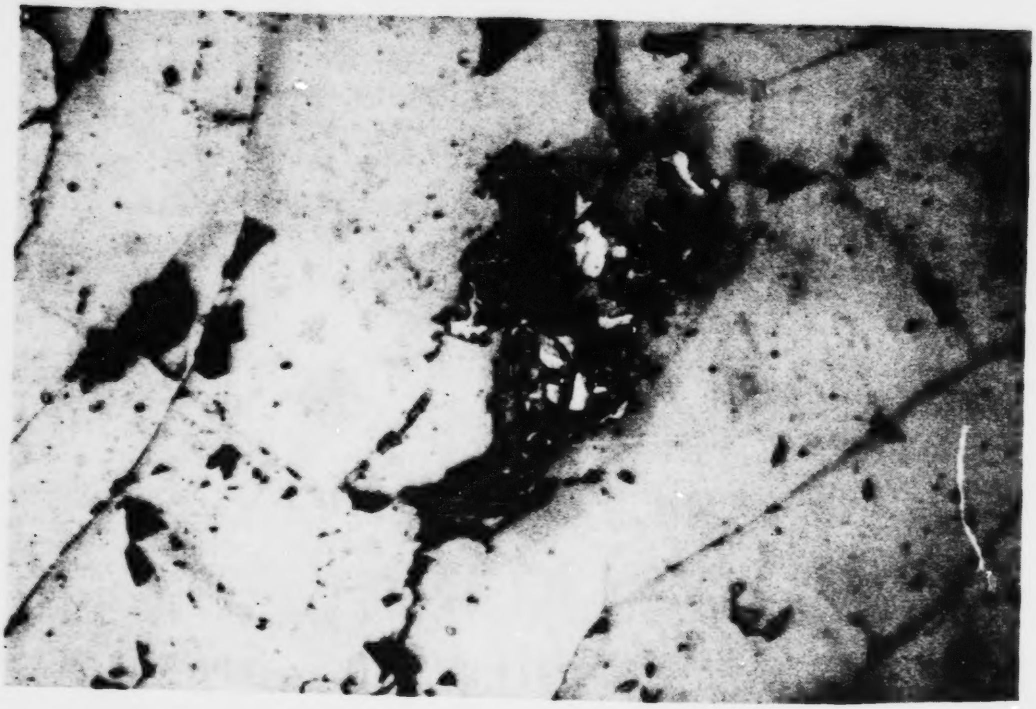

Figure 66 : Gold grains, up to 25 microns, associated with quartz-carbonate threads cutting earlier gangue, Hard Rock Open Stope, Geraldton.

The other principal gold site is in hydrothermal alteration selvages distributed symmetrically about quartz-carbonate veins cutting BIF. For example, Figure 67 shows a 5 to 20 cm wide altered zone on both sides of a 2-3 cm wide quartz-carbonate vein. The geometry of the vein and asymmetrically folded BIF is identical to that in Figure 62. Quartz-carbonate veins, with attendant bilateral deformed and altered zones, are commonly subparallel to lithological layering but are clearly late tectonic features. For example, Figure 68 shows a quartz vein, with disrupted and altered wallrock BIF on both sides of the vein, subparallel to bedding in less deformed BIF, but cutting a folded clastic dike (c.f. Figure 38). Deformation adjacent to the vein is sufficiently intense that fragments of disrupted clastic dikes were not identifiable within the more highly deformed rocks.

The alteration selvage (Figure 67) consists of altered BIF and sulphides, dominantly pyrite, arsenopyrite and minor pyrrhotite (Figure 69). Note in Figure 67 that folded bedding is still visible within the altered rock. The apparent "bedded" sulphides have led to suggestions that the BIF contained an original, syn-sedimentary, sulphide component. Figure 67 indicates that, on the contrary, sulphides are only present within BIF as haloes distributed on either side of veins. Petrographic analysis of the rock demonstrates that sulphides replace the oxide component of BIF (Figure 70). The "well-bedded" nature of the sulphides attests to the efficiency of the replacement process, selectively altering magnetite-bearing mesobands within the BIF and retaining the integrity of original stratigraphy.

Sulphur replacement of oxygen to form iron-bearing sulphides from iron-oxides is a feature common to BIF-hosted gold deposits at Pickle Lake, Opapamiskan Lake, Emerald Lake and Carshaw deposits in Ontario (Barrett and Johnson 1948; Hall and Rigg 1986;

Macdonald 1984a and in press; Fyon et al. 1983. Phillips and Groves (1984) have described similar processes at Mount Magnet, Australia.

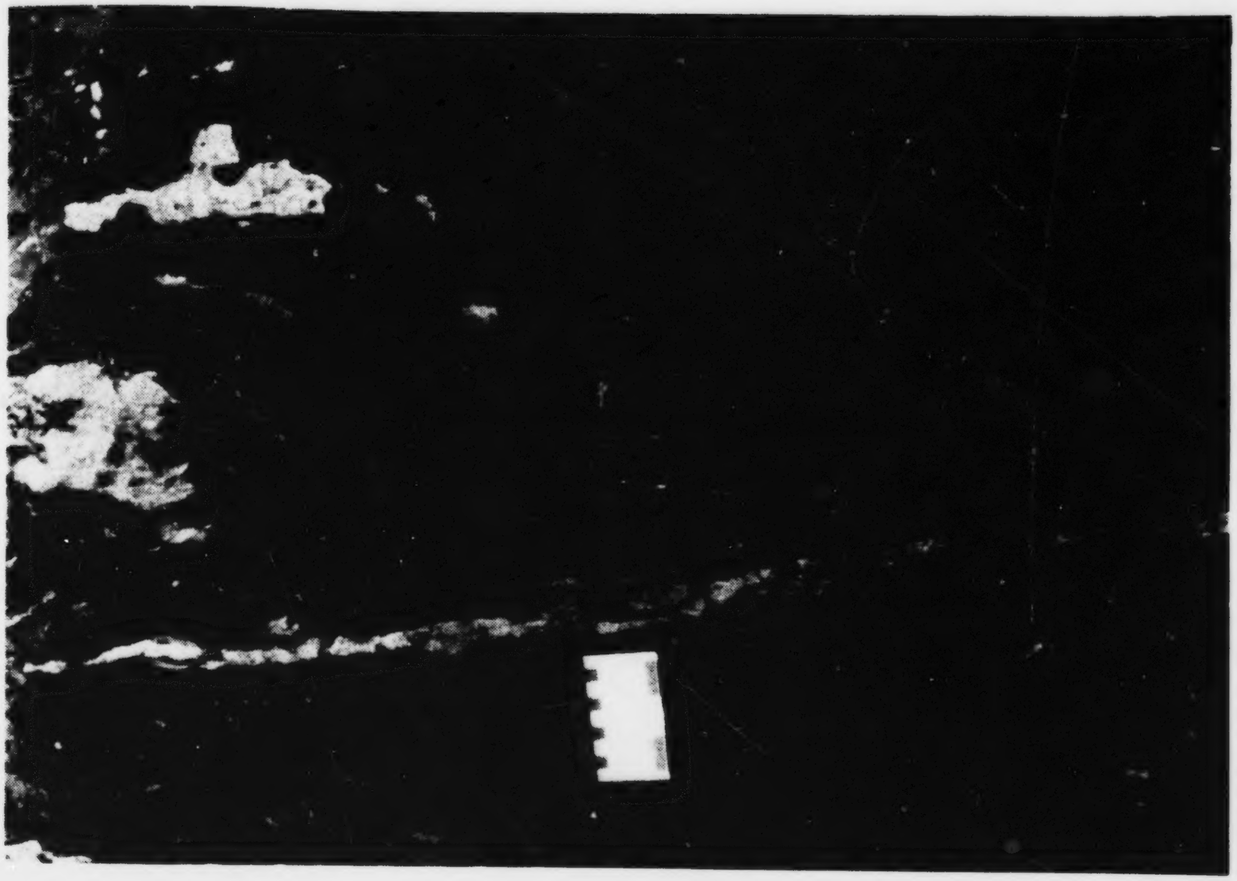

Figure 67 : Zone of sulphidation, bilaterally distributed around quartz-carbonate vein, Hard Rock Open Stope, Geraldton.

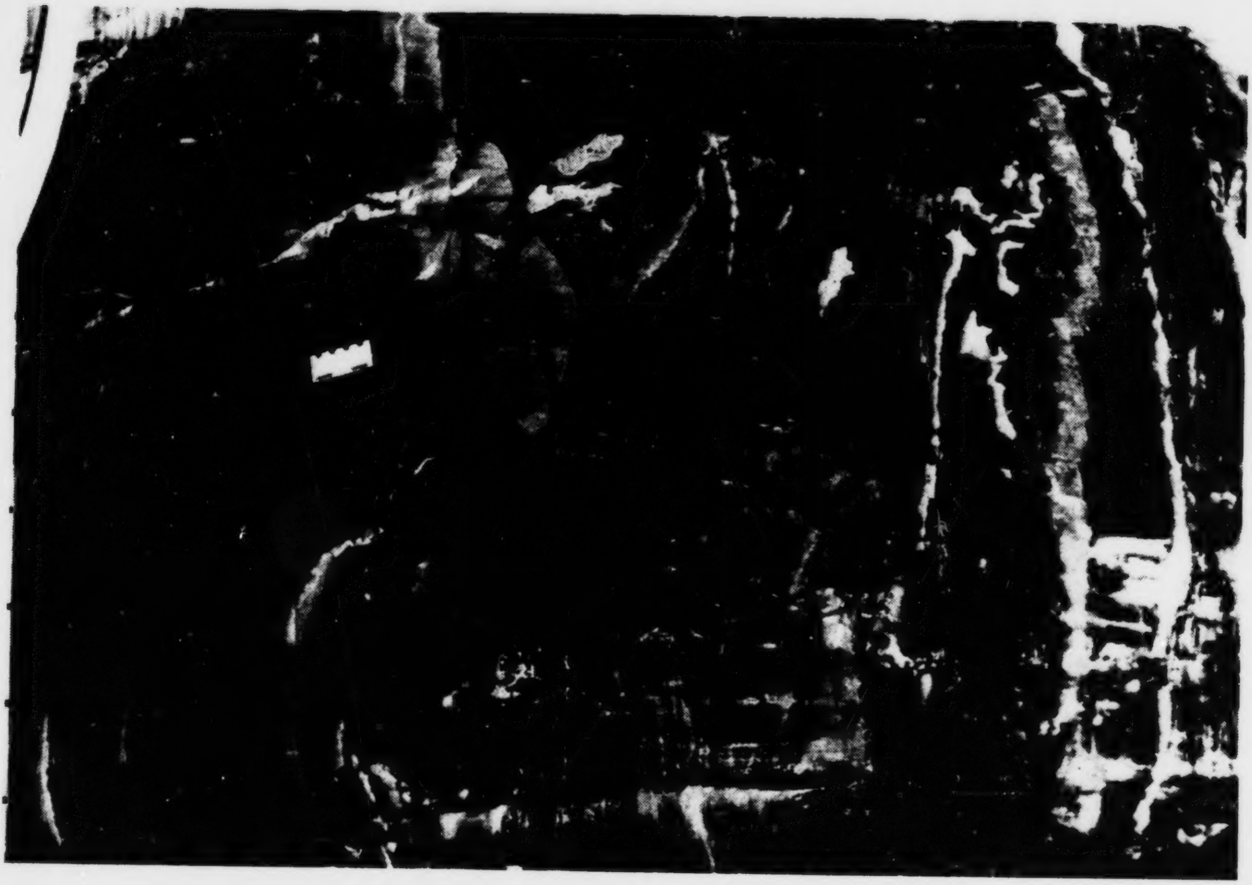

Figure 68 : Quartz-carbonate vein in bedding-parallel deformation zone that cuts folded clastic dike, Hard Rock Open Stope, Geraldton.

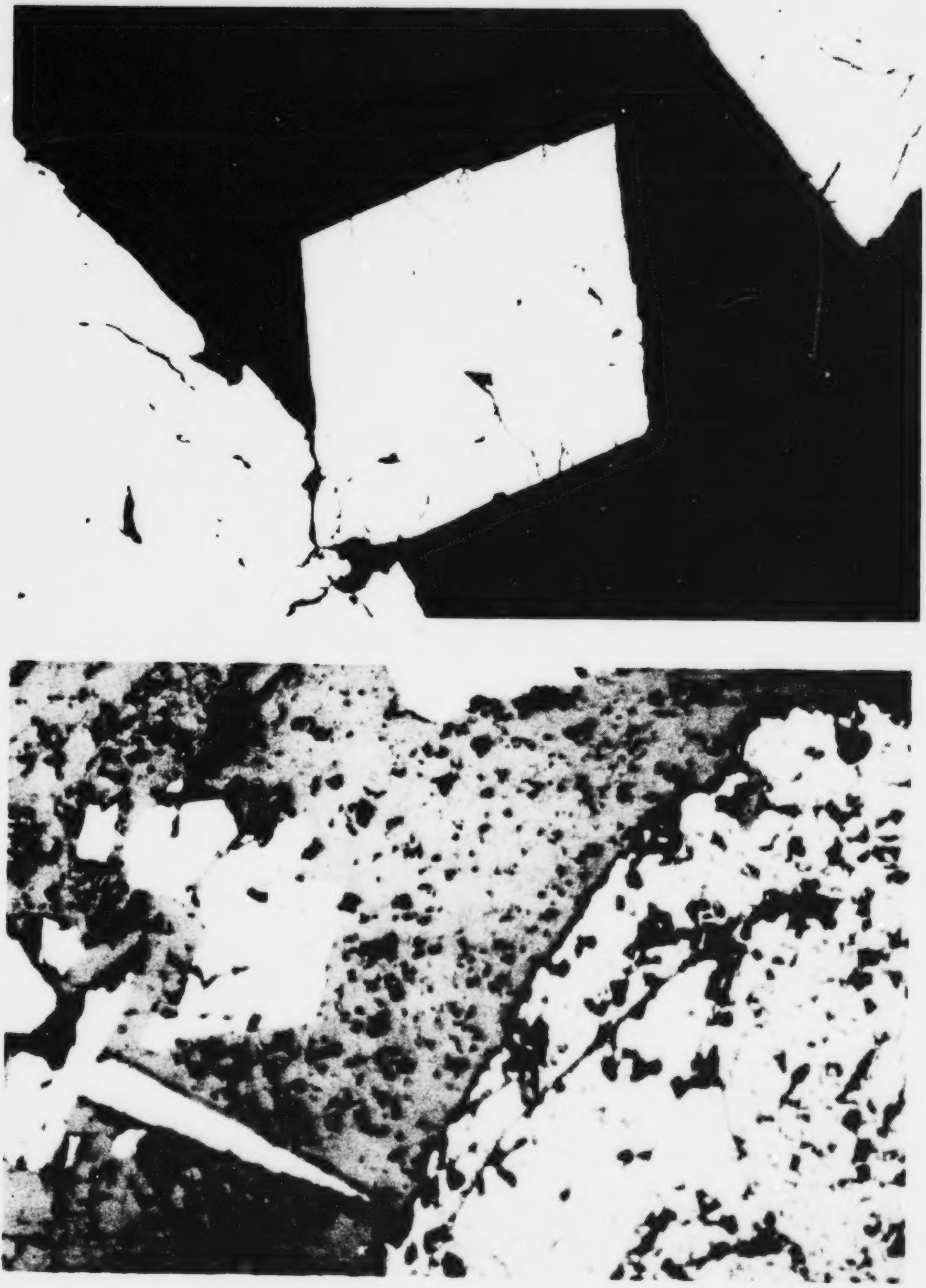

Figure 69 (a) and (b) : Arsenopyrite rhombs (and pyrite, chalcopyrite) in sulphidation selvages, Hard Rock Open Stope, Geraldton. Field of view : (a) 1 mm, (b) 2 mm.

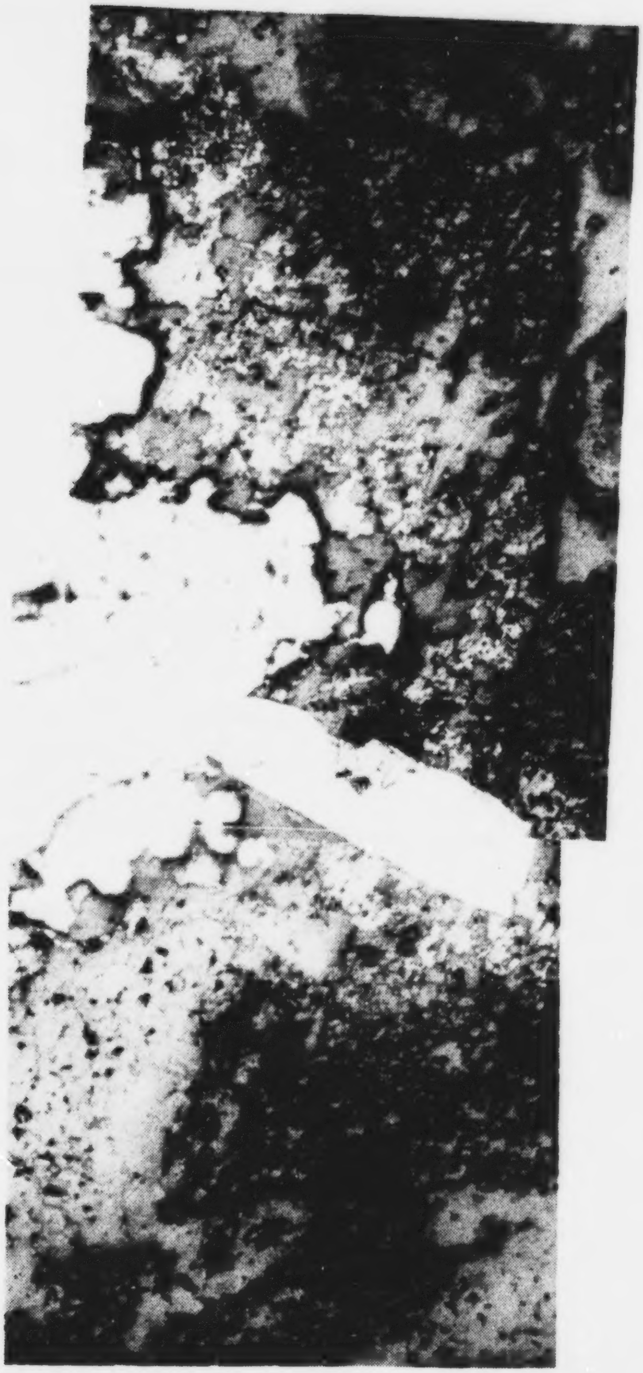

Figure 70 : Arsenopyrite and pyrite (white) replacing magnetite, Hard Rock Open Stope, Geraldton; Field of View 3 mm.

TABLE V : CHEMISTRY OF ALTERED IRON FORMATION, HARD ROCK OPEN STOPE.

	82-004	82-039	83-330a	83-330b	83-330d	83-330e
SiO_2	30.0	23.5	32.4	28.2	23.4	52.6
TiO_2	0.14	0.21	0.16	0.25	0.25	0.02
Al_2O_3	5.7	4.8	3.68	5.9	2.2	0.78
Fe_2O_3	24.6	35.1	26.8	30.0	41.98	26.8
FeO	11.1	17.8	19.7	6.76	3.71	13.6
MnO	0.09	0.06	0.07	0.05	0.04	0.03
MgO	1.86	1.53	1.87	1.5	0.5	0.29
CaO	1.58	3.81	1.90	2.1	1.3	1.35
Na_2O	0.0	2.01	0.97	0.32	0.19	0.18
K_2O	1.16	0.46	0.27	1.18	0.48	0.0
P_2O_5	0.19	0.09	0.16	0.18	0.16	0.1
CO_2	6.73	5.46	7.36	1.16	2.16	2.07
S	18.1	2.25	2.08	23.4	30.5	0.35
H_2O^+	2.14	0.59	1.48	2.6	2.38	0.27
H_2O^-	0.3	0.12	0.16	0.2	0.3	0.03
LOI	(19.5)	(2.00)	(8.7)	(20.0)	(23.6)	(0.9)
TOTAL	103.6	97.79	99.06	103.8	109.55	98.47
As	2.6%	1640	920	7600	3.8%	120
Au(ppb)	12,900	480	360	31,400	18,500	60
B	170		20	120	22	dl
Ba		760	270	140	200	50
Co	7	9	dl	5	dl	dl
Cr	54	56	40	48	26	10
Cu	16	66	13	22	15	12
Nb		8	8	6	5	4
Ni	26	16	12	19	dl	dl
Sb	170	23	25	42	59	12
Sr	65	100	85	90	55	45
V	95	80	50	45	20	10
Y	8	6	6	7	4	3
Zn	40	58	70	63	30	16
Zr		35	16	30	11	3

All samples {AJM} Series
dl : below detection limit
All trace elements in ppm unless specified otherwise

A 5 cm wide, 5 cm deep channel sample was taken across a vein and sulphide selvage from the HRos (Figure 71). Figure 72 shows the distribution of certain elements and oxides from the channel sample, with data plotted for the marginal carbonate altered BIF, the sulphide selvage and the central quartz-carbonate vein ignoring volume effects (c.f. Gresens 1967). The data show (1) a general increase in Fe_2O_3 in the sulphide selvages; (2) a decrease in FeO from altered BIF into the vein; (3) a marked addition of [S] in the vein and selvage; (4) an addition of B to the vein and selvages; (5) considerable As, Sb and Au addition to the vein selvages.

While gold is elevated in both vein and selvage, it is highest in the latter. Table V gives data for altered BIF samples selected from vein selvages in the HRos. In comparing Tables V and III, the data indicate that BIF in close proximity to a vein displays the features shown graphically in Figure 72, i.e. elevated Au, S, Sb, As, B and in many cases, elevated CO_2 incorporated as the iron-bearing carbonate.

One such quartz-carbonate vein and alteration selvage displays associated fibrous quartz-carbonate "ladder" veins at a high angle to the main quartz-carbonate vein (Figure 73), shown in close-up in Figures 74 and 75. The ladder veins consist of alternating quartz and red weathering carbonate fibres. These extension fissures usually initiate in a direction perpendicular to the maximum, incremental, longitudinal strain acting at the time of initiation (Ramsay and Huber, 1983, p.235). Fibres in the extension veins link points that were once in contact; i.e. if fibres are straight, they indicate that progressive strain occurred without change in attitude of the strain ellipse, while curved fibres would indicate an incrementally rotating strain ellipse. Figures 73 to 75 display generally straight fibres, although vein extension is not perpendicular to vein walls; in both Figures 74 and 75, the fibre attitudes indicate that there is a component of dextral motion accompanying progressive opening.

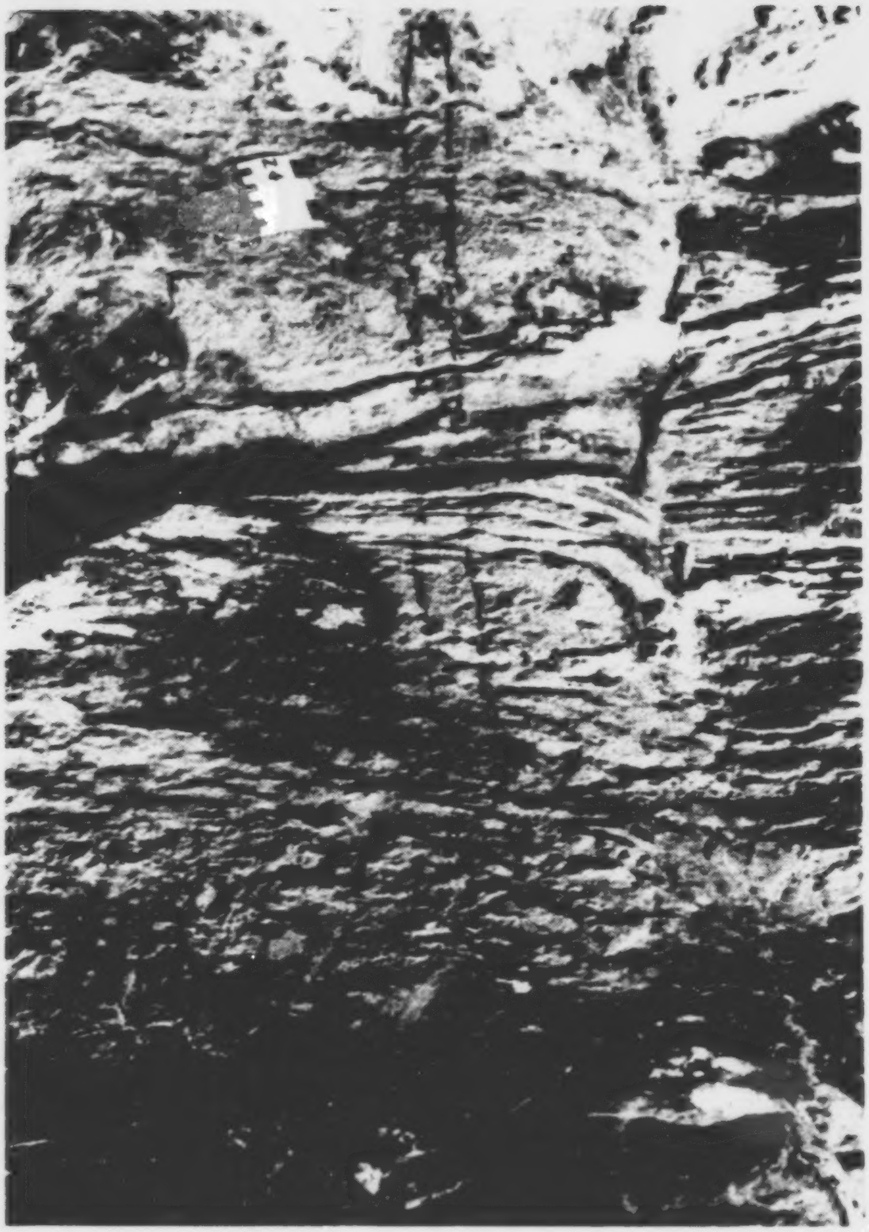

Figure 71 : Location of channel cut across quartz-carbonate vein and bilateral zones of sulphidation, Hard Rock Open Stope, Geraldton.

Mineralized BIF, HROS, Geraldton

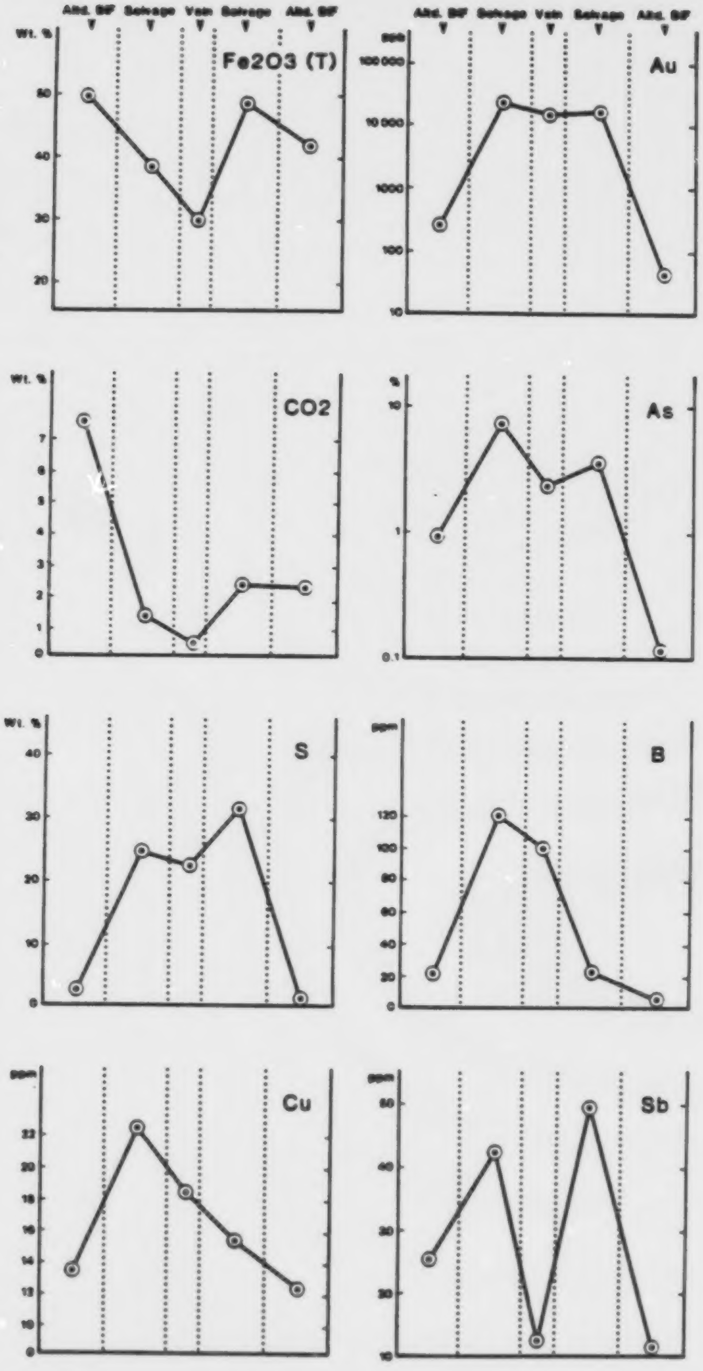

Figure 72 : Oxide and trace element variability across vein and sulphide selvage in Figure 71.

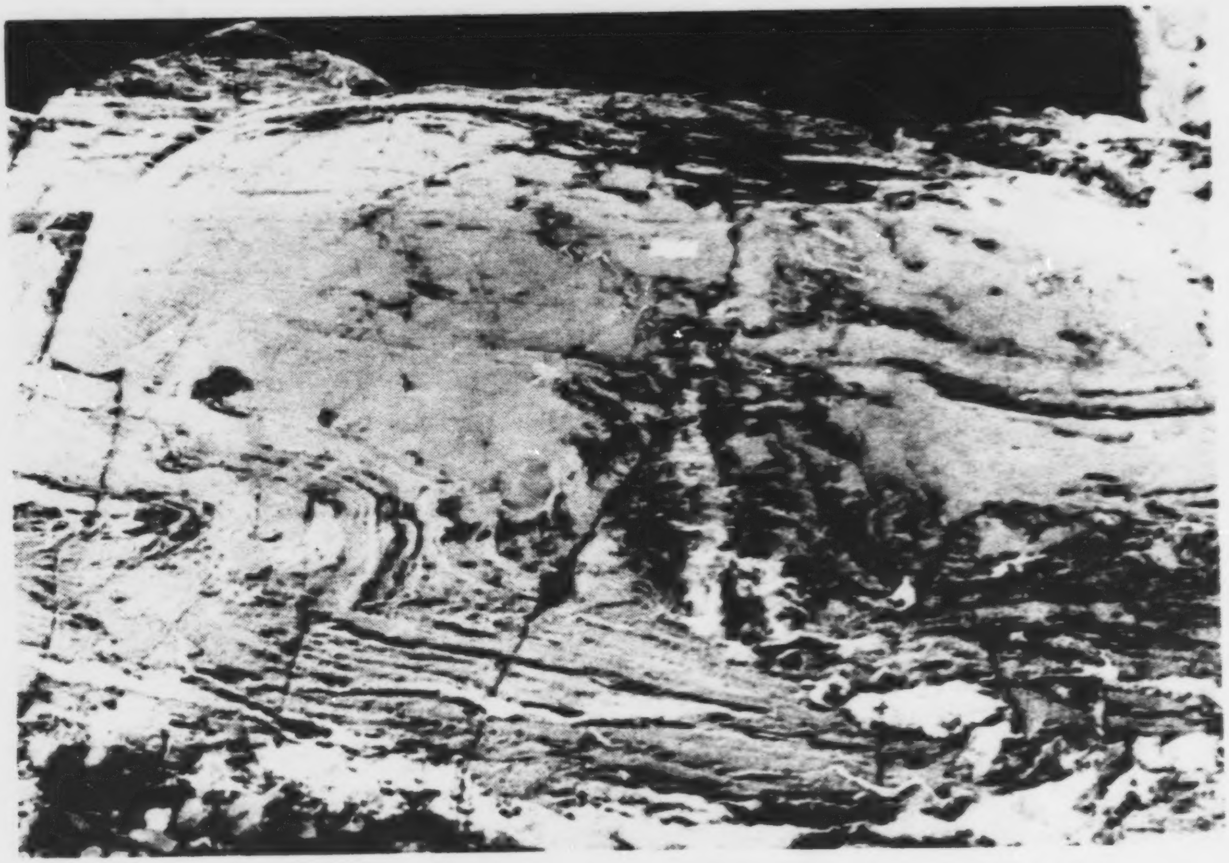

Figure 73 : Extensional quartz-carbonate veins at steep angle to principal vein, Hard Rock Open Stope, Geraldton.

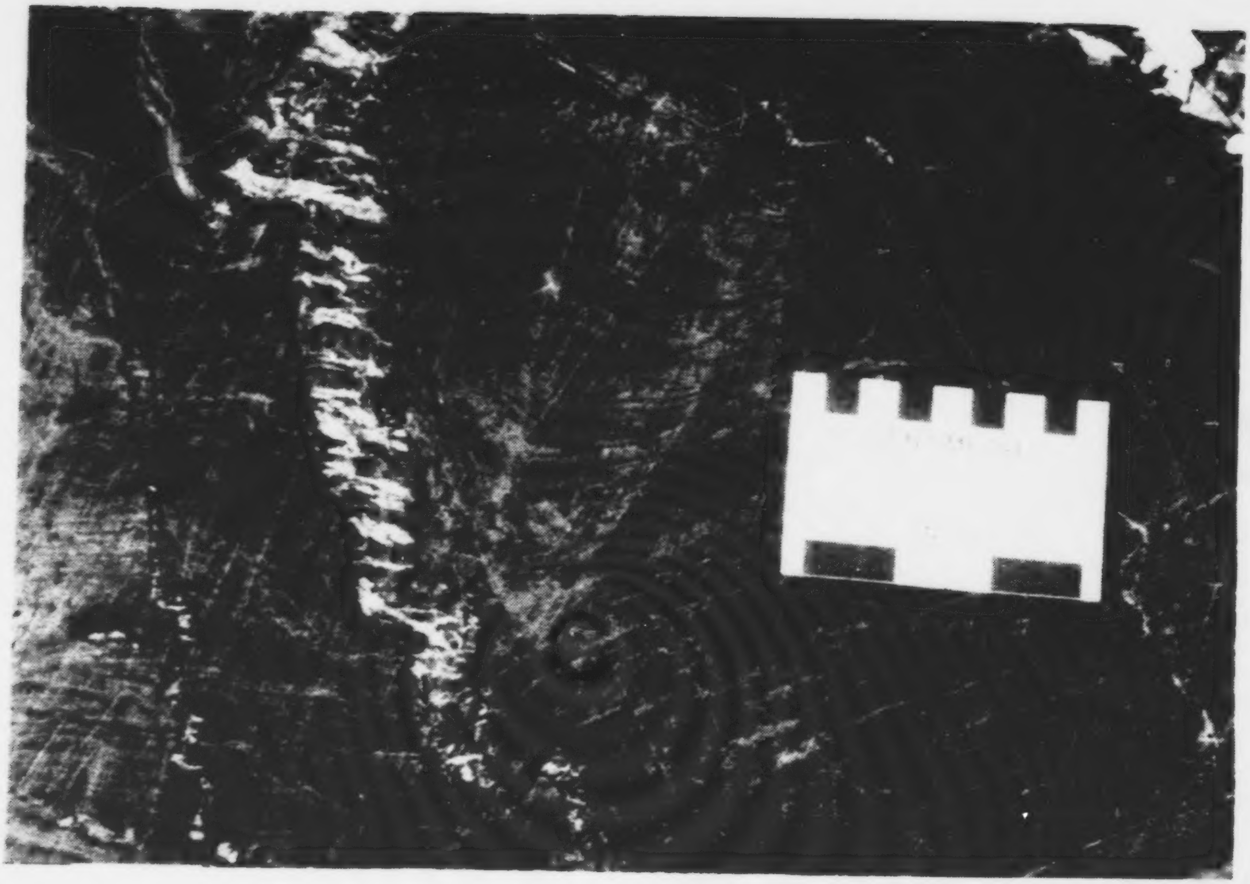

Figure 74 : Close up of extensional quartz-carbonate vein in Figure 73.

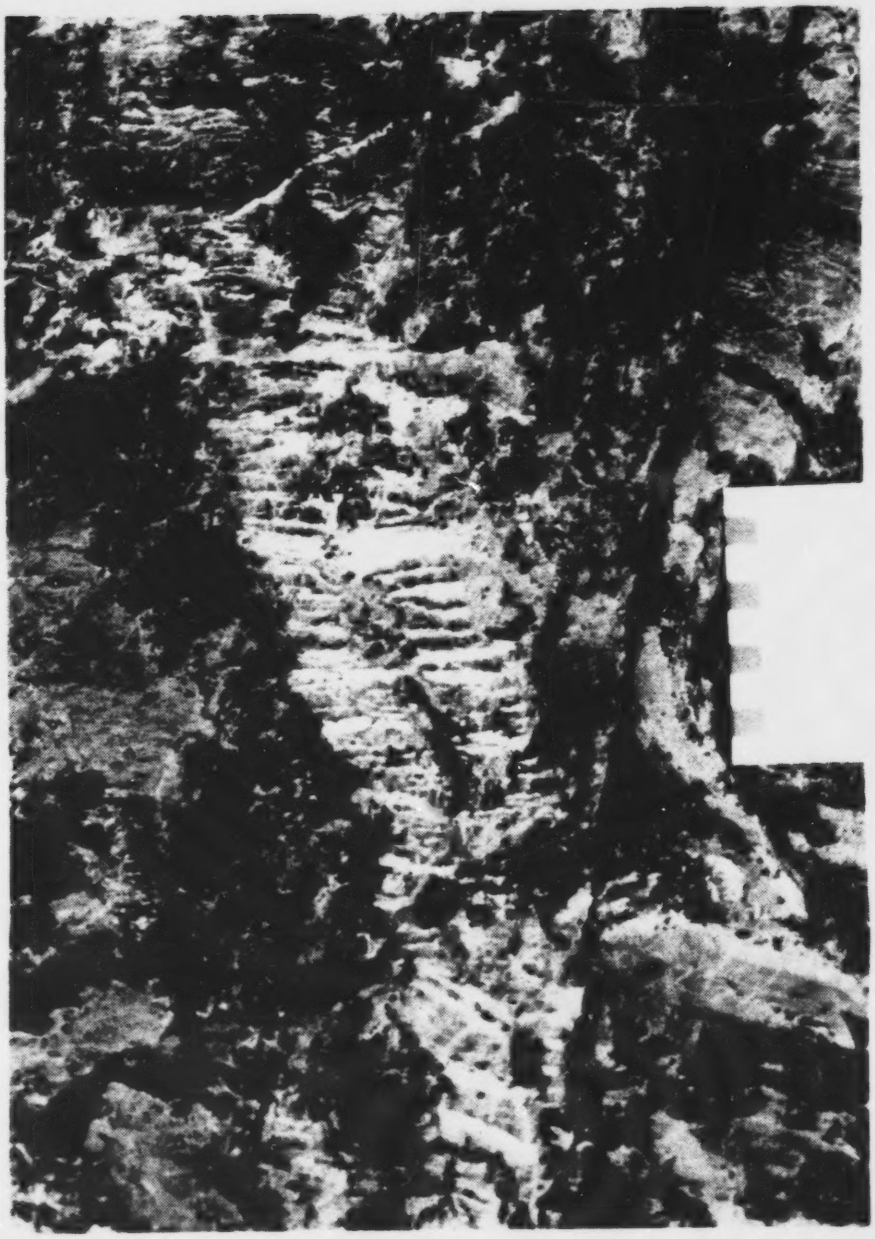

Figure 75 : Close up of extensional quartz-carbonate vein in Figure 73.

While most veins and alteration selvages exposed in BIF within the Hros are associated with asymmetric folds (c.f. Figures 62, 67), a small number also occur at the contact between BIF and porphyry. This relationship (Figure 14) was first pointed out by Horwood and Pye (1951, Figure 10). Where the porphyritic unit is parallel to stratigraphy, veins do not cut across bedding in BIF. Where, however, the porphyry cuts BIF (Figure 14), the vein separating BIF and porphyry of necessity transgresses relict bedding in the sediment. These relationships suggest that hydrothermal fluids utilized space generated between the porphyritic unit and enclosing host rock, with the implication that the contact delaminated during deformation and provided the hydrothermal conduits. It is likely that delamination occurred in response to differing strain exhibited by the two rock types, as a function of their differing rheology.

9.4 Veins in Porphyry

In outcrop, carbonate veinlets are not visible due to intense alteration. Thin sections reveal, however, that early carbonate-bearing veinlets, oblique to the stretching lineation, are cut subsequently by veins carrying quartz and ferroan-dolomite or ankerite (Figure 76), i.e. showing a similar paragenesis to those seen in BIF.

As discussed previously, asymmetric folds with wavelengths of less than 50 cm (c.f. Figure 62) are not seen in the porphyritic unit. While the unit does contain quartz-carbonate veins subparallel to those in BIF (see section on structural analysis, 9.6) they are not associated with asymmetric folds (Figure 77).

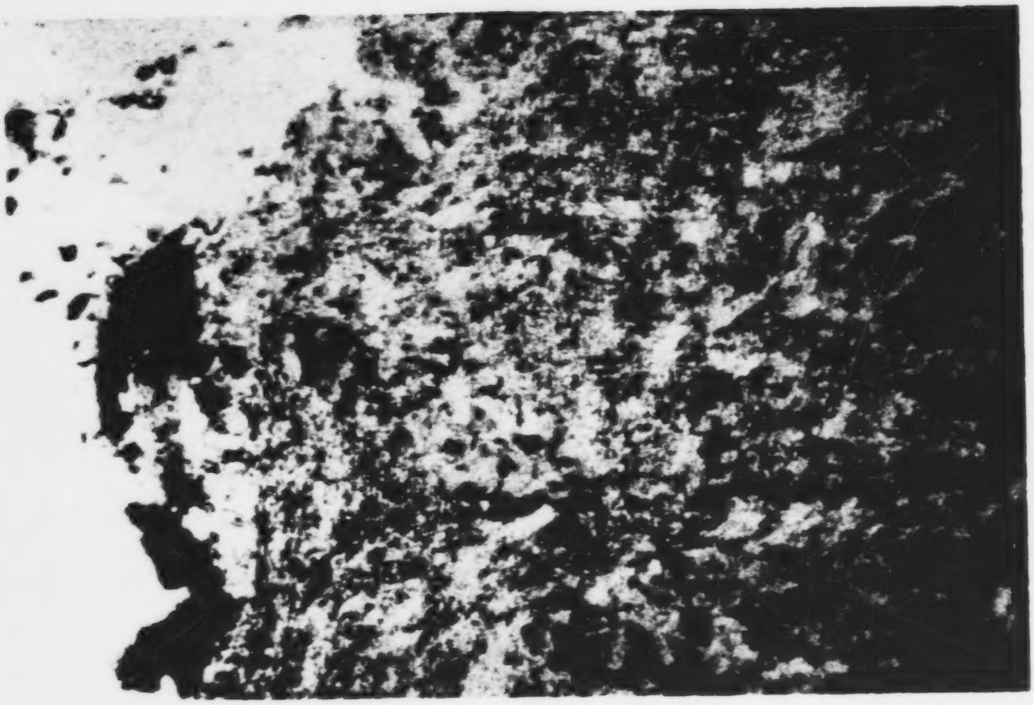

Figure 76 : Quartz-carbonate vein (white) cutting folded iron-cabonate veinlet, in turn cutting foliated porphyry, Hard Rock Open Stope, Geraldton. Field of view 1 cm.

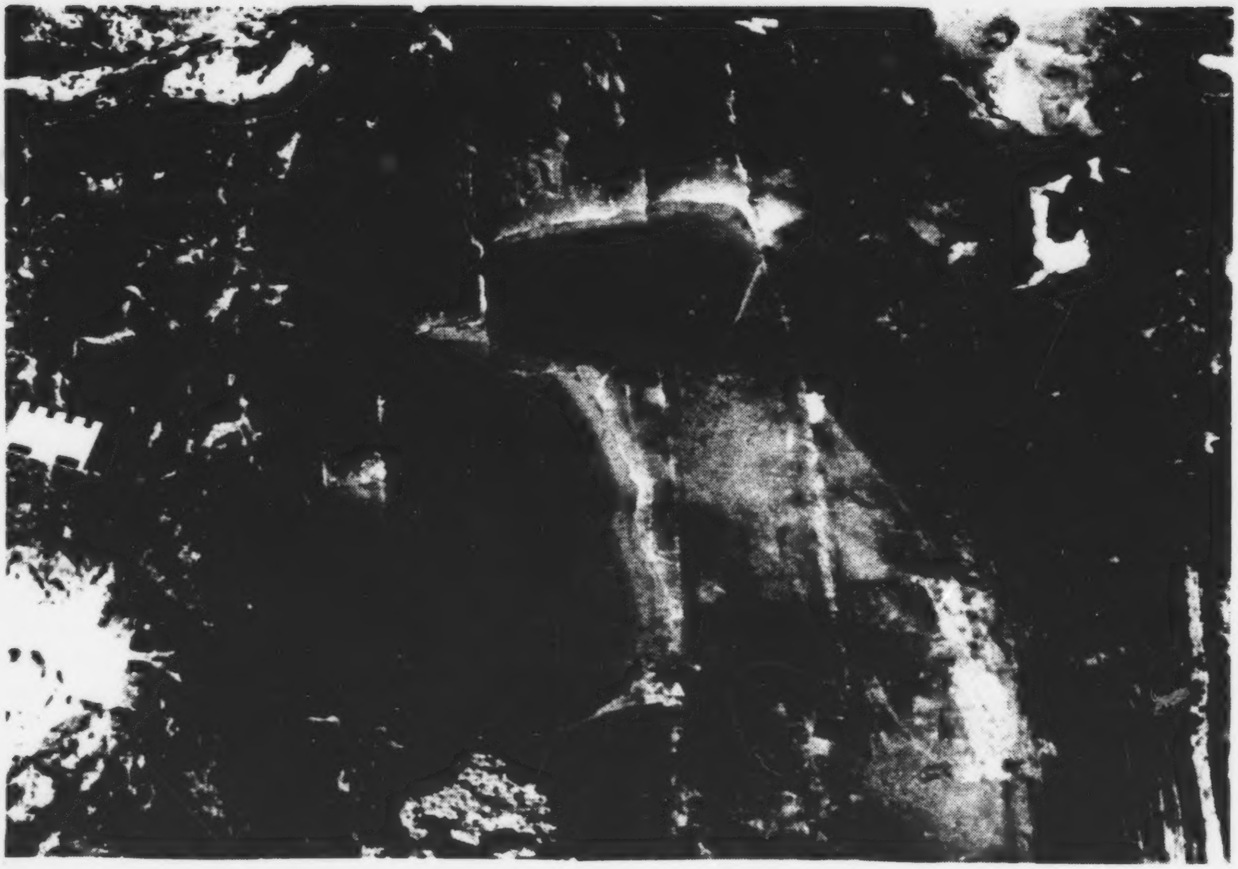

Figure 77 : Quartz-carbonate veins restricted to porphyry, Hard Rock Open Stope, Geraldton.

Within the porphyry, quartz-carbonate + tourmaline + sulphide veins are present in subparallel, sheeted vein sets that do not pass into adjacent BIF (Figure 77), but tend to terminate within porphyry, one or two centimetres from the contact between the two rock types. An exposure on the vertical rock wall of the HRos shows folded porphyry with sub-parallel, northward dipping, sheeted veins restricted to the porphyry unit (Figure 78). Reconnaissance mapping of the north wall of the HRos revealed that over 90% of the veins exposed in a 45 m x 20 m face are hosted by the porphyritic unit as opposed to BIF, in which the porphyry is interleaved.

An alteration selvage is well developed on both sides of quartz ankerite veinlets that cut the porphyritic unit (Figure 79). Most apparent is a 5-10 cm bleached zone in which, in addition to bleaching, several mineral changes are apparent: relict (?) feldspar takes on a green colour, apparently resulting from sheet silicate alteration. The green sheet silicate is often identical in the field as "fuchsite", implying a significant Cr content. It will be recalled from a previous section of this report, that altered porphyry carries anomalous Cr. Whether the Cr is located in green mica is not currently known. Also present within the bleached zone are secondary, sub- to euhedral pyrite crystals, up to 7 mm across. Thus pyritiferous alteration selvages about veins are not restricted to BIF.

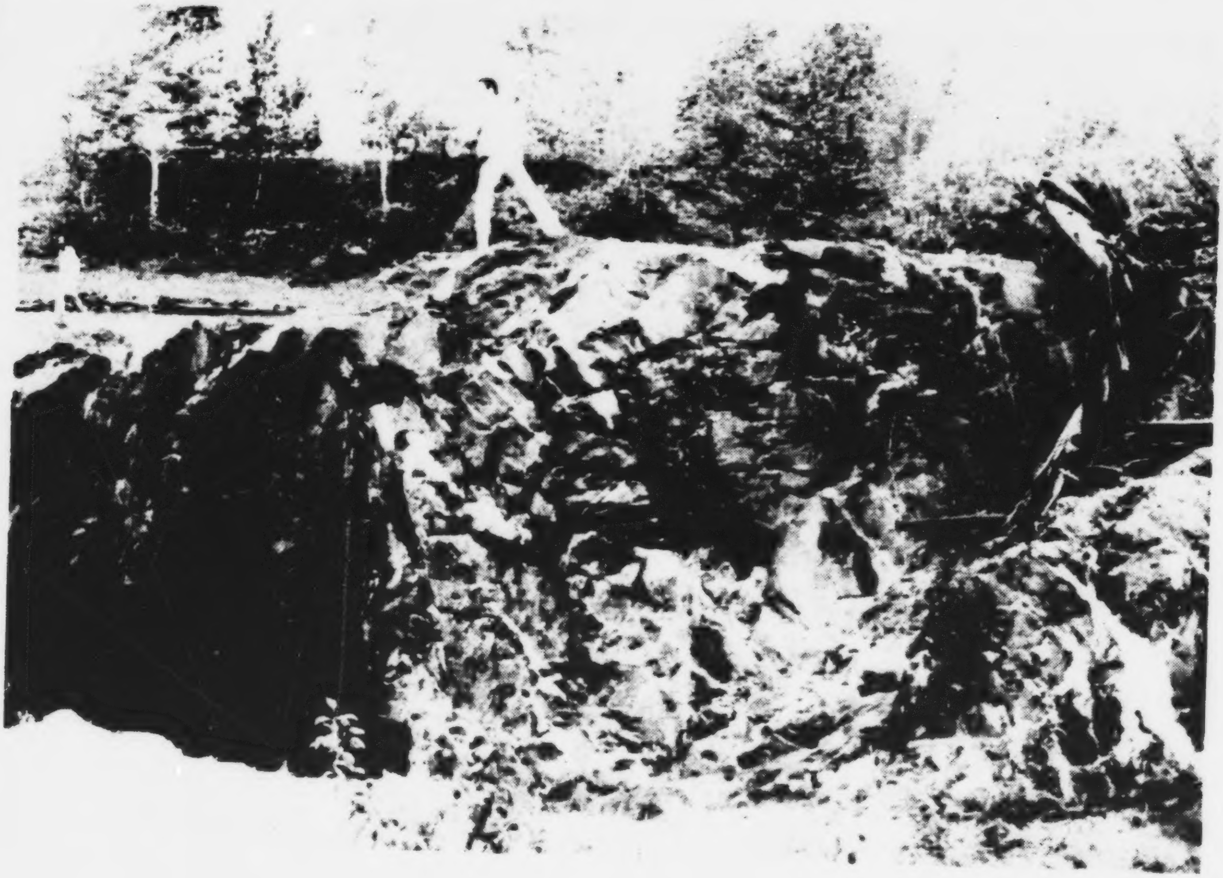

Figure 78 : Sheeted quartz-carbonate veins restricted to folded porphyry, Hard Rock Open Stope, Geraldton.

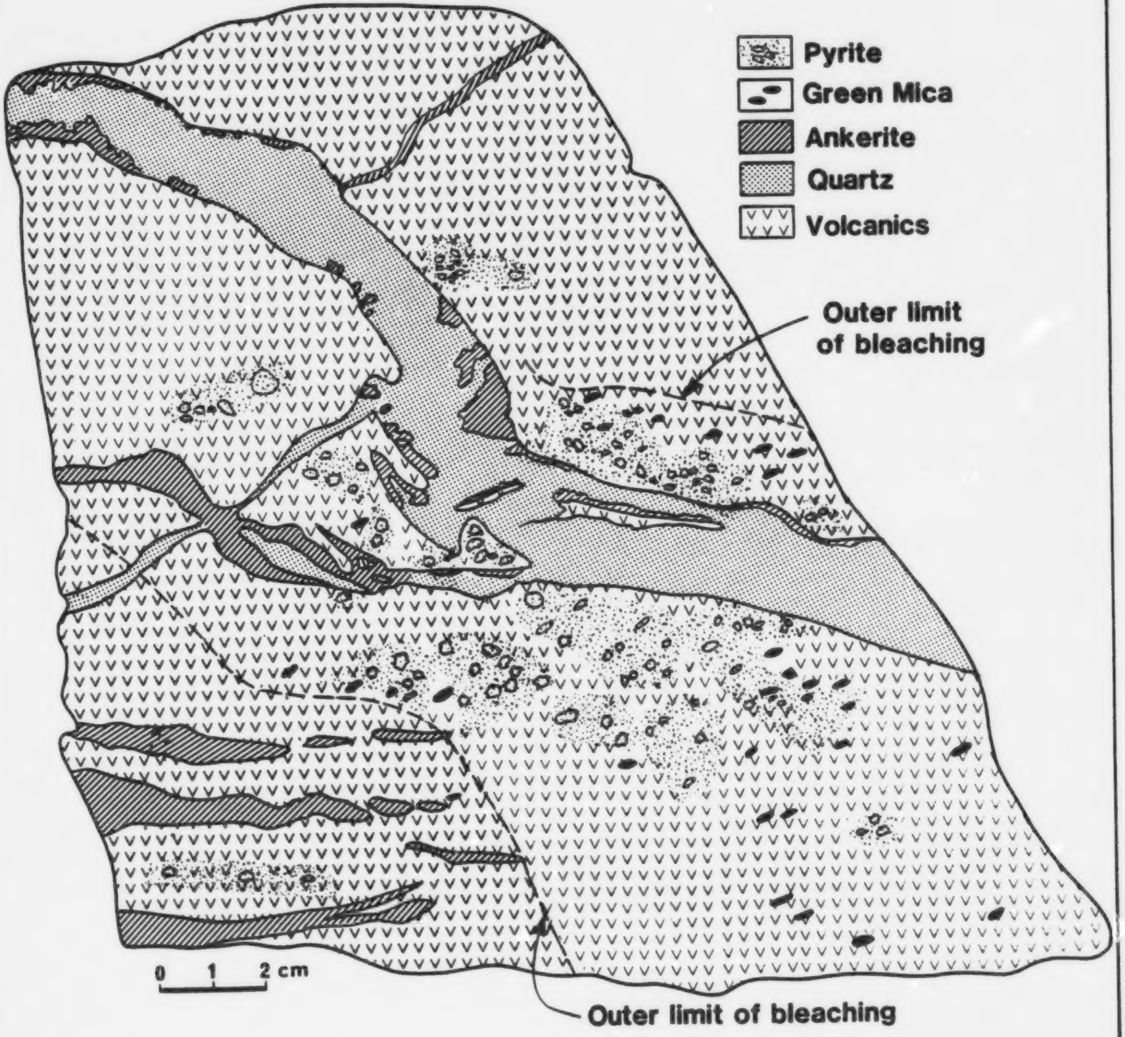
Pyrite
Green Mica
Ankerite
Quartz
Volcanics
Outer limit of bleaching
0 1 2 cm
Outer limit of bleaching

Figure 79 : Sketch of a slab of porphyry, Hard Rock Open Stope, Geraldton. Note quartz-carbonate vein with associated secondary pyrite and alteration selvage.

9.5 Veins in Wacke

Vein density in wacke is considerably less than observed in BIF and porphyry. This may result from the more ductile response to stress exhibited by the wacke in comparison to the other lithologies (see above); wacke being less susceptible to brittle failure, and consequently a less amenable host for vein-style mineralization. Veins exposed around the periphery of the HRos within clastic sediments, principally wacke with minor siltstone, display a greater variability in geometry than veins exposed in either the porphyry or BIF units. As in the other host rocks, veins are either 100% carbonate or quartz-carbonate + tourmaline + sulphides. Earliest veins are, as in the above examples, dominated by iron-bearing carbonate and are foliation-parallel, cutting across bedding (Figure 80). A foliation-parallel quartz-carbonate vein is also shown on Figure 80. The attitude of any vein with respect to foliation determines the degree of *apparent* deformation. For example, the carbonate vein in Figure 80 does not appear, superficially, to be highly deformed. The same vein is cut, however, by a foliation-oblique, quartz-carbonate vein (Figure 81), indicating that the carbonate vein is the older of the two. The younger discordant quartz-carbonate vein is apparently more highly deformed than the carbonate vein. As a result, the degree of apparent deformation (folding, boudinage, etc.) may not reflect relative age. One can infer that the carbonate vein in Figure 81 has at the very least experienced the same strain regime as the quartz-carbonate vein, but that it is manifested as a different strain, i.e. slippage parallel to the vein.

Quartz-carbonate veins cutting wacke are commonly flanked by a 1 cm wide, dark green, chloritic alteration selvage, and may be parallel or oblique to foliation. Foliation-parallel veins exhibit asymmetric intrafolial folding and/or boudinage. In certain locations, these two strain phenomena occur within centimetres of each other

(Figure 82). The asymmetric fold is indicative of a component of dextral shear, while the pinch and swell boudinage suggests stretching in the plane of the vein, i.e. compression perpendicular to the plane. This is yet another example of the complex strain history exhibited by rocks in the HRos.

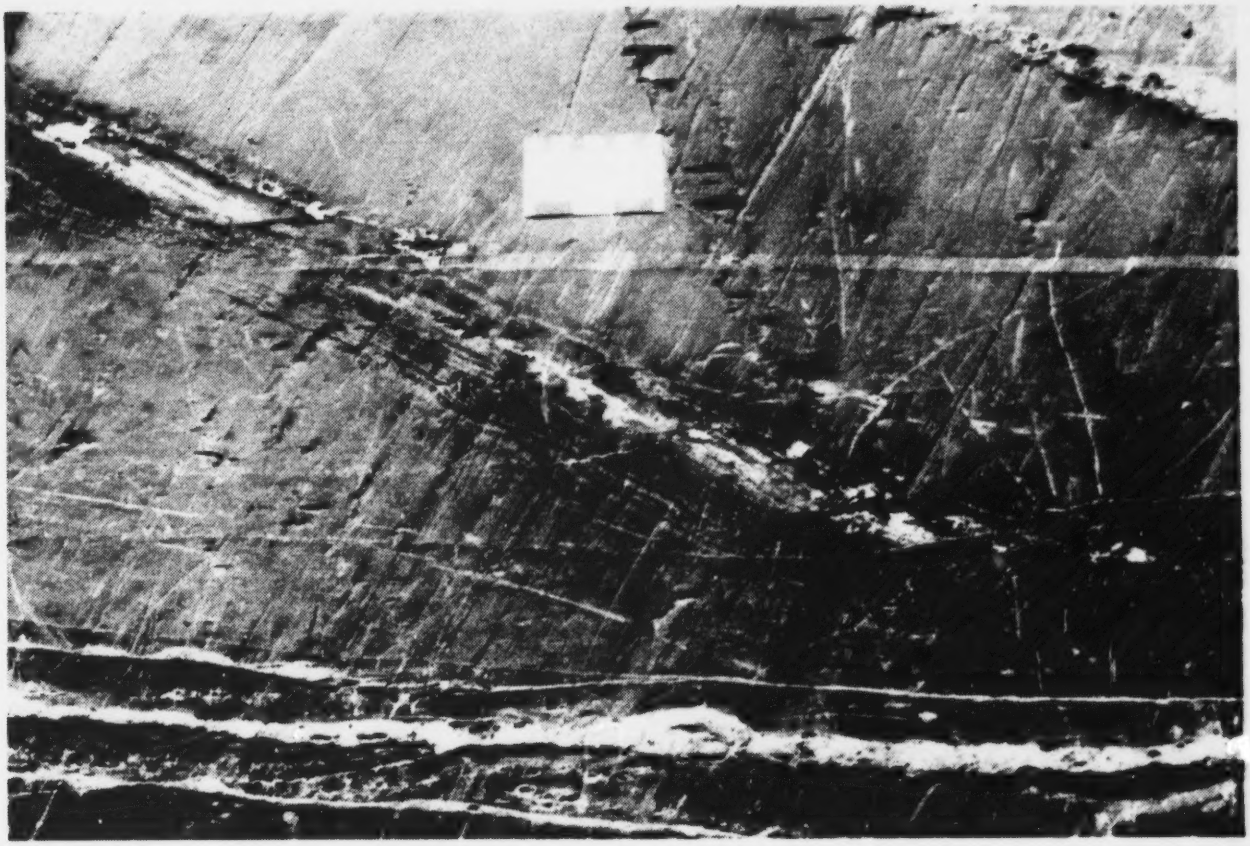

Figure 80 : Foliation-parallel carbonate vein (horizontal, beneath scale card) cuts magnetite beds (oblique, top left to bottom right), Hard Rock Open Stope, Geraldton.

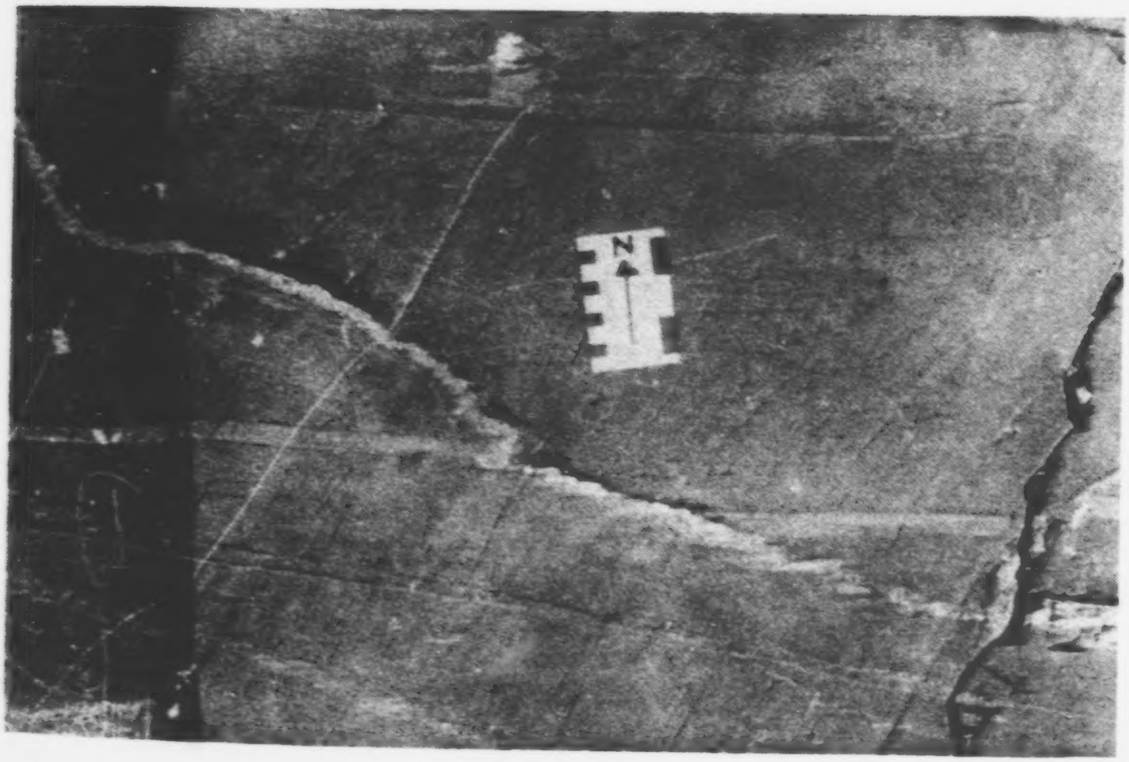

Figure 81 : Carbonate vein in Figure 80 is cut by younger quartz-carbonate vein, that appears superficially to be more highly strained.

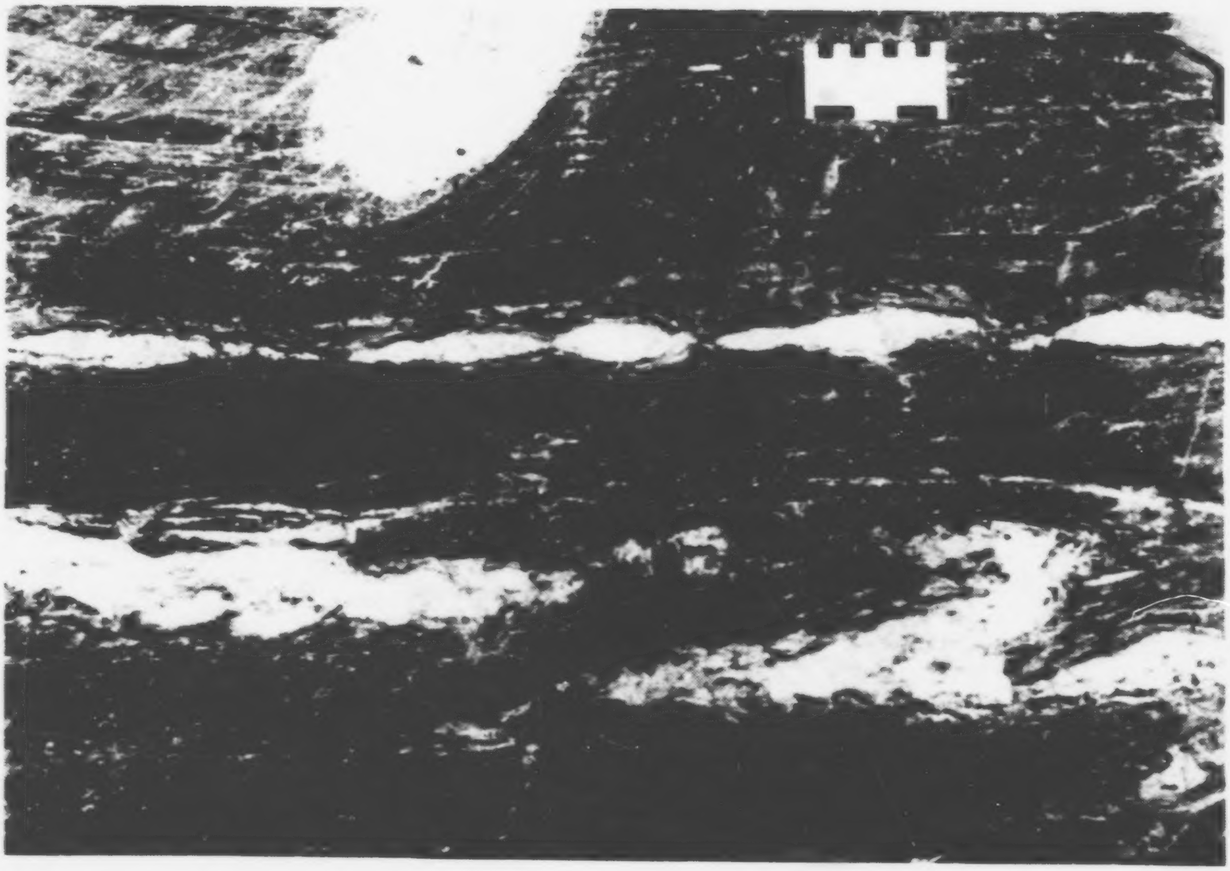

Figure 82 : Adjacent quartz-carbonate veins in silstone displaying boudinage and kink folds, Hard Rock Open Stope, Geraldton.

Clear cross-cutting relationships between different generations of quartz-carbonate veins are not common. Some outcrops suggest at least two generations. For example, Figure 83 shows two foliation-oblique, quartz-carbonate veins, one of which is in an intrafolial fold hinge, whose limbs have been tectonically dismembered; the other vein, although deformed, remains intact. Ramsay (1967) and Ramsay and Huber (1983) point out that formation of intrafolial folds indicates a period of fold formation followed by a period of strong extension, tending to rupture and isolate fold hinges of the more competent layers, apparently free-swimming in the incompetent matrix. The presence of an apparently less deformed quartz-carbonate vein in Figure 83 may suggest that it did not "see" the total deformation history experienced by the dismembered intrafolial fold hinge, even bearing in mind the caveat presented above.

The most intensely foliated quartz-carbonate veins are those which exhibit the greatest degree of obliquity to foliation, up to 90°. Quartz-carbonate veinlets develop fold structures known as elasticas, the tightest of folds, in which the inter-limb angle is negative (Ramsay 1967, p.349) and a characteristic shape of ptygmatic folds (Figure 84). Note, in Figure 84, that as the general strike of the vein becomes more oblique to foliation, the degree of ptygmatic folding increases until the folded vein suffers intense transposition (dextral sense). Figure 85 is a quartz-carbonate veinlet that is ptygmatically folded and at a high angle to foliation. Horwood and Pye (1951) and Pye (1951) referred to these structures as "wiggly veins", locally constituting important components of the Hardrock A and B ore zones (see Horwood and Pye 1951, p.61 - 65).

Ramsay (1967) indicates that ptygmatic folds, such as those in Figure 85, are formed by shortening of a competent layer within a more incompetent matrix. Experimental generation of ptygmatic folds (Ramsay and Huber 1983, Figure 1.9B) suggests that the principal direction of shortening is perpendicular to the ptygmatic fold axes;

i.e. in Figure 85, approximately parallel to the long edge of the scale card, or perpendicular to foliation.

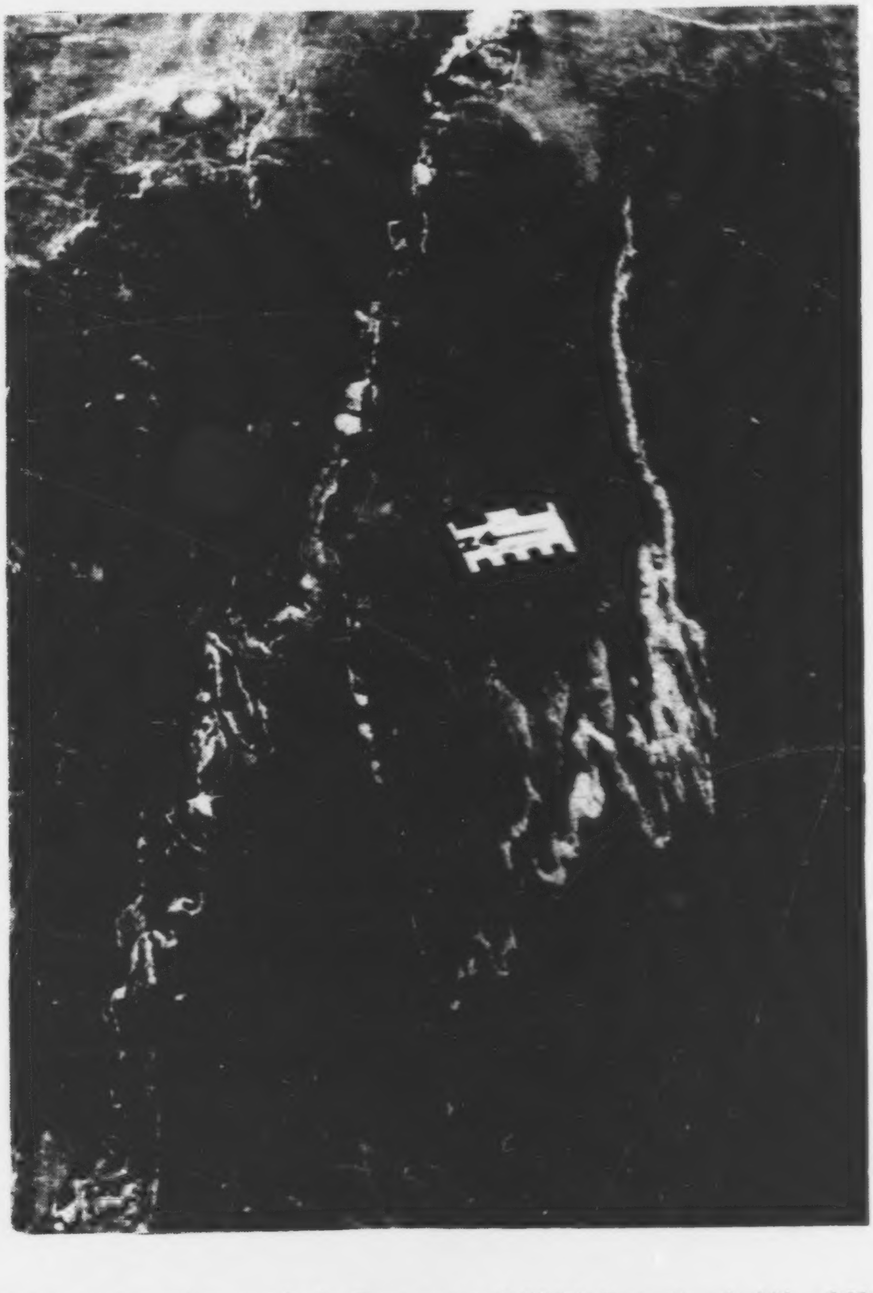

Figure 83 : Two quartz-carbonate veins in siltstone, one of which is dismembered within a fold hinge, Hard Rock Open Stope, Geraldton.

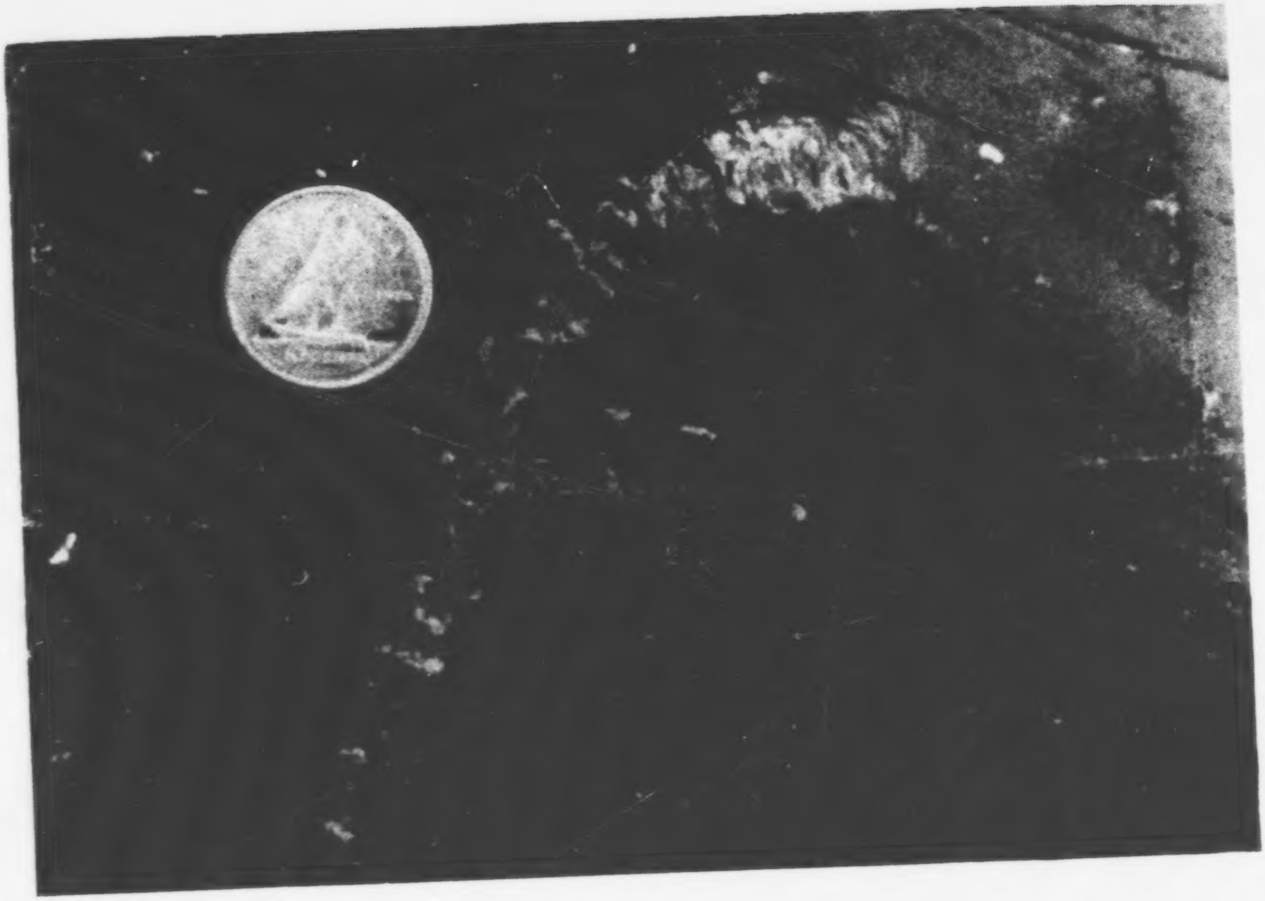

Figure 84 : Ptygmatic or elastica vein, Hard Rock Open Stope, Geraldton, 10 cent coin for scale.

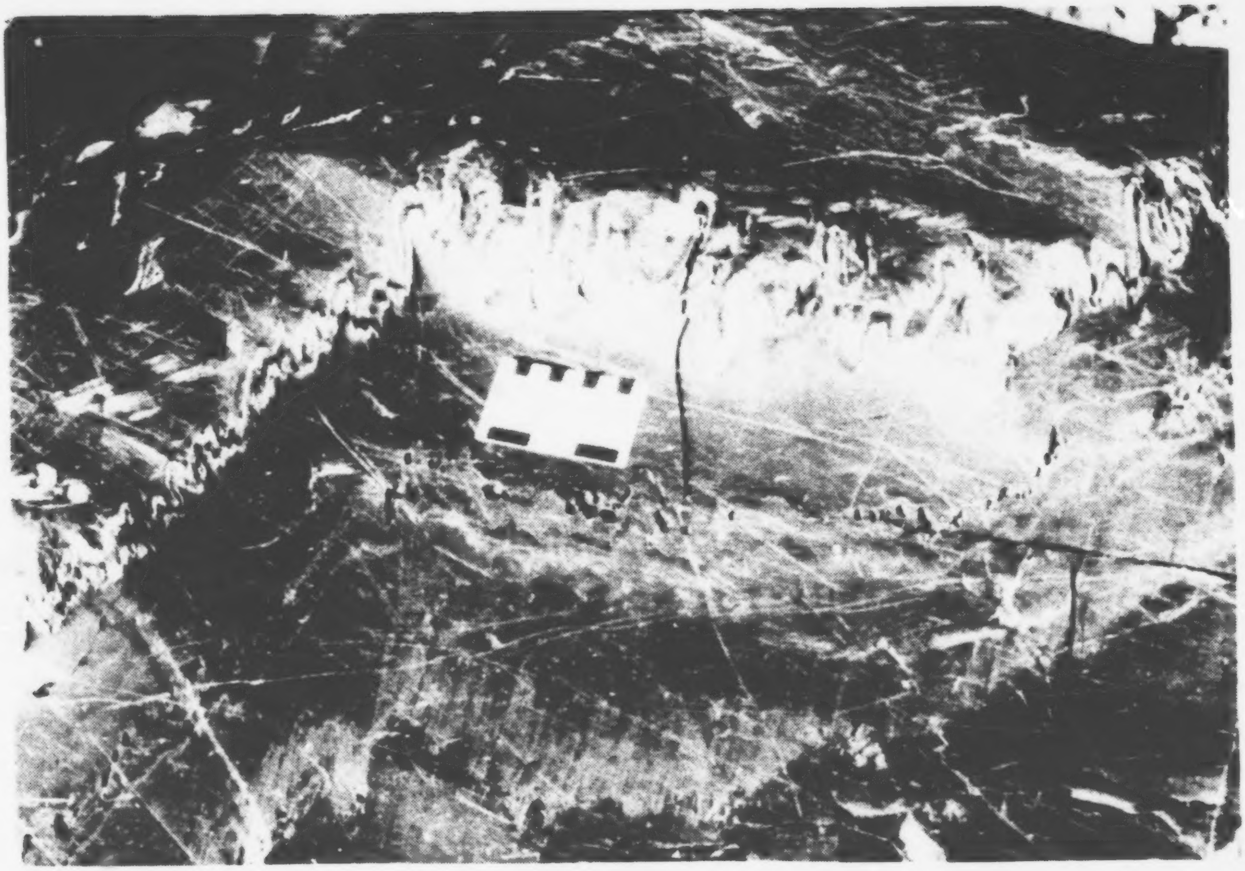

Figure 85 : Ptygmatic or elastica vein, Hard Rock Open Stope, Geraldton.

9.6. Summary of vein structures

All rock types in the HRos contain an early carbonate vein/veinlet set cut by younger quartz-carbonate + sulphide + tourmaline vein set(s). The relationships between various vein sets, stratigraphy and structural features shed light upon the stress pattern in which the different veins were formed.

METHOD

Structural measurements were hampered in the HRos by the presence of magnetite-rich iron formation. Azimuth measurements could not be made with a standard compass, although dip/plunge readings could be taken with a clinometer. Accordingly a sun compass was constructed using a clear plastic circular protractor, a 10 cm bolt and nuts. A hole was drilled in the centre of the protractor, to allow insertion of the bolt which was fixed rigidly in place with a nut either side of the plastic. When the protractor was held horizontally, the sun would cast a shadow of the bolt onto the protractor degree markings. Visibility of the shadow was enhanced by attaching a white or pale coloured, opaque fabric or tape to the base of the protractor.

At regular (15 minute) intervals during the day, a bearing is taken with a standard compass on the azimuth of a shadow cast by the sun, at some location distant from the source of magnetic interference. The resulting table of shadow azimuths is then used to calibrate the sun compass. Azimuth readings are recorded using the compass by first noting the time of day, secondly recording the angle between the feature being measured and the angle cast by the bolt on the sun compass. The angle in question is then compared with the measured azimuth of a shadow cast at that time of day in order to obtain the bearing, strike, etc. of the feature being investigated. In this way, bedding attitudes, fold axes, cleavages, lineations and veins could be measured in the vicinity of the iron formation.

Measurements of penetrative fabric were made throughout the HRos. Figure 86 is a contoured equal areal lower hemisphere projection of cleavage measured in wacke and siltstone. This and following plots are generated by the method of Robin and Jowett (1986); refer to their paper for details of contouring procedure. The data concentrate around a strike of 105^{o} and are steeply dipping. A trend of 95^{o} is present for strike of cleavage in the porphyritic unit, although greater variability is present than within the wacke (Figure 87). Elongated crystals of plagioclase (?) and amphibole (?) are subparallel to the cleavage. One oriented sample of porphyry indicated that the stretching lineation plunged between 20 and 30^{o} on a bearing of 275^{o}.

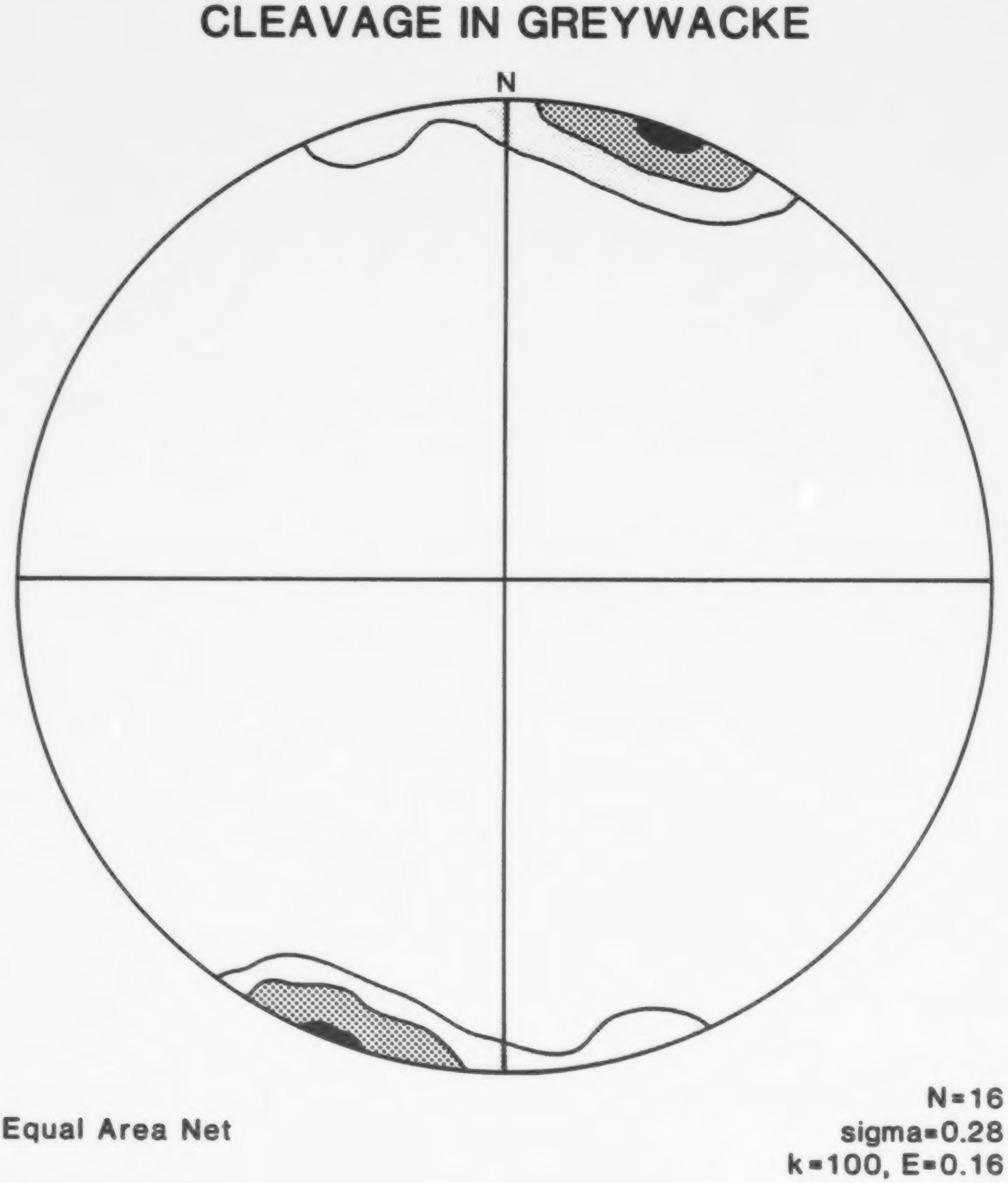

Figure 86 : Poles to cleavage in wacke, Hard Rock Open Stope, Geraldton.

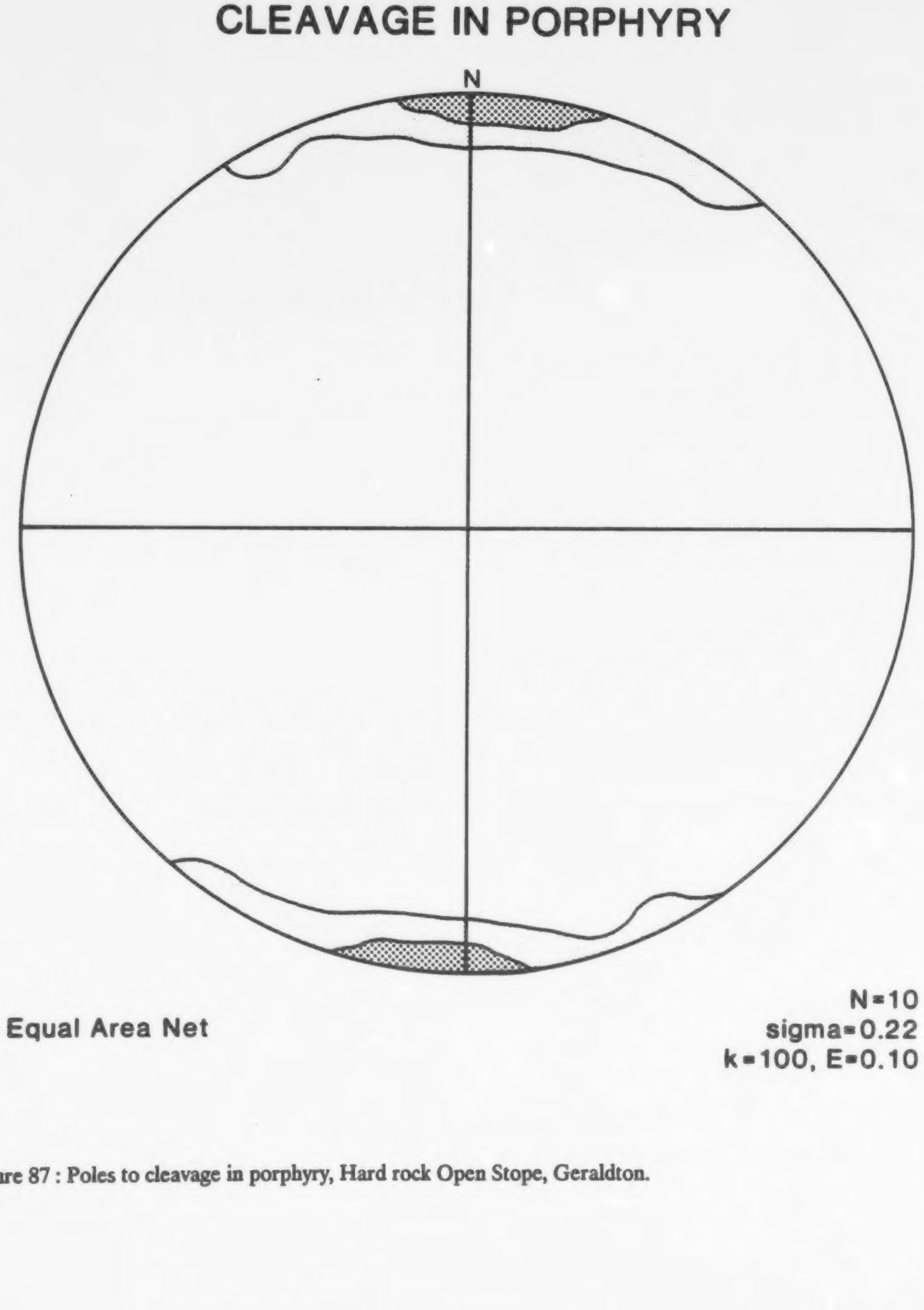

Figure 87 : Poles to cleavage in porphyry, Hard rock Open Stope, Geraldton.

It is important to note that the measured cleavage direction, are not axial planar to the asymmetric folds measured throughout the HRos. Folds with amplitudes and wavelength on the 1-2 metre scale (see Map, back pocket) have a mean axial azimuth of $263^{o} \pm 7^{o}$ (1 standard deviation, 23 measurements). The folds most commonly plunge westwards at 28 to 29^{o}, as first pointed out by Horwood and Pye (1951).

Quartz-carbonate vein attitudes in BIF are shown in Figure 88. There are two sets of quartz-carbonate veins in the porphyritic unit, as mentioned above. The attitudes of the major vein set are shown in Figure 89. These show a similar mean azimuth (094^{o}) to those in BIF (092^{o}) but tend to dip less steeply to the north (c.f. Figure 78). Attitudes of the minor quartz-carbonate vein set in the porphyry are given in Figure 90, with a mean azimuth of 64^{o}, and a dip comparable to that of other veins in the porphyritic unit.

Veins in wacke (see above) are relatively rare when compared with BIF and porphyry, as the rock exhibited less brittle failure, a frequent precursor to veining. As described above, veins in wackes are either foliation-parallel (azimuth approximately 105^{o}) or foliation-oblique, in which case ptygmatic folding (Figure 85) and transposition (Figure 84) render meaningless any azimuth measurements.

By inspection of structural data from fabrics and veins in the HRos (Figures 86-90) with minor fold azimuths (mean $263^{o} \pm 7^{o}$, 1 standard deviation, 23 measurements), it is apparent that close, but not exact, parallelism is shown between the principal fabrics, a cleavage, a stretching lineation, fold axes of asymmetric folds and principal vein azimuths; i.e. penetrative deformation (the cleavage) and veins are not axial planar to the minor, asymmetric folds. An extensive interpretation on a larger scale is considered by Buck (1986), and awaits the structural analyses of Lavigne (in preparation).

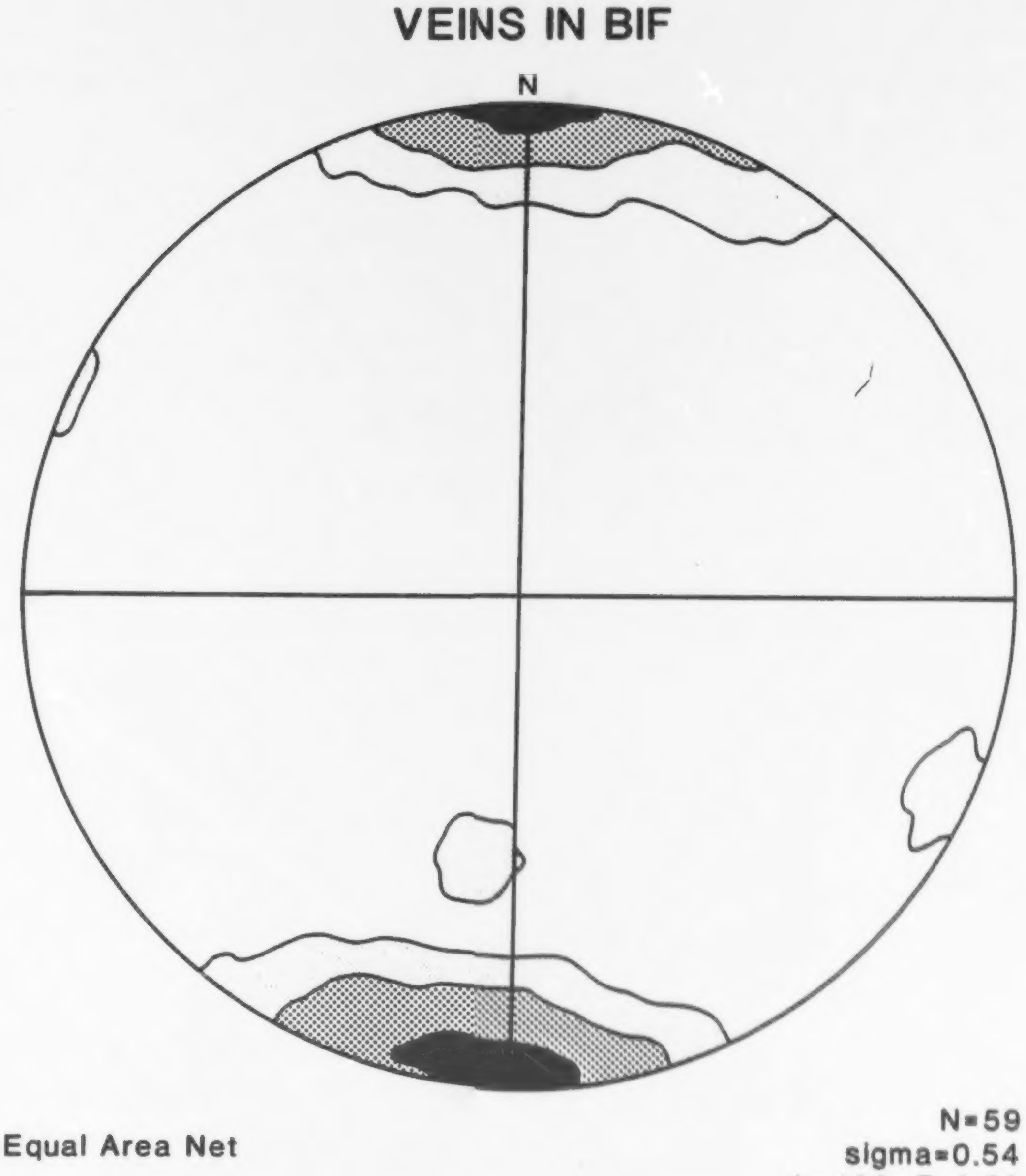

Figure 88 : Poles to veins in iron formation, Hard Rock Open Stope, Geraldton.

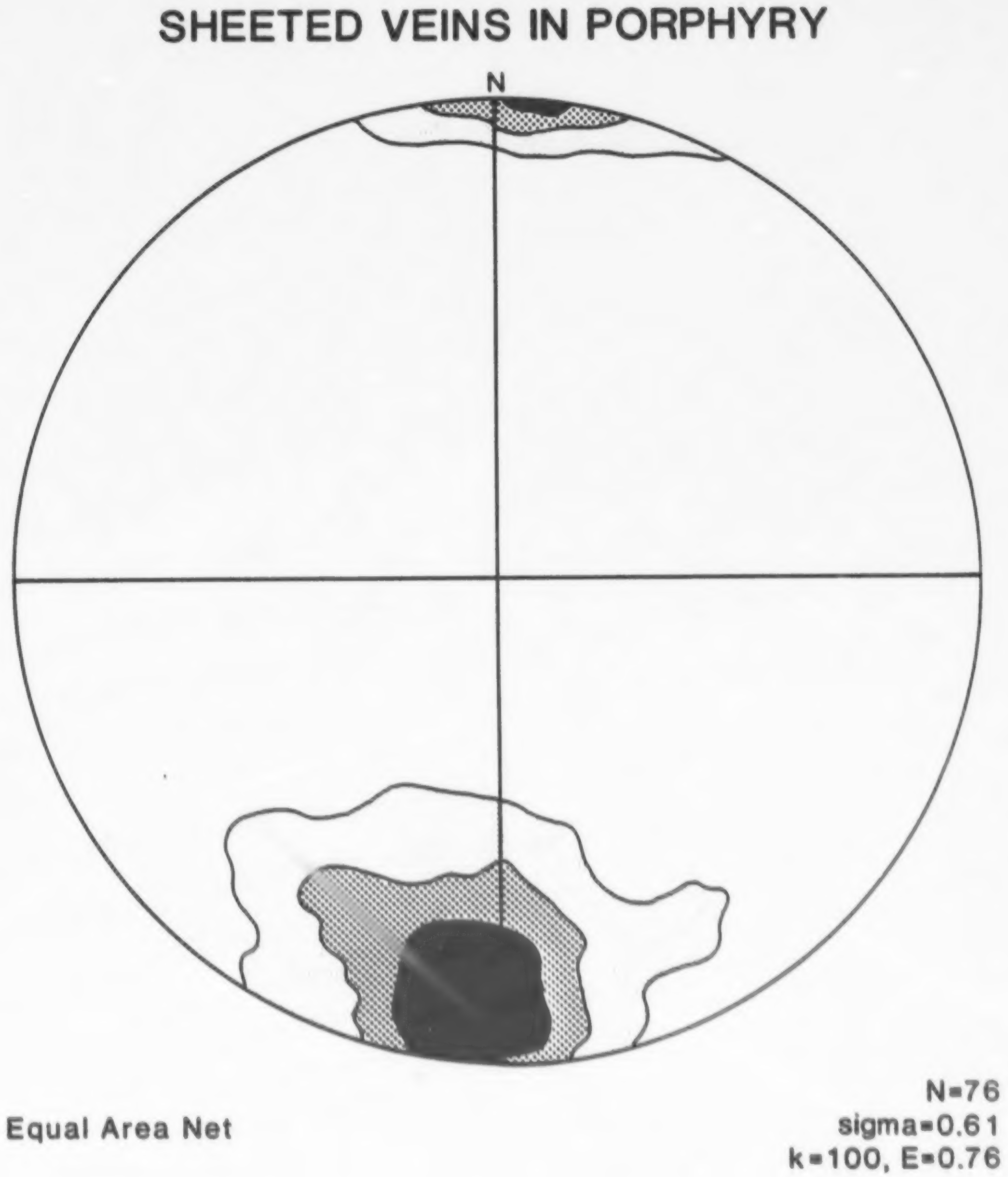

Figure 89 : Poles to sheeted veins in porphyry, Hard Rock Open Stope, Geraldton.

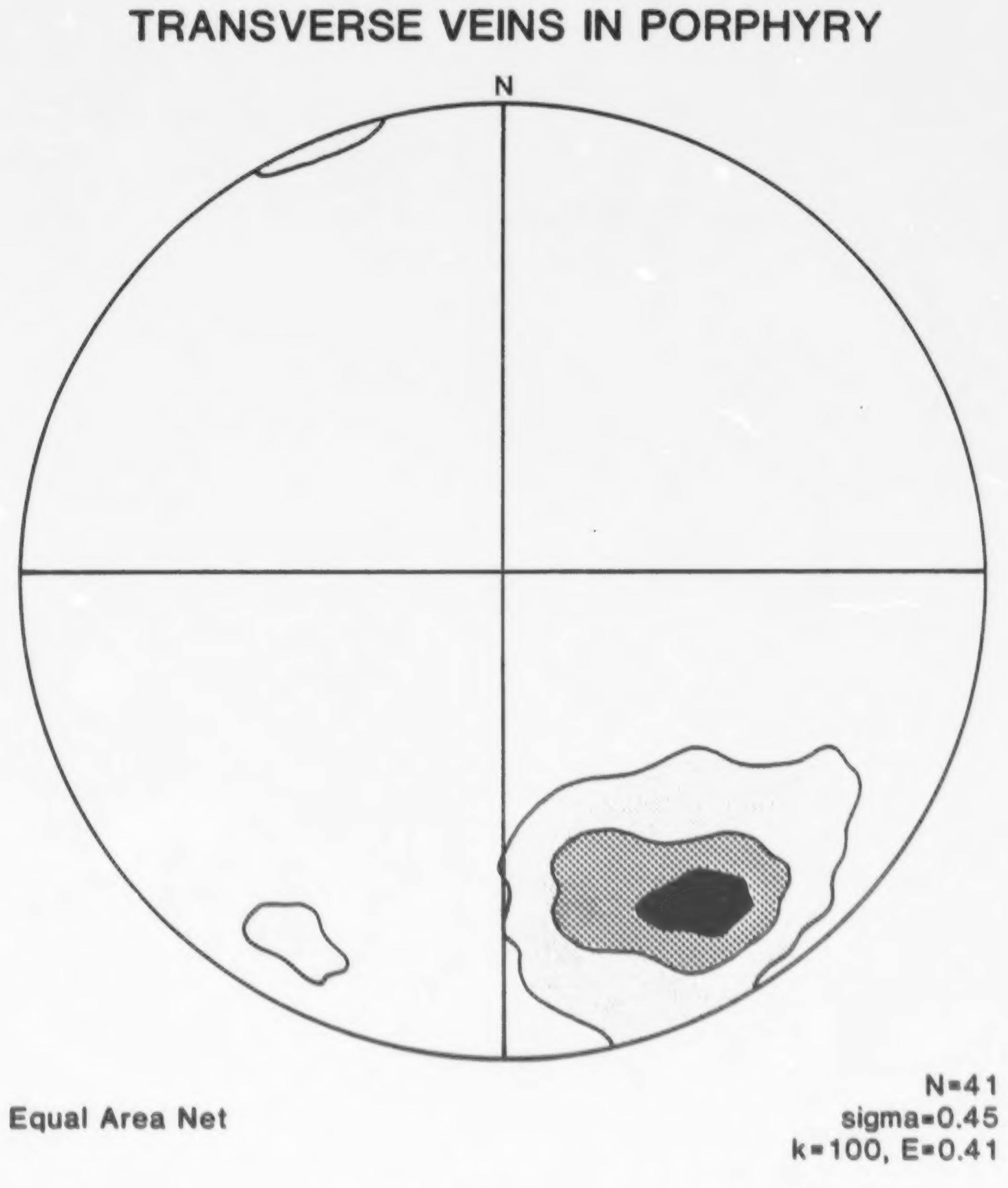

Figure 90 : Poles to transverse veins in porphyry, Hard Rock Open Stope, Geraldton.

The principal fabric, a foliation, is subparallel to the mapped boundary of the Barton Bay Lithotectonic Zone (Figure 3) and can be considered analogous to a C fabric, using terminology of Berthe et al. (1979) and shown in Figure 91. Carbonate veins and some quartz-carbonate veins in wacke are parallel to this fabric. The principal quartz-carbonate + tourmaline + sulphide veins are compatible with P shear fractures in Figure 91, are late Riedel shears. No early Riedel (R) shear fractures are recognized. The sense of motion observed on the veins in the HRos is dextral (c.f. Figure 62) as predicted in the geometric model of Harris and Cobbold (1984). The minor vein set in the porphyritic unit does not have a geometric equivalent in the model of Hugon and Schwerdtner (1985) (Figure 91). Coeval thick and thin vein sets are recognized, features typical of some gold deposits (Hodgson, in press) resulting from bulk inhomogeneous strain, in which one vein set tends to open in preference to the other member of the conjugate pair.

Considering the asymmetric fold structures and stretching lineations exposed in the HRos in terms of the finite strain ellipsoid, the X direction is parallel to the stretching lineation (azimuth: 95^{o}-105^{o}, depending upon rock type; plunge 20^{o}-39^{o}W). The Z axis of the strain ellipsoid is approximately normal to the fold axial plane (83^{o}, sub-vertical) i.e. an azimuth of 173^{o}, or nearly north-south.

This may be an over simplification of the fold/strain ellipse relationship, as folds that form in shear zones are subject to re-orientation through rotation, resulting from shear (e.g. Bell 1978). Escher and Watterson (1974) demonstrated that as shear strain is intensified, passive linear features, such as fold axes, are rotated into parallelism with the stretching lineation. There is no clear indication as to when the folds formed within the whole deformation history in the Geraldton Camp, or (b) to what extent rotation of fold axes has modified the fold attitudes. The approximate but not exact parallelism shown by many of the structural features of the HRos (e.g. Figures 86-90) may support the hypothesis that intense deformation resulting from shear in the BBLZ has rotated linear features towards the azimuth of the stretching lineation.

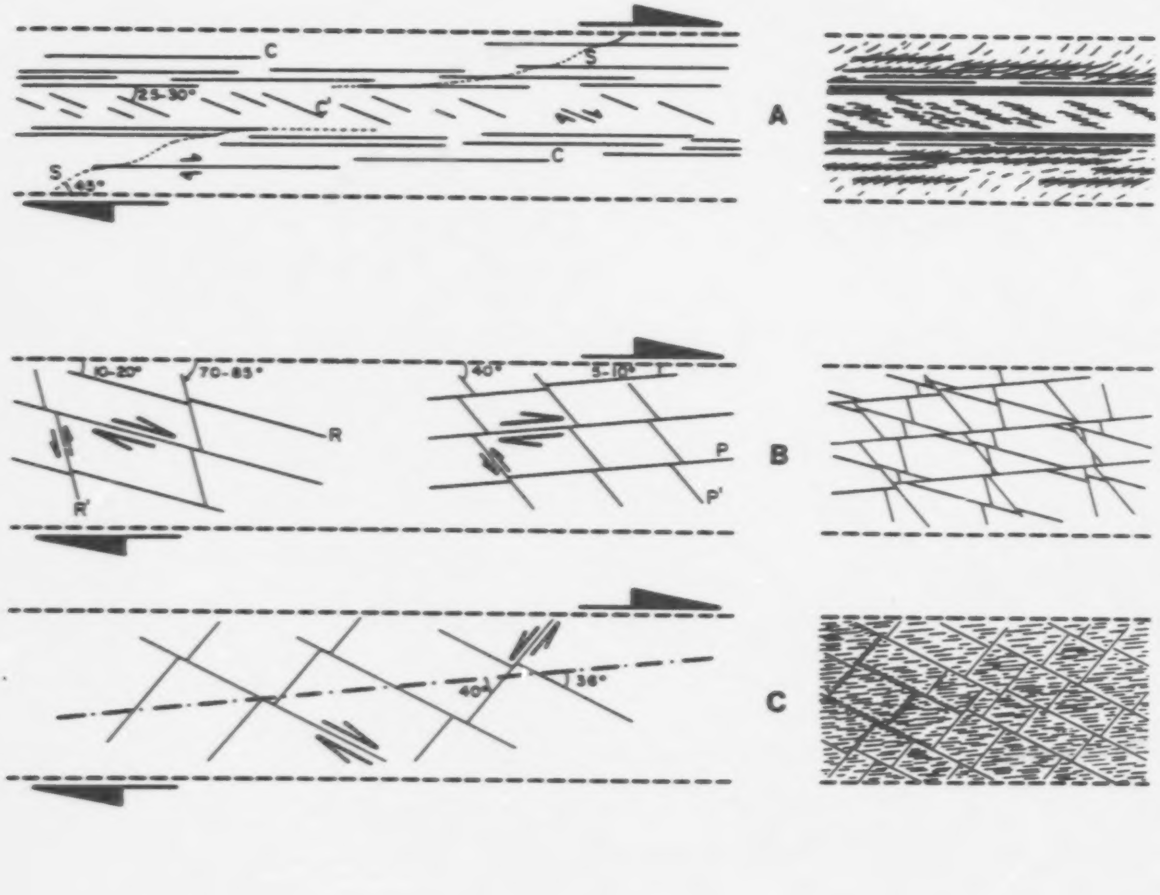
C
S
25-30°
C'
C
S
45°
A
10-20°
70-85°
R
R'
40°
5-10°
P
P'
B
40°
36°
C

Figure 91 : Fabrics developed in a dextral shear zone, based upon Berthe et al. (1979), from Hugon and Schwerdtner (1985).

10.0 Summary

Three different lithologic units are exposed in the HRos: BIF, porphyry and clastic sediments, mainly wacke and siltstone. Each unit has responded to stress uniquely, exhibiting different degrees of both brittle and ductile deformation. Small asymmetric folds are well developed in BIF, with local lithologic failure in a brittle manner in the areas of higher strain, allowing influx of hydrothermal fluids to form veins. A penetrative stretching which developed either before or during asymmetric folding lineation is characteristic of the porphyry. Brittle failure, in two directions, permitted veins to fill wider fractures in one direction (094^{o}) than the other (064^{o}). Pressure solution cleavages developed spectacularly in siltstone, parallel to cleavage in wacke units. Ductile disruption of bedding in wacke destroyed most original stratigraphic layering. Cleavage-parallel carbonate veins and rare quartz-carbonate veins *appear* to be on an outcrop-scale less-deformed than cleavage-oblique, quartz-carbonate veins that have suffered considerable shortening and ptygmatic folding.

The excellent exposure afforded by ice-polished surfaces on the rim of the Hard Rock Open Stope has provided an opportunity to investigate the variability in strain exhibited by rocks of differing physical properties, in response to a shearing regime acting over a volume of rock far greater than the exposure itself. Local heterogeneity or strain is enhanced or caused by contrasts in rheology of adjacent rock types. Accommodation of this heterogeneity commonly involved delamination and brittle failure, permitting influx of hydrothermal fluids. Without the physical heterogeneities present within the non-cylindrical fold structure hosting the North Zone, strain might have been dominantly homogenous and ductile, prohibiting influx of auriferous hydrothermal fluids along zones of enhanced permeability provided by brittle fractures.

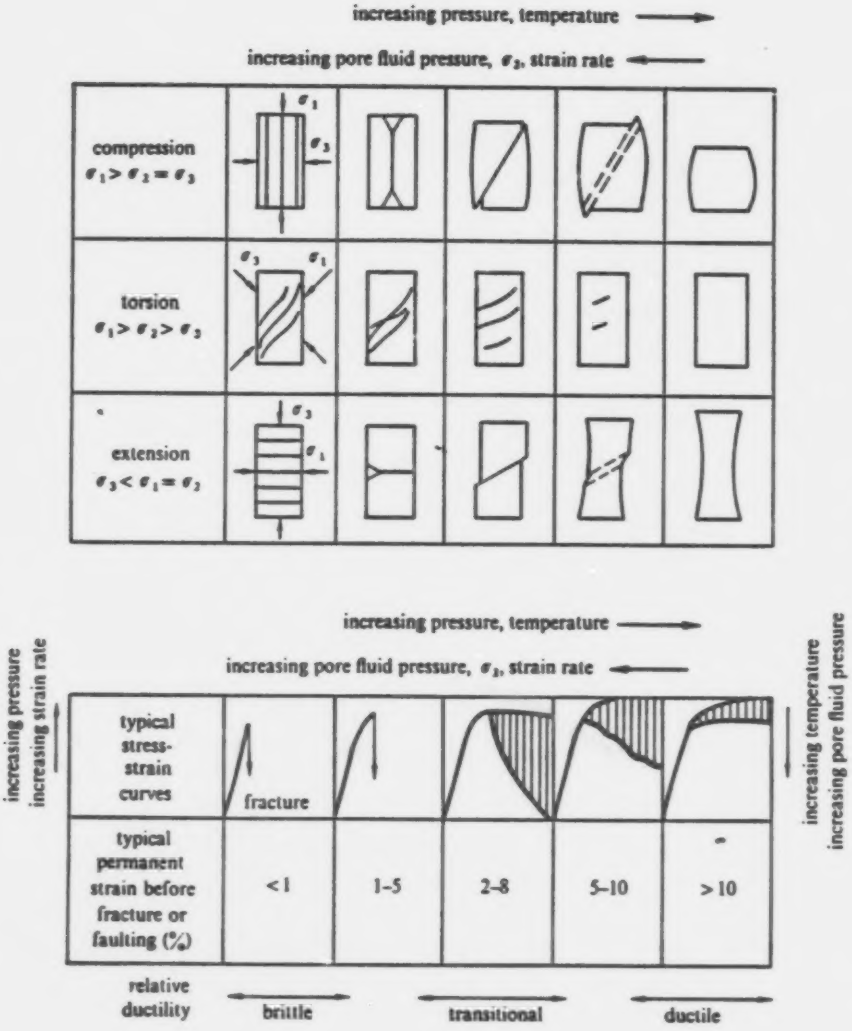
increasing pressure, temperature
increasing pore fluid pressure, σ_3, strain rate
compression
$\sigma_1 > \sigma_2 = \sigma_3$
torsion
$\sigma_1 > \sigma_2 > \sigma_3$
extension
$\sigma_3 < \sigma_1 = \sigma_2$
σ_1
σ_3
increasing pressure, temperature
increasing pore fluid pressure, σ_3, strain rate
increasing pressure
increasing strain rate
increasing temperature
increasing pore fluid pressure
typical stress-strain curves
fracture
typical permanent strain before fracture or faulting (%)
< 1
1–5
2–8
5–10
> 10
relative ductility
brittle
transitional
ductile

Figure 92 : Effects of pressure, temperature and fluid pressure upon strain style, from Heard (1976).

While other studies (e.g. Colvine et al. 1984) have suggested that large scale, discrete domains within a greenstone belt may deform by contrasting structural styles, e.g. brittle in one domain, ductile in another - with consequent effect for morphology of mineralization, detailed mapping of the Hard Rock open stope demonstrates great complexity on a small scale. While mineralization is hosted by brittle features, the overwhelming style of deformation exhibited by *all* rock types is ductile. In terms of their contribution to bulk strain, the brittle features receive undue attention, only because of economic significance. The observation that at least three brittle, veining events occurred during overall ductile deformation suggests the following hypothesis:

During ductile deformation, introduction of hydrothermal fluids was accompanied by transient brittle failure and vein formation. Following each brief period of brittle fracturing, and crystallization of vein-fill minerals in the resultant openings, the dominant ductile deformation style was re-established until interrupted by a further brittle event, coincident with a younger vein set. As it seems unlikely that, in each case, the association between transient brittle failure and hydrothermal influx is merely coincidental, the possibility that there exists a cause-and-effect relationship may be considered.

Heard (1976) gives a graphical representation of the effects of pressure, temperature, pore-fluid pressure and strain rate upon deformation style (Figure 92). If a rock mass is undergoing dominantly ductile deformation (right hand side of Figure 92), then transition to a brief period of brittle failure followed by a return to the ductile regime, can be accomplished under the following scenarios:

1) rapid decrease, followed by increase, in P or T;

2) rapid increase, and then decrease, in strain rate;

3) rapid increase, and then decrease, in pore fluid pressure.
i.e hydrofracturing.

It seems unlikely that pressure and/or temperature could change significantly to enable the rock to cross the ductile-brittle-ductile transitions on several occasions throughout the deformational event, although the possibility cannot be ruled out. There is, however, no evidence to support highly variable ambient physical conditions. It is much more likely that strain rate would show short bursts of high rate, as is typical in high strain zones at present (c.f. San Andreas fault system, California). There is no intuitive reason, however, why a rapid increase in strain rate, accompanying an earthquake in a fault zone, should be necessarily accompanied by fluid influx to seal cracks generated during brittle failure.

Figure 92 **does** suggest, on the other hand, that an increase in fluid pressure, produced possibly by fluid influx from an external source, can be the *cause* of brittle failure. This is an explanation for the strong association between brittle failure and the localization of mineralization: influx of hydrothermal fluid into a zone deforming ductiley, may modify the mechanical response of the host rock and initiate brittle failure. Hydrothermal fluids, concentrated in zones of highest induced permeability (fractured zones), would permit crystallization of minerals to fill the veins. Subsequent reduction of fluid pressure permits a return to ductile flow until perturbed by later fluid influx. As a result of sequential ductile-brittle transitions in one locality, the oldest vein sets in a mineralization sequence exhibit the most extensive effects of ductile deformation.

In summary, the host rocks exposed in the Hard Rock open stope have been deformed in a dominantly ductile fashion. Transient brittle failure, which may be initiated by hydrothermal fluid influx, resulted in localization of auriferous mineralization in veins, veinlets and associated alteration selvages. Following each brittle event, the dominant ductile deformation regime was reimposed, superimposing ductile strain upon the previously formed veins and veinlets and resulting in a protracted sequence of brittle-ductile transitions.

11.0 Implications of the Au-BIF Study for Mineralization in the Geraldton Camp

Detailed field mapping of the HRos has demonstrated unequivocally that gold mineralization is related to fracturing, veining and selvage replacement of host rocks, including BIF, and porphyry, and minor wacke and siltstone. Deformation style is manifested by considerable strain heterogeneity, in response to the very different physical properties of adjacent rock types. In general, however, deformation in the Geraldton Camp is dominated by an easterly directed component of dextral simple shear and a general north-south compression, as first described by Horwood and Pye (1951) and confirmed by Lavigne (1983). No field or geochemical evidence has been found to indicate the presence of an auriferous, precursor protore. Indeed, detailed field mapping throughout the Geraldton Camp indicates that gold was not present in above background concentrations until after mafic and felsic intrusion. Accordingly, the hypothesis that gold represents an integral syn-sedimentary component of banded iron formation (Figure 2) is rejected, and an external source for the gold, and a method of transporting the metal, must be considered. Pye (1951) came to the same conclusion; in Horwood and Pye's (1951, p.47) report, he speculated as to the origin of the ore solutions:

> "The origin of the ore solutions is not known. Since the mineralization in the area occurred subsequent to the emplacement of the albitic porphyries, however, it appears that the ore deposits were formed either concomitantly with or later than the intrusion of the granitic masses flanking the Little Long Lac area on the north and south. A likely source of the ore solutions, if a magmatic origin is to be postulated, is the granitic "finger" or stock, which is exposed in Croll Township, and which plunges westward and probably underlies Ashmore Township at an undetermined depth. The necessary channelways for the upward migration of the ore solutions, whatever their source, are believed to have been provided by the disturbed zone associated with the major east-west faults and their subsidiary structures."

Pye (1951, Figure 7) noted that the contained gold content of deposits in the Geraldton Camp showed an exponential decrease from east to west (Figure 93), implying a source to the east.

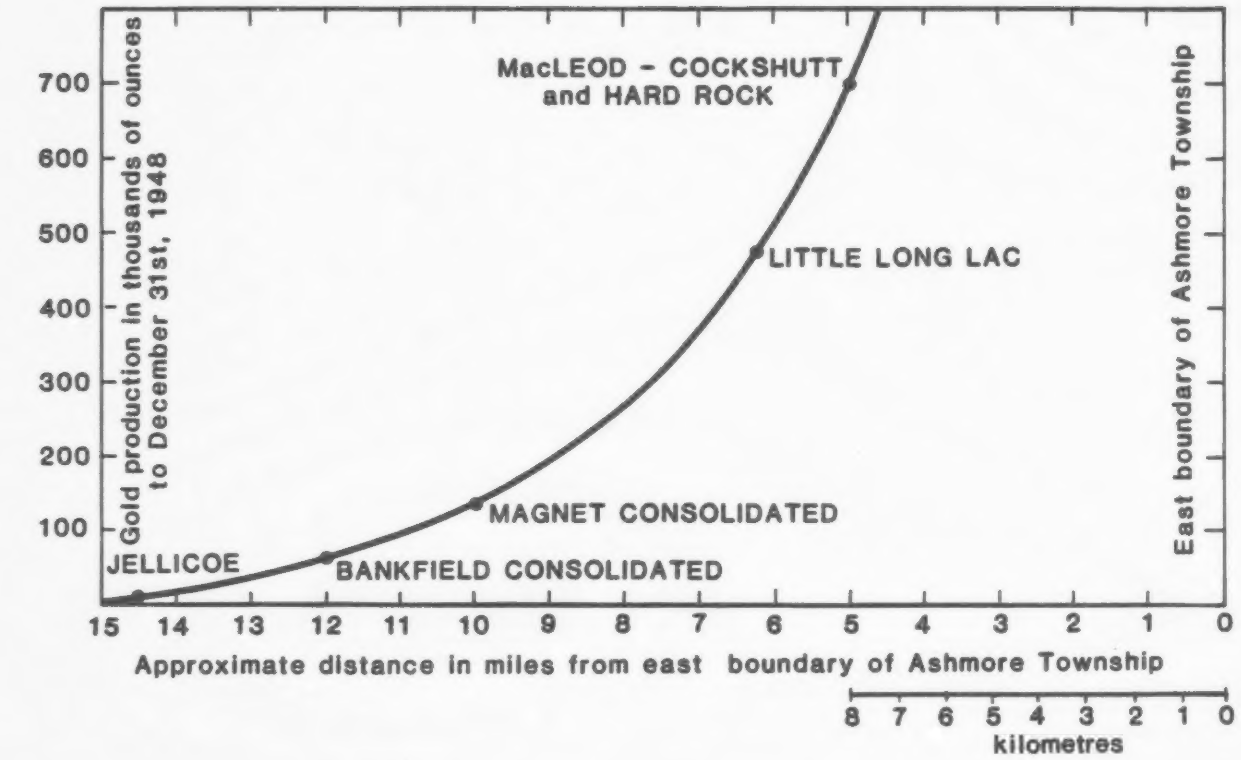

Figure 93 : Relationship between contained gold in various mines of the Geraldton Camp and distance from the eastern margin of Ashmore Township and the Croll Lake felsic intrusion (modified from Pye, 1951).

Based upon mapping during this study, which confirmed the syntectonic nature of gold mineralization, and observations and hypotheses presented by Pye (1951) and Horwood and Pye (1951), reconnaissance traverses into Croll Township (Figure 3) were made in late 1982. Large (greater than 1m) boulders of tourmaline- and molybdenite-bearing quartz were encountered. This was considered as possible support for the hypotheses of Horwood and Pye (1951, see above). Accordingly a study was initiated to map in detail portions of the Croll Lake Stock in 1983 (Macdonald, 1983b, 1984b).

12.0 Acknowledgements

I received field assistance during 1982 from Tina Eng (University of Western Ontario) and logistical support from David Slater and the staff of the Geraldton Fire Centre. Their co-operation is very much appreciated. John Mason, George Patterson and the staff of the Resident Geologist's Office, Thunder Bay are warmly thanked for their help in focussing this study and constant assistance throughout all phases of the research. John Mason's geological knowledge proved invaluable and I am most grateful for his continued support.

I have benefited greatly from discussions with my colleagues in the Mineral Deposits Section of the OGS, with Federal Government geologists, especially Jim Franklin and Howard Poulsen, and other researchers in the Geraldton gold camp, with special thanks to Lyn Anglin (Memorial University and the Geological Survey of Canada), Maurice J. Lavigne, Jr. (Ministry of Northern Development and Mines), Shane Buck and Howard Williams (Brock University). This report has improved considerably as a result of discussions and, in some cases, reviews, by these geologists, although the concepts and conclusions are wholly my responsibility.

I thank Mrs. I. Sherrett for typing the manuscript, and Mrs. G. Atkinson and Ms. J. van Kralingen for drafting some of the figures.

13.0 References

Andrews, A.J., Hugon, H., Durocher, M., Corfu, F., and Lavigne, M.J.
1986: The Anatomy of a gold-bearing Greenstone Belt, Red Lake, Northwestern Ontario, Canada; p. 3 -22, in Macdonald, A.J., editor, Proceedings of GOLD 86 : An International Symposium on the Geology of Gold Deposits, Toronto, 1986.

Anglin, C.D., and Franklin, J.M.
1985: Gold Mineralization in the Beardmore-Geraldton area of Northwestern Ontario: Structural Considerations and The Role of Iron Formation; in Current Research, part A, Geological Survey of Canada,Paper 81-1A, p. 193-201.

Armstrong, H.S.
1943: Gold Ores of the Little Long Lac Area; Economic Geology, Volume 38, no. 3, p. 234.

Ayres, L.D.
1969: Early Precambrian Stratigraphy of Part of Lake Superior Provincial Park, Ontario, Canada, and its implications for the Origin of the Superior Province; Unpublished Ph.D. Thesis, Princeton University, 399 p.

Barrett, T.J., and Fralick, P.W.
1985: Sediment Redeposition in Archean Iron Formation: Examples from the Beardmore-Geraldton Greenstone Belt, Ontario; Journal of Sedimentary Petrology, Vol. 55, No. 2, p. 205-212.

Barrett, R.E., and Johnston, A.W.
1948: Central Patricia Mine; p. 268-372, in Structural Geology of Canadian Ore Deposits, CIMM, 1948, 948 p.

Beakhouse, G.P.
1984: Geology of the Grenville Lake Area, Thunder Bay District; Ontario Geological Survey Open File Report 5513, 146p., 13 tables, 17 Figures, 12 photos, and 2 Prelim maps in back pocket (maps P.2592, 2593).

Bell, T.H.
1978: Progressive deformation and reorientation of fold axes in a ductile mylonite zone: the Woodroffe Thrust; Tectonophysics, volume 44, p. 285-320.

Berthe, D., Choukoune, P. and Gapais, D.
1979: Orientations prefentielles du quartz et orthogneissification progressive en regime cisaillement: l'example du cisaillement sud armoricain; Bull. Mineral.. vol 102, p. 265 -272.

Borradaile G.J., Bayly, M.B., and Powell, C.McA. (editors)
1982: Atlas of deformational and metamorphic rock fabrics; Springer, Berlin.

Boyle, R.W.
1979: The Geochemistry of Gold and its Deposits; Geological Survey of Canada, Bulletin 280, 584p.

Bruce, E.L.
1935: Little Long Lac Gold Area; Ontario Department of mines, 44th Annual Report, Volume XLIV, Part III, 60 p.

Bruce, E.L.
1946: The Hard Rock "Porphyry" of Little Longlac; Economic Geology, Volume 41, p. 282-283.

Bruce, E.L., and Samuel, W.
1937: Geology of the Little Long Lac Mine; Economic Geology, Volume 32, p. 318-334.

Buck, S.
1986: Structural Studies and Gabbro Mylonitization within the Barton Bay Deformation Zone, Geraldton, Ontario; M.Sc.Thesis, Brock University, 96p.

Buck, S. and Williams, H.R.
1984: Structural Studies in the Geraldton Area; p. 208-211, in Summary of Field Work, 1984, edited by J. Wood, O.L. White, R.B. Barlow and A.C. Colvine, Ontario Geological Survey Miscellaneous Paper 119, 309p.

Cobbold, P.R., and Quinquis, H.
1980: Development of Sheath Folds in Shear Regimes; Journal of Structural Geology, Volume 2, No. 12, p. 119-126.

Colvine, A.C. and Corfu, F.
1985: Archean Gold Mineralization and Metamorphism: Timing Constraints from Precise U-Pb Dating; p. 551 in Abstracts with Programs, Geological Society of America, Annual General Meeting, Orlando, Florida.

Colvine, A.C., Andrews, A.J., Cherry, M.E., Durocher, M.E., Fyon, J.A., Lavigne, M.J. Jr., Macdonald, A.J., Marmont, S., Poulsen, K.H., Springer, J.S., and Troop, D.G.
1984: An Integrated Model for the Origin of Archean Lode Gold Deposits; Ontario Geological Survey Open File Report 5524, 98p., 7 tables, 53 figs., and 2 appendices.

Corking, W.P.
1948: Pickle Crow Mine; p. 373-376, in Structural Geology of Canadian Ore Deposits, CIMM.

de Sitter, L.V.
1964: Structural Geolgy, Second Edition, New York, McGraw Hill, 587 p.

Devaney, J.R., and Fralick, P.W.
1985: Regional Sedimentology of the Namewaminikan Group, Northern Ontario; Archean Fluvial Fans, Braided Rivers, Deltas and an Aquabasin; p. 125-132 in Geological Survey of Canada, Current Research , Part B, Paper 85-1B.

Escher, A., and Waterson, J.
1974: Stretching fabrics, folds and crustal shortening; Tectonophysics, volume 22, p. 223-231.

Ferguson, S.A.
1967: MacLeod-Mosher Gold Mines Limited. Subsurface Plans and Longitudinal Projection, Parts of Errington and Ashmore Townships, Ontario; Ontario Department of Mines, Preliminary map P-436.

Fralick, P.W., and Barrett, T.J.
1983: The sedimentology of Banded Iron Formation in the Beardmore-Gertaldton Greenstone Belt: A Preliminary Appraisal; p. 204-206 in Summary of Field Work 1983, Ontario Geological Survey, Miscellaneous Paper 116, 313 p.

Fyon, J.A., Crocket, J.H. and Schwarcz, H.P.
1983: The Carshaw and Malga iron formation-hosted gold deposits of the Timmins area; p. 98-110 in Colvine, A.C., editor, The Geolgy of Gold in Ontario, Ontario Geological Survey, Miscellaneous Paper 110.

Gresens, R.L.
1967: Composition-Volume Relationships of Metasomatism; Chemical Geology, Volume 2, p. 47-65.

Gross, G.A.
1965: Geology of Iron Deposits, Volume I: General Geology and Evaluation of iron deposits; Economic Geology Report Number 22, Geological Survey of Canada.

Grout, F.F.
1932: Petrography and Petrology; First Edition, McGraw-Hill, New York.

Harris, L.B., and Cobbold, P.R.
1984: Development of conjugate shear bands during bulk simple shearing; Journal of Structural Geology, volume 7, p. 37-44.

Hall R.S., and Rigg, D.M.
1986: Geology of the West Anticline Zone, Musselwhite Prospect, Opapimiskan Lake, Ontario, Canada; p. 124-136, in Macdonald, A.J., editor, Proceedings of GOLD 86 : An International Symposium on the Geology of Gold Deposits, Toronto, 1986.

Heard, H.C.
1976: Comparison of flow properties of rocks at crustal conditions. Philosophical Transactions of the Royal Society of London, volume 283, p. 173-186.

Hobbs, B.E., Means, W.D., and Williams, P.F.
1976: An Outline of Structural Geology; J. Wiley and Sons, 571 p.

Hodgson C.J.
In Press: The structure of a vein-type gold deposits; Ore Geology Reviews.

Horwood, H.C., and Pye, E.G.
1951: Geology of Ashmore Township, Little Long Lac Area; Ontario Department of Mines, Annual Report, Volume 60, Pt. 5, 105 p., accompanied by Map 1951-2.

Hugon, H., & Schwerdtner, W.F.
1985: Structural Signature and Tectonic History of Deformed Gold-bearing Rocks in Northwestern Ontario, p. 62-72, in Milne, V.G., editor, Geoscience Research Grant Program, Ontario Geological Survey, Miscellaneous Paper 127.

Kehlenbeck, M.M.
1986: Folds and Folding in the Beardmore-Geraldton Fold Belt; Canadian Journal of Earth Sciences, Vol. 23, p. 158-171.

Karvinen, W.O.
1981: Geology and Evolution of Gold Deposits, Timmins Area, Ontario; p. 29-46 in Genesis of Archean, Volcanic-Hosted Gold Deposits, Symposium Held At the The University of Waterloo, March 7, 1980, Ontario Geological Survey, Miscellaneous Paper 97, 175p.

Lavigne, M.J.
1983: Gold Deposits of the Geraldton Area; p. 198-200 in Summary of Field Work 1983, Ontario

Geological Survey, Miscellaneous Paper 116, 313 p.

Macdonald, A.J.
1982: The MacLeod-Cockshutt and Hard Rock Mines, Geraldton; Examples of an Iron Formation-Related Gold Deposit; p. 188-191 in Wood, J., White, O.L., Barlow, R.B., and Colvine, A.C., editors, Summary of Field Work 1982, Ontario Geological Survey, Miscellaneous Paper 106, 235 p.

Macdonald, A.J.
1983a: Iron Formation-Gold Association: Evidence from Geraldton Area; p. 75-83, in the Geology of Gold in Ontario, Colvine, A.C., editor, Ontario Geological Survey, Miscellaneous Paper 110, 278 p.

Macdonald, A.J.
1983b: A Re-appraisal of the Geraldton Gold Camp, p. 194-197, in Wood, J., White, O.L., Barlow, R.B., and Colvine, A.C., editors, Summary of Field Work, Ontario Geological Survey, Miscellaneous Paper 116.

Macdonald, A.J.
1984a: Gold Mineralisation in Ontario, I : The role of banded iron formation; Canadian Institute of Mining and Metallurgy, Special Volume 34, p. 412-430.

Macdonald, A.J.
1984b: The Au-CO_2 association, evolving hydrothermal fluids and precipitating mechanisms; p. 581, in Geological Society of America, Abstracts with Programs, Annual General Meeting, Reno, Nevada, November, 1984.

Macdonald, A.J.
In Press: Banded Oxide-Facies Iron Formation as a Host For Gold Mineralization; in Ancient Banded Iron Formations and Deposits (Regional Presentations), Theophrastus (publishers), Athens.

Macdonald, R.D.
1944: Regional Metamorphism in the Kenogamisis River Area; Journal of Geology, Vol. 52, p. 414 -423.

Marmont, S.
1984: Temporal Relationships of Archean Gold Mineralization to Volcanism, Tectonism and Intrusion; p. 584 in Geological Society of America, Annual General Meeting, Reno, Nevada.

Mason, J., White, G., and McConnell, C.
1985: Field guide to the Beardmore-Geraldton Metasedimentary-Metavolcanic Belt; Ontario Geological Survey, Open File Report 5538, 73 p.

Mason, J., and White, G.
1986: Gold Occurrences, Propspects, and Deposits of the Beardmore-GeraldtonArea, Districts of Thunder Bay and Cochrane; Ontario Geological Survey, Open File report 5630, 2 volumes, 680 p.

Matheson, A.F., and Douglas, J.H.
1948: Hard Rock Mine; p. 406-412, in Structural Geology of Canadian Ore Deposits, CIMM, 1948, 948 p.

McGlynn, J.C.
1970: Geology of the Canadian Shield-Superior Province; in Geology and Economic Minerals of Canada, Geological Survey of Canada, Economic Report 1, p. 66.

Oliver, J.L.

1985: Characteristics of Gold Mineralisation, Geraldton-Beardmore District, Northwestern Ontario; M.Sc. Thesis, Queen's University, Kingston.

Phillips, G.N., and Groves, D.I.
1984: Fluid access and fluid-wall rock interaction in the genesis of the Archean gold-quartz vein deposit at Hunt Mine, Kambalda, Western Australia; p. 389-416 in Foster, R.L., editor, GOLD '82, A.A. Balkema, publisher.

Pirie, J., and Mackasey, W.O.
1978: Preliminary Explanation of Regional Metamorphism in Parts of Quetico Metasedimentary Belt, Superior Province, Ontario; p. 37-48, in Metamorphism in the Canadian Shield, Geological Survey of Canada, Paper 78-10.

Pye, E.G.
1951: Geology of Errington Township, Little Long Lac Area; Ontario Department of Mines, Annual Report, Volume 60, Pt. 6, 140 p., Accompanied by Map 1951-7.

Ramsay, J.G.
1967: Folding and Fracturing of Rocks; McGraw Hill, New York, 568 p.

Ramsay, J.G., and Huber, M.I.
1983: The Techniques of Modern Structural Geology,; Volume 1 : Strain Analysis. Academic Press, Toronto, 307 p.

Reid, J.A.,
1945: The Hard Rock Porphyry of Little Long Lac; Economic Geology, Volume 40, No. 8, p. 509-516.

Ridler, R.H.
1970: Relationship of Mineralization to Volcanic Stratigraphy in the Kirkland-Larder Lakes Area, Ontario; Proceedings of the Geological Society of Canada, Vol. 21, p. 33-42.

Ridler, R.H.
1976: Regional Metallogeny and Volcanic Stratigraphy of the Superior Province; Geological Survey of Canada, Paper 76-1A, p. 399-405.

Robin, P.F., and Jowett E.C.
1986: Computerised density contouring and statistical evaluation of orientation data using counting circles and continuous weighting functions; Tectonophysics 121, p. 207-223.

Snow, D.T.
1969: Anisotropic Permeability of Fractured Media; Water Reserves and Resources, vol.5, no. 6, p. 1273-1289.

Stockwell, C.H.
1964: Fourth Report on Structural Provinces, Orogenies, and Time Classification of Rocks in the Canadian Precambrian Shield; in Age Determinations and Geological Studies, Part II. Geological Studies: Geological Survey of Canada, Paper 64-17 (Part II), p. 1-21.

Streckeisen, A.
1973: IUGS Subcomissions on the Systematics of Igneous Rocks: classification and nomenclature of Plutonic Rocks; N. Jb. Miner. Mh., 1973, p. 149-164.

Trendall, A.F., and Blockley, J.G.
1970: The Iron Formations of Western Australia, with Special Reference to the Associated

Crocidolite: West Australia Geological Survey, Bulletin 119, 353 p.

Williams, H.R.
1986: Structural Studies in the Beardmore-Geraldton Belt, Northern Ontario; p. 138-146 in Geoscience Research Grant Program, Summary of Research 1985-86, edited by V.G. Milne, Ontario Gological Survey, Miscellaneous Paper 130, 255p.

3268
ISSN 0826-9580
ISBN 0-7729-4445-8

MAPS
NOT
FILMED

CARTES
OMISES